



Search for dark matter in association with an energetic photon in pp collisions at $\sqrt{s} = 13$ TeV with the ATLAS detector

The ATLAS Collaboration

A search for dark matter is conducted in final states containing a photon and missing transverse momentum in proton–proton collisions at $\sqrt{s} = 13$ TeV. The data, collected during 2015–2018 by the ATLAS experiment at the CERN LHC, correspond to an integrated luminosity of 139 fb^{-1} . No deviations from the predictions of the Standard Model are observed and 95% confidence-level upper limits between 2.45 fb and 0.5 fb are set on the visible cross section for contributions from physics beyond the Standard Model, in different ranges of the missing transverse momentum. The results are interpreted as 95% confidence-level limits in models where weakly interacting dark-matter candidates are pair-produced via an s -channel axial-vector or vector mediator. Dark-matter candidates with masses up to 415 (580) GeV are excluded for axial-vector (vector) mediators, while the maximum excluded mass of the mediator is 1460 (1470) GeV. In addition, the results are expressed in terms of 95% confidence-level limits on the parameters of a model with an axion-like particle produced in association with a photon, and are used to constrain the coupling $g_{aZ\gamma}$ of an axion-like particle to the electroweak gauge bosons.

Contents

1	Introduction	2
2	ATLAS detector	4
3	Dataset and simulated events	4
4	Event reconstruction and selection	6
5	Strategy for background estimation	9
6	Results	11
7	Interpretations	15
8	Conclusion	23

1 Introduction

Despite its astounding success, the Standard Model (SM) of particle physics is considered to be a low-energy approximation to some fundamental theory of nature, with new degrees of freedom and symmetries that would be evident at a higher energy. Numerous attempts have been made to figure out a footprint of physics beyond the Standard Model (BSM) at the Large Hadron Collider (LHC), but no significant sign of new physics has been observed yet. In this paper, proton–proton collisions at the LHC are used to explore the production of events with an energetic photon and large missing transverse momentum (E_T^{miss} , with magnitude E_T^{miss}), as it may constitute a striking signature of BSM physics, including extensions that account for particle dark matter (DM) [1].

Understanding the nature of dark matter has provided some of the strongest motivations to search for BSM physics at the LHC. Recent advances in theory and experiment combining high-energy physics, astrophysics and cosmology have led to a potential DM phenomenology with a variety of experimental signatures that could be observed in proton–proton collisions at the LHC. Among the searches are those focusing on final states that try to replicate the annihilation processes which could have led to dark-matter freeze-out in the early universe. This is the case for direct DM pair-production yielding large E_T^{miss} in association with a visible particle (X) that, in most searches, originates from initial-state radiation [2]. The X + E_T^{miss} signature is the hallmark of this type of search.

Axion-like particles (ALPs), originally motivated by the QCD axion from the dynamical solution to the strong CP problem of the SM [3], provide a compelling and elegant explanation of DM. More generally, ALPs appear in any theory with a spontaneously broken global symmetry. They could be non-thermal DM candidates [4] or mediators to a dark sector. Depending on the different ALP production mechanisms at the LHC, it is possible to probe a large range of masses and couplings over several orders of magnitude [5]. Masses from keV to MeV are conducive to a stable ALP and are best searched for in association with either a photon or a jet, and hence the expected final states are events with a photon or a jet plus E_T^{miss} [6–8].

This paper presents the results of a search for an excess of events with a $\gamma + E_T^{\text{miss}}$ final state over the SM prediction. The search is performed using the full Run-2 dataset collected by the ATLAS experiment at the

LHC in proton–proton collisions at a centre-of-mass energy of $\sqrt{s} = 13$ TeV. The $\gamma + E_T^{\text{miss}}$ final state has the advantage of a clean signature that nicely complements the other $X + E_T^{\text{miss}}$ processes. The sensitivity of this search is enhanced compared to a previous search using 36.1 fb^{-1} [9] due to the increased size of the dataset and by incorporating new criteria for reconstructed objects. The $X + E_T^{\text{miss}}$ signatures have been explored by the LHC experiments for the cases where X is a photon [9, 10], a jet [11, 12], a heavy quark [13, 14], a vector boson [12, 15, 16] or a Higgs boson [17, 18].

The results are interpreted using simplified models where Dirac-fermion DM candidates (denoted by χ) interact with quarks through the exchange of a mediator in the s -channel via vector or axial-vector interactions [19–21]. A photon can be radiated from the initial state and the $\chi\bar{\chi}$ pair is invisible to the detector, resulting in a $\gamma + E_T^{\text{miss}}$ final state as shown in Figure 1 (left).

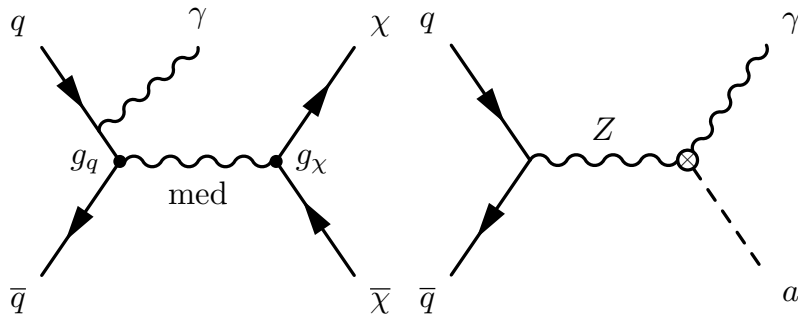


Figure 1: Feynman diagrams corresponding to the simplified DM model (left) and ALP DM model (right) considered.

The free parameters in models of this kind are the mass of the mediator, m_{med} , the mass of the DM particle, m_χ , the couplings g_q , g_ℓ and g_χ of the mediator to quarks, leptons and DM particles respectively, and the width of the mediator, Γ_{med} [22]. The latter is computed as the minimum width allowed given the couplings and masses.

In addition, a model with an ALP (denoted by a) produced in association with a photon is used. The model considered is an effective field theory (EFT) that extends the SM Lagrangian, by using effective operators to describe the interactions of ordinary matter with an additional particle. This particle is a generic CP-odd (pseudo-)Nambu–Goldstone boson of a spontaneously broken symmetry at energies below a scale higher than the electroweak scale, singlet under the SM charges and playing the role of the ALP [8].

Signals from this model consist of events having the ALP generated in association to a photon as shown in Figure 1 (right). In this ALP EFT, the new physics scale to be considered is the ALP decay constant f_a , which regulates the dimension-5 operators built from the SM fields and a . After electroweak symmetry breaking, the couplings of ALPs to the electroweak gauge bosons can be obtained as a linear combination of the relevant free parameters, namely the real operator coefficients c_i in the effective Lagrangian describing bosonic ALP couplings, and the effective scale f_a . The ALP mass is supposed to be a free parameter, but since the ALP is considered a light particle (~ 1 MeV) it does not affect the kinematics. The coupling of ALPs to two photons is tightly constrained by experimental observations, and it is taken to be zero, which allows a further reduction in the number of parameters (see Ref. [8] and the references therein). The resulting limits for this model are set on the energy scale f_a and $c_{\tilde{W}}$, the coefficient for the operator built from the $SU(2)_L$ gauge group field and a . The signal cross section depends on the square of the ratio of an operator coefficient to the effective scale, $(c_i/f_a)^2$, and hence the ratio $c_{\tilde{W}}/f_a$ is the relevant combination of parameters provided by this analysis.

2 ATLAS detector

The ATLAS experiment is a multipurpose detector [23–25] with a cylindrical geometry and almost 4π coverage in solid angle.¹ The collision point is surrounded by tracking detectors, collectively referred to as the inner detector (ID), followed by a superconducting solenoid providing a 2 T axial magnetic field, a calorimeter system and a muon spectrometer.

The ID provides precise measurements of charged-particle tracks in the pseudorapidity range $|\eta| < 2.5$. It consists of three subdetectors arranged in a coaxial geometry around the beam axis: a silicon pixel detector, a silicon microstrip detector and a transition radiation tracker.

The electromagnetic (EM) calorimeter covers the region $|\eta| < 3.2$ and is based on a high-granularity, lead/liquid-argon (LAr) sampling technology. It is segmented longitudinally in shower depth. The first layer has a high granularity in the η direction in order to provide efficient discrimination between single-photon showers and two overlapping photons originating from a π^0 decay. The second layer is where most of the energy, deposited in the calorimeter by electron- or photon-initiated electromagnetic showers, is collected. Significant energy deposits can be left in the third layer by very high energy showers; this layer can also be used to correct for energy leakage beyond the electromagnetic calorimeter.

The hadronic calorimeter uses a steel/scintillator-tile sampling detector in the region $|\eta| < 1.7$ and a copper/LAr detector in the region $1.5 < |\eta| < 3.2$. The forward calorimeter (FCAL) covers the range $3.2 < |\eta| < 4.9$ and uses LAr as the active material and copper or tungsten as absorbers for the EM and hadronic sections, respectively.

The muon spectrometer (MS) consists of separate trigger and high-precision tracking chambers to measure the deflection of muons in a magnetic field generated by three large superconducting toroids arranged with an eightfold azimuthal coil symmetry around the calorimeters. The high-precision chambers cover the range of $|\eta| < 2.7$. The muon trigger system covers the range $|\eta| < 2.4$ with resistive-plate chambers in the barrel and thin-gap chambers in the endcap regions.

A two-level trigger system is used to select events in real time [26]. It consists of a hardware-based first-level trigger and a software-based high-level trigger. The latter employs algorithms similar to those used in the offline reconstruction.

3 Dataset and simulated events

The analysis is performed on a set of proton-proton collision data collected by the ATLAS detector at $\sqrt{s} = 13$ TeV between 2015 and 2018. In this period, the LHC delivered colliding beams with a peak instantaneous luminosity up to $L = 2.1 \times 10^{34} \text{ cm}^{-2}\text{s}^{-1}$ and an average number of interactions in the same or neighbouring bunch crossings of $\langle \mu \rangle = 33.7$. With requirements on the stability of the beams, the operational status of all ATLAS detector components, and the quality of the recorded data, the total integrated luminosity of the dataset is 139 fb^{-1} with an uncertainty of 1.7%. It is derived from the

¹ ATLAS uses a right-handed coordinate system with its origin at the nominal interaction point (IP) in the centre of the detector and the z -axis along the beam pipe. The x -axis points from the IP to the centre of the LHC ring, and the y -axis points upward. Cylindrical coordinates (r, ϕ) are used in the transverse plane, ϕ being the azimuthal angle around the beam pipe. The pseudorapidity is defined in terms of the polar θ angle as $\eta = -\ln[\tan(\theta/2)]$.

calibration of the luminosity scale using x - y beam-separation scans, following a methodology similar to that detailed in Ref. [27], and using the LUCID-2 detector [28] for the baseline luminosity measurements.

To evaluate the effects of the detector efficiency and acceptance on the signal and background, and to estimate SM backgrounds, simulated event samples were produced using Monte Carlo (MC) generators. Inelastic collisions were simulated using PYTHIA 8.186 [29] with a set of tuned parameters called the A2 tune [30] and the MSTW2008LO parton distribution function (PDF) [31] set and overlaid on the signal and background MC samples. These simulated events are reweighted to accurately reproduce the average number of proton-proton interactions in the same or neighbouring bunch crossings (referred to as pile-up).

Samples of simulated events for DM production in simplified models were generated for the case of an s -channel mediator with axial-vector interactions. MADGRAPH5_aMC@NLO v2.6.2 [32] was used in conjunction with PYTHIA 8.235 with the A14 tune [30] for modelling of parton showering, hadronisation, and the underlying event. The PDF set used is NNPDF3.0NLO [33]. A photon with a transverse energy above 130 GeV was required at the matrix-element level in MADGRAPH5_aMC@NLO. The DMsimp [34] implementation of the model at next-to-leading order (NLO) in QCD was used. The g_q coupling was set to be universal in quark flavour and equal to 0.25, g_χ was set to 1.0, and $\Gamma_{m_{\text{med}}}$ was computed as the minimum width allowed given the couplings and masses. Different choices of the couplings and a model with a vector mediator were also considered [22]. A grid of signal samples was generated spanning the m_χ - m_{med} plane for m_χ values from 10 to 500 GeV and m_{med} values from 10 to 1700 GeV.

Samples for ALP production in association with a photon were generated at NLO with MADGRAPH5_aMC@NLO v2.6.2 and interfaced to PYTHIA 8.240 with the A14 tune for modelling of parton showering, hadronisation, and the underlying event. The PDF set used for the generation is NNPDF23LO, and the renormalisation and factorisation scales were set to half of the transverse mass of the ALP and photon system. Effective scales f_a in the range between 1 TeV and 5 TeV are explored.

Samples of SM backgrounds were produced using the SHERPA 2.2 MC event generator [35, 36]. The leading-order (LO) and NLO matrix elements were generated using the Comix [37] and OpenLoops [38] matrix-element generators, and the merging with the parton shower is done using the ME+PS@NLO prescription [39]. The NNPDF3.0NNLO [33] PDF set was used in conjunction with a dedicated parton shower tuning developed by the SHERPA authors [40]. For $W\gamma$ and $Z\gamma$ backgrounds, events containing a charged lepton (e , μ or τ) and a neutrino or a pair of charged leptons together with a photon and associated jets were simulated by SHERPA 2.2.2 and the matrix elements were calculated for up to one parton at NLO and up to three partons at LO. For γ^*/Z decays into charged leptons, a requirement on the dilepton invariant mass of $m_{\ell\ell} > 10$ GeV was applied at generator level. Events containing a photon with associated jets were also simulated using SHERPA 2.2.2, and the matrix elements were calculated for up to two partons at NLO and up to four partons at LO. Events containing W or Z bosons with associated jets were simulated using SHERPA 2.2.1 and the matrix elements were calculated for up to two partons at NLO and up to four partons at LO. The W/Z +jets events are normalised to next-to-next-to-leading order (NNLO) inclusive cross-section predictions [41].

Table 1 summarises the details of the generation of events for the signal samples and SM background processes considered in the analysis.

All background samples were simulated with a full ATLAS detector simulation [42] based on GEANT4 [43], while the signal samples were processed through a fast simulation of the ATLAS detector using a parameterisation of the calorimeter response and GEANT4 for the ID and MS. The simulated events are

Table 1: Details of the generation of events for the signal samples and SM backgrounds considered in the analysis.

Process	Generators	PDF sets	Order
DMsimp model	MG5_aMC@NLO v2.6.2 + PYTHIA 8.235	NNPDF3.0NLO	NLO
ALP model	MG5_aMC@NLO v2.6.2 + PYTHIA 8.240	NNPDF23LO	NLO
$W/Z + \gamma$	SHERPA 2.2.2	NNPDF3.0NNLO	0,1j@NLO + 2,3j@LO
γ +jets	SHERPA 2.2.2	NNPDF3.0NNLO	1,2j@NLO + 3,4j@LO
W/Z +jets	SHERPA 2.2.1	NNPDF3.0NNLO	0,1,2j@NLO + 3,4j@LO

reconstructed and analysed with the same analysis chain as for the data, using the same trigger and event selection criteria discussed in Section 4.

4 Event reconstruction and selection

All the events in the analysis must satisfy beam, detector and data-quality criteria. They are selected by a trigger requiring at least one photon candidate with transverse energy E_T^γ above a threshold of 140 GeV and passing ‘loose’ identification requirements [44]. Events are required to have at least one candidate for primary vertex, defined as the vertex with the highest sum of the squared transverse momenta of its associated tracks and reconstructed from at least two good-quality tracks [45] with $p_T > 0.5$ GeV. Events are removed if they contain a poor-quality photon or jet arising from instrumental problems or non-collision background [46].

Depending on the quality and kinematic requirements imposed, physics objects are labelled either as candidate or selected, where the latter is a subset of the former, with tighter selection criteria applied. Candidate physics objects are used when classifying overlapping selected objects and for vetoing events.

Photons are reconstructed from clusters of energy deposits in the electromagnetic calorimeter, together with information about charged-particle tracks reconstructed in the ID [47]. Photon candidates are classified either as converted (the photon cluster is matched to a reconstructed conversion vertex) or as unconverted (matched to neither a conversion vertex nor an electron track). Both the converted and unconverted photon candidates are used in the analysis. The calibration of the photon energy in the calorimeter accounts for upstream energy loss as well as lateral and longitudinal leakages. The energy of the cluster of calorimeter cells associated with the photon candidate is corrected using a combination of simulation-based and data-driven calibration factors determined from $Z \rightarrow e^+e^-$ events. Photon candidates are also required to fulfill ‘loose’ or ‘tight’ identification criteria based on observables that reflect the shape of the electromagnetic showers in the calorimeter, especially in the finely segmented first layer. All the reconstructed photons of ‘loose’ quality with $E_T^\gamma > 10$ GeV and $|\eta| < 2.37$ are considered as photon candidates. Selected photons must additionally satisfy the ‘tight’ identification criteria, have $|\eta| < 1.37$ or $1.52 < |\eta| < 2.37$, and be isolated to avoid contamination coming from π^0 or other neutral hadrons decaying into an almost-collinear photon pair; the isolation condition is imposed by requiring the transverse energy in the calorimeters in a cone of size $\Delta R = \sqrt{(\Delta\eta)^2 + (\Delta\phi)^2} = 0.4$ around the cluster barycentre, excluding the transverse energy associated with the photon cluster, to be less than $2.45 \text{ GeV} + 0.022E_T^\gamma$. This transverse energy in the cone is corrected for photon energy leakage from the central core and for the

effects of pile-up and the underlying event. In addition, the scalar sum of the p_T of non-conversion tracks in a cone of size $\Delta R = 0.2$ around the cluster barycentre is required to be less than $0.05E_T^\gamma$.

Electron candidates are reconstructed from energy clusters in the electromagnetic calorimeter matched to charged-particle tracks in the ID. A procedure similar to that for photons is applied for their identification and calibration [47]. They must fulfil the ‘medium’ identification requirement and are required to have $p_T > 7$ GeV and $|\eta| < 2.47$. Selected electrons must be isolated according to ‘loose’ criteria.

Muon candidates are reconstructed by searching for track segments in different layers of the MS. These segments are combined and matched with tracks found in the ID. The candidates are re-fitted using the complete track information from both detector systems. Muon candidates must pass the ‘medium’ identification requirement [48] and are required to have $p_T > 6$ GeV and $|\eta| < 2.7$. Selected muons are also required to pass the ‘loose’ isolation requirement.

To achieve additional rejection of background electrons and muons from non-prompt sources, electron and muon tracks must be matched to the primary vertex with a longitudinal impact parameter $|z_0 \sin \theta| < 0.5$ mm and a transverse impact parameter significance, defined as the transverse impact parameter d_0 divided by its estimated uncertainty σ_{d_0} , satisfying $|d_0|/\sigma_{d_0} < 5.0$ for electrons and $|d_0|/\sigma_{d_0} < 3.0$ for muons.

Jets are reconstructed from topological clusters of energy in the calorimeter [49] using the anti- k_t jet clustering algorithm [50, 51] with a radius parameter $R = 0.4$. The reconstructed jets are then calibrated by the application of a jet energy scale derived from 13 TeV data and simulation [52]. Only candidate jets with $p_T > 20$ GeV and $|\eta| < 4.5$ are considered. To reduce the effects of pile-up, for jets with $|\eta| < 2.5$ and $p_T < 120$ GeV a significant fraction of the tracks associated with each jet must have an origin compatible with the primary vertex, as defined by the jet vertex tagger [53]. Selected jets are required to have $p_T > 30$ GeV and $|\eta| < 4.5$.

Hadronically decaying τ -lepton candidates are reconstructed by combining information from the calorimeters and the ID. The τ -lepton reconstruction algorithm is seeded by jets reconstructed as described above and the reconstructed energy is corrected to the τ -lepton energy scale [54]. Hadronically decaying τ -lepton candidates are required to have one or three associated charged-particle tracks (prongs) and $p_T > 20$ GeV. To improve the discrimination between hadronically decaying τ -leptons and jets, a multivariate algorithm is used; selected τ -leptons are required to fulfil the ‘loose’ identification criteria.

Possible double counting of reconstructed candidate physics objects is resolved in the following order. If any electron shares its inner detector track with a selected muon, the electron is removed and the muon is kept, in order to remove electron candidates originating from muon bremsstrahlung followed by photon conversion. If a photon and an electron or a muon are closer than $\Delta R = 0.4$ the photon is removed. If an electron lies within $\Delta R = 0.2$ of a jet, the jet is removed, while if an electron lies within $0.2 < \Delta R < 0.4$ of a jet, the electron is removed. Muons lying within $\Delta R = 0.4$ of jets are removed, except if the number of tracks with $p_T > 0.5$ GeV associated with the jet is less than three. In the latter case, the muon is kept and the jet is discarded. If a jet lies within $\Delta R = 0.4$ of a photon, the jet is removed. Hadronically decaying τ -leptons close to electrons or muons ($\Delta R < 0.2$) are removed. Any remaining jet within $\Delta R = 0.2$ of a hadronically decaying τ -lepton is removed.

The missing transverse momentum E_T^{miss} is measured as the negative vectorial sum of the transverse momenta of all candidate electrons, photons, hadronically decaying τ -leptons, jets, and muons, plus an additional ‘soft term’ [55]. The ‘soft term’ is constructed from high-quality charged-particle tracks associated with the primary vertex but not with such physics objects. This allows the E_T^{miss} calculation to adopt the best calibration for all the identified particles, while maintaining pile-up independence in

the ‘soft term’. Possible double counting of contributions from reconstructed charged-particle tracks, energy deposits in the calorimeter, and reconstructed muons is avoided by applying a signal ambiguity resolution procedure which rejects already used signals when combining the various E_T^{miss} contributions. A powerful quantity used to discriminate between events with E_T^{miss} arising from poorly reconstructed physics objects and events with E_T^{miss} originating from weakly interacting particles is the E_T^{miss} significance, which is calculated as $|E_T^{\text{miss}}| / [\sigma_L^2 (1 - \rho_{LT}^2)]^{1/2}$, where σ_L is the total standard deviation in the direction longitudinal to the E_T^{miss} corresponding to the summation of the covariance matrices from resolution effects of physics objects and ‘soft term’ entering the E_T^{miss} calculation, ρ_{LT} is the correlation factor of the longitudinal (L) and transverse (T) measurements [56].

The signal region (SR) is defined by requiring events to have a selected leading photon that satisfies the criteria defined in Section 4 and has $E_T^\gamma > 150$ GeV.

The ‘photon pointing’, $|\Delta z_\gamma|$, defined as the separation, measured along the beam line, between the extrapolated origin of the photon and the position of the event’s identified primary vertex is required to be smaller than 250 mm. This criterion suppresses the non-collision background in the data-driven method used to estimate the contribution from events in which jets are misidentified as photons, as described in Section 6.

To ensure that the leading photon and E_T^{miss} do not overlap in the transverse plane, $\Delta\phi(\gamma, E_T^{\text{miss}}) > 0.4$ is required. In order to reduce the number of background events characterised by E_T^{miss} arising from poorly reconstructed physics objects, events are required to have $E_T^{\text{miss}} > 200$ GeV and E_T^{miss} significance > 8.5 . To suppress multi-jet background, events with more than one selected jet or with a jet with $\Delta\phi(\text{jet}, E_T^{\text{miss}}) < 0.4$ are rejected. Events are required to have no candidate electrons, muons or hadronically decaying τ -leptons passing the requirements described in Section 4. This lepton veto mainly rejects W/Z events.

To improve the sensitivity of the analysis, seven SRs are defined corresponding to different E_T^{miss} ranges: four inclusive (SRI1–SRI4) and three exclusive (SRE1–SRE3), their use will be explained in Section 5. Table 2 summarises the SR definitions and the selection criteria described above.

Table 2: Selection criteria for the SRs.

Event cleaning	Detector quality conditions and primary vertex						
Leading γ	$E_T^\gamma > 150$ GeV, $ \eta < 1.37$ or $1.52 < \eta < 2.37$, tight, isolated, $ \Delta z_\gamma < 250$ mm, $\Delta\phi(\gamma, E_T^{\text{miss}}) > 0.4$						
E_T^{miss} significance	> 8.5						
Jets	0 or 1 with $p_T > 30$ GeV, $ \eta < 4.5$ and $\Delta\phi(\text{jet}, E_T^{\text{miss}}) > 0.4$						
Leptons	veto on e, μ and τ						
E_T^{miss} [GeV]	SRI1	SRI2	SRI3	SRI4	SRE1	SRE2	SRE3
	> 200	> 250	> 300	> 375	200–250	250–300	300–375

5 Strategy for background estimation

Backgrounds in the various SRs arise from a number of processes that generate real photons and from events in which one or more energetic jets or electrons are misidentified as photons. The latter are estimated through the use of control samples including jets or electrons, scaled by misidentification rates determined from data. The background where isolated photons are accompanied by significant E_T^{miss} is expected to receive contributions from processes with energetic neutrinos providing genuine E_T^{miss} and from events where the E_T^{miss} arises from instrumental sources or poorly reconstructed physics objects. These contributions are obtained using MC simulations constrained by observed event counts in dedicated control regions (CRs) through the estimation of normalisation factors. Control regions are built by inverting one or more of the selection criteria used to define the SRs, allowing one of the background processes to become dominant but otherwise kinematically similar to the given SR. The contribution of these backgrounds is determined separately for each SR, as defined in Table 2, with a maximum-likelihood fit, referred to as the ‘background-only fit’. This procedure constrains the normalisation of the dominant backgrounds to the observed event yields in the associated CRs, assuming that no signal is present in the CRs and including the background contribution from the misidentification of electrons and jets as photons estimated with data-driven techniques.

The inputs to the fit for each SR include the number of events observed in its associated CRs and the number of events predicted by simulation in the SR and CRs for each background process. The latter are described by Poisson statistics. The systematic uncertainties in the expected values (see Section 6) are included in the fit as nuisance parameters, modelled by Gaussian distributions with widths corresponding to the sizes of the associated uncertainties. Using a simultaneous fit technique allows a straightforward combination of multiple CRs and permits a coherent treatment of the correlation of the systematic uncertainties across the different regions. The product of the various probability distributions forms the likelihood, which the fit maximises by adjusting the background normalisations and the nuisance parameters.

Moreover, a simultaneous fit is performed using the CRs associated to the exclusive SRs plus the inclusive SR corresponding to the highest E_T^{miss} range (SRI4) as shown in Table 2. This allows normalisation factors for the background contributions in each E_T^{miss} bin to be extracted by exploiting the E_T^{miss} shape information. Since the shape of BSM signal models over multiple E_T^{miss} bins is different from the background prediction, this technique, known as ‘simplified shape fit’, permits to better discriminate signal from background and it is used to set exclusion limits in the models studied, if no excess is found in the data.

Four control regions are defined in order to estimate the contributions of the dominant $Z(\rightarrow \nu\nu)\gamma$ background and secondary $W(\rightarrow \ell\nu)\gamma$, $Z(\rightarrow \ell\ell)\gamma$ and γ + jets backgrounds, making use of the maximum-likelihood approach described above.

The Single-Muon CR used to extract the normalisation of the $W(\rightarrow \ell\nu)\gamma$ background in the corresponding signal regions is built by selecting events with the same criteria used for each SR, except for the muon veto. Exactly one selected muon must be present in each event. In addition, since background events characterised by fake E_T^{miss} arising from poorly reconstructed jets are not expected to contribute significantly in the leptonic CRs, the requirement on the E_T^{miss} significance is not applied. For this control region the E_T^{miss} is defined as described in Section 4 but the muon contribution is not taken into account in the computation to emulate the E_T^{miss} distribution in the SR. A similar Single-Electron CR is not needed to constrain the $W(\rightarrow \ell\nu)\gamma$ normalisation because the Single-Muon CR has enough events and is less contaminated by events with fake photons and fake E_T^{miss} .

To constrain the normalisation of both the $Z(\rightarrow \nu\nu)\gamma$ and the $Z(\rightarrow \ell\ell)\gamma$ processes in each SR, two control regions are defined similarly, with the corresponding E_T^{miss} criteria but inverting the lepton veto. In the Z -enriched Two-Muon and Two-Electron CRs, exactly two selected muons/electrons are required in the event, with a dilepton invariant mass $m_{\ell\ell}$ greater than 10 GeV. Similarly to the Single-Muon CR, the E_T^{miss} in the Two-Muon CR and the Two-Electron CR is computed disregarding the contributions from selected muons or electrons, respectively.

The γ + jets background in the SRs consists of events characterised by fake E_T^{miss} originating from jet energy mismeasurements or wrong jet-to-vertex matching amplified by the high pile-up conditions. This QCD background is largely suppressed by the large E_T^{miss} requirement, the jet- E_T^{miss} azimuthal separation and the requirement on the E_T^{miss} significance described in Section 4. The control region used to estimate the normalisation of the residual γ + jets background (Photon-Jet CR) is defined by lowering the E_T^{miss} requirement to the range $85 \text{ GeV} < E_T^{\text{miss}} < 110 \text{ GeV}$ and removing the requirement on the E_T^{miss} significance. In addition, the requirement $\Delta\phi(\gamma, \mathbf{E}_T^{\text{miss}}) < 3.0$ is applied to reduce possible signal contamination, thus providing a region dominated by real photons arising from radiative QCD processes.

The background contribution from events in which jets are misidentified as photons, mainly due to Z + jet or W + jet processes, is estimated using a sideband counting method [57]. This method relies on counting photon candidates in four regions of a two-dimensional plane defined by the amount of transverse energy deposited in cell-clusters within a cone of size $\Delta R = 0.4$ around the photon, excluding the photon cluster itself (isolation), and by the quality of the photon identification criteria (tightness). A photon signal region (region A) is defined by photon candidates that are isolated and satisfy ‘tight’ identification as explained in Section 4. Three background regions are defined in the isolation-tightness plane, consisting of photon candidates which are tight and non-isolated (region B), non-tight and isolated (region C) or non-tight and non-isolated (region D). A non-isolated photon candidate is defined by inverting the requirement in the amount of isolation transverse energy. A photon candidate is classified as non-tight if it fails the tight identification but satisfies a modified set of requirements related to four of the selections associated with the shower-shape variables computed from the energy deposits in the first layer of the EM calorimeter. Complete independence between the photon identification and isolation would imply that the numbers of photon candidates in the four regions (A, B, C, D) satisfy the condition $N^A/N^B = N^C/N^D$. Although this condition is almost fully satisfied, to estimate the number of background candidates in the region A there is a residual correlation that has to be taken into account. Besides, a correction to the method is added in order to consider the effect of contamination by real photon events in the three background regions (B, C, D). MC simulations are used to estimate both the correlation factor and the signal leakage coefficients. This method is then used to evaluate the contribution of jets misidentified as photons in all analysis regions: the SRs and their associated four CRs used for the dominant background.

Electrons or positrons can be misidentified as photons and represent an additional source of background. This contribution is estimated by using a control sample with an electron- E_T^{miss} final state and scaling the event yield by the probability for such an electron to be misreconstructed as a tight photon as determined from a comparison of the rate of Z boson reconstruction in the $e\gamma$ and ee final states. The full Run-2 dataset is used to select $Z \rightarrow ee$ events where the two electrons (actually, one of the two electrons is a positron, but they are referred to as electrons in what follows) in the final state are reconstructed either as an ee pair or as an $e\gamma$ pair. The invariant mass m_{ee} or $m_{e\gamma}$ is required to be consistent with the Z boson mass to within 10 GeV. The yields of Z events are then obtained from a fit to the m_{ee} and $m_{e\gamma}$ distributions, in order to subtract the contamination from misidentified jets in the sample as modelled from the sidebands. The electron-to-photon scale factor, measured as a function of $|\eta|$ and p_T varies between 1.5% and 9%, with larger factors associated with larger values of $|\eta|$, since the misidentification rate depends on the amount of

material in front of the calorimeter. Background estimates are then also made for the various signal regions as well as for their associated four control regions by applying the electron-to-photon misidentification factor to events selected with the same criteria as used in these regions but requiring an electron instead of a photon.

6 Results

The background-only simultaneous fit, described in Section 5, is performed to evaluate the SM background expectations in all regions of the analysis.

Systematic uncertainties in each of the background components are taken into account in the fit as described in Section 5. Uncertainties arising from experimental and theoretical sources are estimated for the $Z(\rightarrow \nu\nu)\gamma$, $W(\rightarrow \ell\nu)\gamma$, $Z(\rightarrow \ell\ell)\gamma$ and γ + jets backgrounds. Experimental uncertainties related to the energy and momentum scale of all the physics objects described in Section 4, and to their identification, reconstruction and isolation efficiencies, are taken into account. The uncertainties of the different physics objects are propagated to the E_T^{miss} calculation, as are the uncertainties in the ‘soft term’ resolution and scale. The uncertainty in the integrated luminosity and pile-up reweighting, reported in Section 3, is also considered.

Theoretical uncertainties affecting the SHERPA MC event generator predictions include an uncertainty in the NLO cross section as well as uncertainties from variations of the QCD factorisation and renormalisation scales [58], in the strong coupling constant α_S , and from the choice of parton distribution functions. The effects of the latter ‘PDF+ α_S ’ uncertainties are calculated using the PDF4LHC prescription [59]. The theoretical uncertainties affect the dominant $W/Z + \gamma$ backgrounds by less than about 7%.

Both the experimental and theoretical systematic uncertainties are considered fully correlated between the different control and signal regions allowing a partial cancellation in the fitting procedure.

Uncertainties in the estimates of jets and electrons misidentified as photons are evaluated with the in situ techniques explained in Section 5. The main systematic uncertainty for the sideband counting method is evaluated by varying the criteria for photon tightness and isolation used to define the four regions (A,B,C,D). Uncertainties related to signal leakage were considered in order to account for differences between $W\gamma$ and $Z\gamma$ samples. The sources of systematic uncertainties related to the methodology used to estimate the contribution of electrons misidentified as photons are the choice of invariant mass window, the background subtraction and the energy scale of the misidentified photons; the last of these has the dominant effect.

Table 3 shows the observed number of events and the expected SM background contribution in SR11, which is the most inclusive SR and covers $E_T^{\text{miss}} > 200$ GeV, and in its associated CRs: three leptonic CRs and the Photon–Jet CR. For the SM predictions, both the statistical and systematic uncertainties are included.

The observed number of events and the expected SM background contribution resulting from the background-only fit are reported in Table 4 for each inclusive SR. The values of the normalisation factors for $W/Z + \gamma$ and γ + jets backgrounds ($k_{Z\gamma}$, $k_{W\gamma}$, $k_{\gamma+\text{jets}}$) are also shown. A summary of the data event yields and the background expectations broken down into their contributing SM sources in the inclusive regions is shown in Figure 2, which also presents the significance of the difference between data and the SM background prediction, calculated with the method described in Ref. [60].

Results from the ‘simplified shape fit’ described in Section 5, are shown in Table 5 together with the fitted normalisation factors. The fit is performed simultaneously in the CRs associated with each of the exclusive

SRs and with the inclusive SR with the highest E_T^{miss} range (SRI4). The Photon–Jet CR is common to all SRs as it corresponds to a lower E_T^{miss} range, while the leptonic CRs span the same E_T^{miss} ranges of the SRs involved. A summary of the data event yields and the SM expectations in all the regions used for the ‘simplified shape fit’ to extract the model-dependent limits is shown in Figure 3.

The distributions of E_T^{miss} in data and for the expected SM background obtained after performing the ‘simplified shape fit’ are shown in Figure 4 for the SRs and the leptonic CRs. The distributions of the expected SM backgrounds include the $W/Z + \gamma$ and $\gamma + \text{jets}$ backgrounds normalised with the corresponding k -factors reported in Table 5 and the data-driven estimates for the backgrounds produced by events in which electrons or jets are misidentified as photons.

Table 3: Observed and expected yields from SM backgrounds in SRI1 corresponding to $E_T^{\text{miss}} > 200$ GeV and in its associated four CRs. The expected event yields from SM processes are obtained from the background-only fit, described in Section 5. The uncertainty includes both the statistical and systematic uncertainties. The individual uncertainties can be correlated and do not necessarily add in quadrature to equal the total background uncertainty.

	SRI1	1 Muon CR	2 Muon CR	2 Electron CR	Photon–Jet CR
Observed events	5293	1991	473	378	21991
Expected SM events	5350 ± 190	1991 ± 45	475 ± 18	376 ± 15	21990 ± 150
$Z(\rightarrow \nu\nu)\gamma$	3410 ± 150	1.721 ± 0.094	–	–	372 ± 42
$W(\rightarrow \ell\nu)\gamma$	680 ± 33	1589 ± 68	0.40 ± 0.11	0.81 ± 0.18	530 ± 37
$Z(\rightarrow \ell\ell)\gamma$	48.4 ± 2.9	131.5 ± 8.1	457 ± 19	361 ± 16	35.9 ± 4.8
$\gamma + \text{jets}$	103 ± 41	12.9 ± 7.0	–	–	19610 ± 290
Fake photons from e	860 ± 80	63.9 ± 6.0	1.91 ± 0.31	0.54 ± 0.22	694 ± 65
Fake photons from jets	249 ± 54	192 ± 49	15.3 ± 8.6	13.7 ± 8.5	750 ± 230

Table 6 shows the total relative uncertainty, including systematic and statistical contributions, in the expected SM background yield after the background-only fit for inclusive SRs and after the ‘simplified shape fit’ for exclusive SRs. This total uncertainty ranges from 3.5% to 9.5% depending on the SR. The purely statistical uncertainty is dominant, varying from 2.4% to 8.5% and driven by the statistical precision from the Two-Muon and Two-Electron CRs adopted to constrain the normalisation of the leading $Z(\rightarrow \nu\nu)\gamma$ background.

The relative impact of each source of systematic uncertainty on the total SM background estimates is summarised in Table 6. A large experimental uncertainty is related to jets misidentified as photons and varies from 1.4% to 4.1%. The impact of the uncertainty in the jet energy scale and resolution varies from 1.6% to 2.7%. The uncertainty related to electrons misidentified as photons varies between about 2% and 2.3%. Other experimental systematic uncertainties related to electrons, photons, muons and the E_T^{miss} ‘soft term’ have a relative impact below 1.5% in all SRs. Theoretical systematic uncertainties in the $W/Z + \gamma$ and $\gamma + \text{jets}$ MC estimates have an impact of 0.5% in all SRs.

In all SRs of the analysis, the observations and background predictions are found to be compatible within the uncertainties.

Table 4: Observed and expected yields from SM backgrounds in all inclusive SRs. The expected event yields from SM processes are obtained from the background-only fit, described in Section 5, in each inclusive SR. The normalisation factors obtained from the fit are also shown. The uncertainty includes both the statistical and systematic uncertainties. The individual uncertainties can be correlated and do not necessarily add in quadrature to equal the total background uncertainty.

	SRI1	SRI2	SRI3	SRI4
Observed events	5293	2270	1106	427
Expected SM events	5350 ± 190	2320 ± 110	1134 ± 71	448 ± 42
$Z(\rightarrow \nu\nu)\gamma$	3410 ± 150	1540 ± 95	779 ± 65	306 ± 40
$W(\rightarrow \ell\nu)\gamma$	680 ± 33	285 ± 22	128 ± 12	56.8 ± 7.1
$Z(\rightarrow \ell\ell)\gamma$	48.4 ± 2.9	16.4 ± 1.2	7.01 ± 0.65	2.69 ± 0.37
γ + jets	103 ± 41	17.0 ± 7.0	5.5 ± 2.2	2.9 ± 1.2
Fake photons from e	860 ± 80	349 ± 32	161 ± 15	59.7 ± 5.6
Fake photons from jets	249 ± 54	114 ± 40	54 ± 20	20 ± 11
$k_{Z\gamma}$	0.93 ± 0.07	0.88 ± 0.07	0.88 ± 0.09	0.86 ± 0.12
$k_{W\gamma}$	0.81 ± 0.08	0.80 ± 0.09	0.78 ± 0.10	0.85 ± 0.13
$k_{\gamma+\text{jets}}$	0.82 ± 0.21	0.82 ± 0.20	0.81 ± 0.19	0.82 ± 0.21

Table 5: Observed and expected yields from SM backgrounds obtained from the ‘simplified shape fit’ described in Section 5. The normalisation factors obtained from the fit are also shown. The uncertainty includes both the statistical and systematic uncertainties. The individual uncertainties can be correlated and do not necessarily add in quadrature to equal the total background uncertainty.

	SRE1	SRE2	SRE3	SRI4
Observed events	3023	1164	679	427
Expected SM events	3070 ± 130	1182 ± 75	680 ± 53	448 ± 42
$Z(\rightarrow \nu\nu)\gamma$	1910 ± 110	758 ± 65	468 ± 49	306 ± 40
$W(\rightarrow \ell\nu)\gamma$	394 ± 22	159 ± 15	71.0 ± 8.2	56.7 ± 7.1
$Z(\rightarrow \ell\ell)\gamma$	33.2 ± 2.4	9.32 ± 0.89	4.26 ± 0.48	2.69 ± 0.37
γ + jets	87 ± 35	11.9 ± 4.8	2.7 ± 1.1	3.0 ± 1.2
Fake photons from e	511 ± 48	188 ± 18	100.9 ± 9.5	59.7 ± 5.6
Fake photons from jets	136 ± 28	56 ± 29	33 ± 16	20 ± 11
$k_{Z\gamma}$	0.99 ± 0.08	0.89 ± 0.09	0.90 ± 0.11	0.86 ± 0.12
$k_{W\gamma}$	0.81 ± 0.09	0.84 ± 0.11	0.74 ± 0.11	0.85 ± 0.13
$k_{\gamma+\text{jets}}$		0.82 ± 0.21		

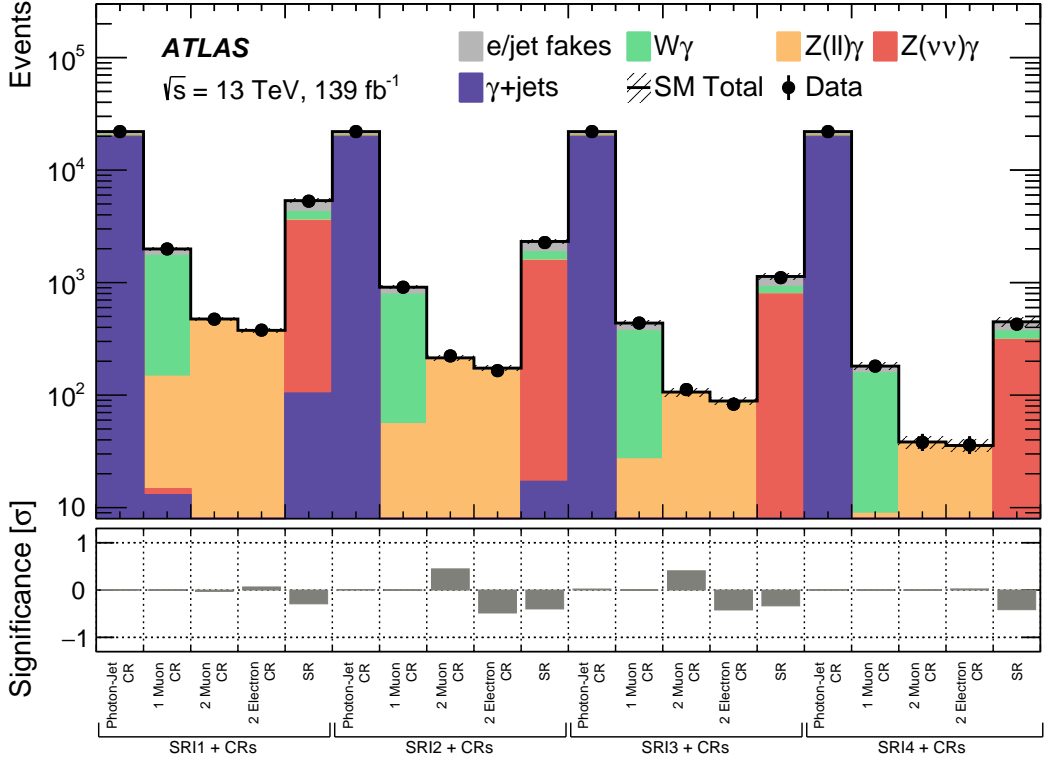


Figure 2: Data event yields and the SM predictions from separate background-only fits in each inclusive SR and its associated CRs. The uncertainties in the expected numbers of events are the combined statistical and systematic uncertainties. The lower panel shows the significance of the difference between data and background prediction.

Table 6: Summary of the uncertainties (%) in the background estimate for inclusive SRs after the background-only fit and for exclusive SRs after the ‘simplified shape fit’. The individual uncertainties can be correlated and do not necessarily add in quadrature to equal the total background uncertainty.

	SRI1	SRI2	SRI3	SRI4	SRE1	SRE2	SRE3
	[%]	[%]	[%]	[%]	[%]	[%]	[%]
Total (statistical+systematic) uncertainty	3.5	4.8	6.2	9.5	4.3	6.3	7.8
Statistical uncertainty	2.4	3.6	5.3	8.5	3.3	5.0	6.7
Fake photons from jets (Section 5)	1.4	2.5	2.8	4.1	1.4	3.6	3.7
Jet energy scale/resol [52]	1.6	2.2	2.5	2.7	2.2	2.2	2.3
Fake photons from electrons (Section 5)	2.1	2.0	2.0	2.0	2.3	2.3	2.1
Electrons reco/id/isolation eff. [47]	1.0	1.2	1.3	1.4	1.0	1.0	1.2
Electron/photon energy scale/resol [47]	0.8	0.6	0.7	0.9	0.9	0.9	0.6
Muon reco/id/isolation eff. [48]	0.7	0.8	0.9	1.0	0.6	0.7	0.9
E_T^{miss} soft term scale/resolution [55]	0.1	0.4	0.7	0.9	0.5	0.2	0.5
Theoretical W/Z + γ , γ + jets	0.5	0.5	0.5	0.5	0.5	0.5	0.5
$\langle\mu\rangle$ reweighting in MC simulation	0.3	0.2	0.2	0.2	0.3	0.2	0.2

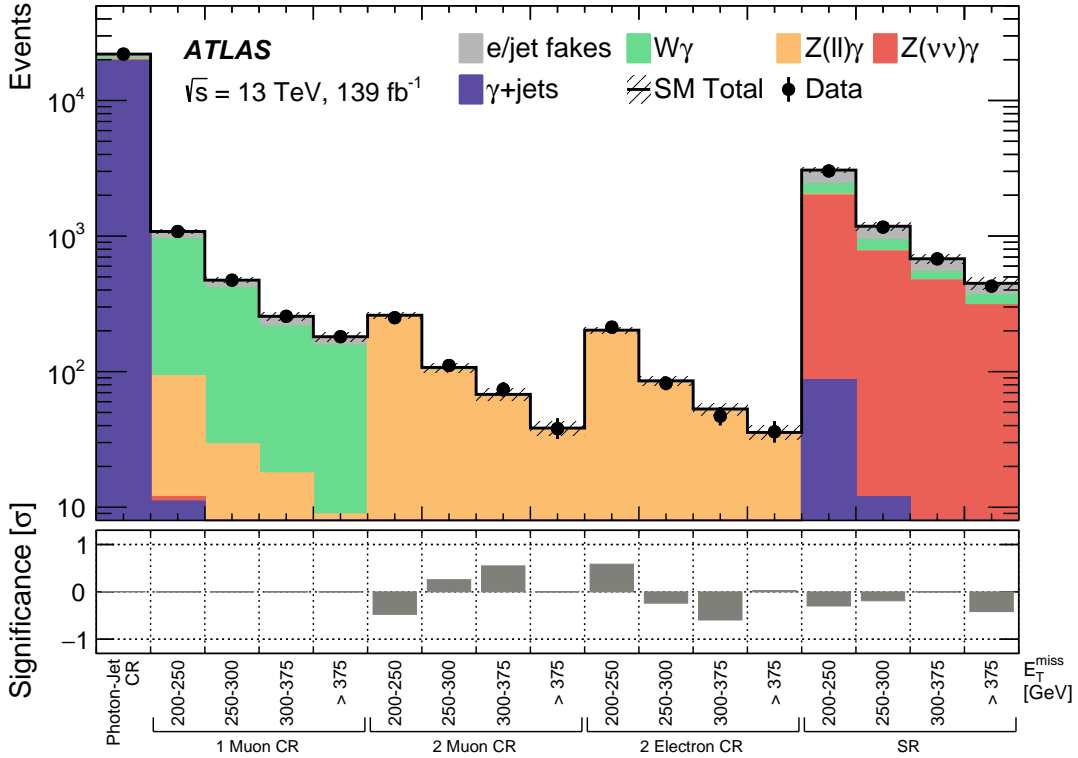


Figure 3: Data event yields and the SM predictions from the ‘simplified shape fit’ in all exclusive SRs plus the inclusive SR with the highest E_T^{miss} range (SRI4) and their associated CRs. The uncertainties in the expected numbers of events are the combined statistical and systematic uncertainties. The lower panel shows the significance of the difference between data and background prediction.

7 Interpretations

For each SR, exclusion upper limits at the 95% confidence level (CL) are set on the number of events from any scenario of physics beyond the SM that would produce an excess in events with a $\gamma + E_T^{\text{miss}}$ final state as presented in this paper. These limits are based on the profile-likelihood-ratio test statistic [61] and CL_s prescriptions [62], evaluated using the asymptotic approximation [63]. A simultaneous fit is performed including both the SR and its associated CRs to obtain the model-independent upper limits on the observed number of such events. Normalising the upper limits on the number of signal events by the integrated luminosity of the data sample provides upper limits on the visible BSM cross section $\sigma \times A \times \epsilon$. Here σ is the production cross section for the BSM signal, and $A \times \epsilon$ is the product of the acceptance (A), defined to be the fraction of events whose underlying objects pass all kinematic selections at the particle level, and the efficiency (ϵ), defined to be the fraction of those events that would be observed after reconstruction in the detector. The expected (in absence of new physics) and observed 95% CL limits on $\sigma \times A \times \epsilon = N^{\text{lim}} / \int L dt$ are shown in Table 7 together with the observed upper limits on the number of events.

In order to provide additional constraints on BSM physics, which can be reinterpreted in terms of the results from this paper, a fiducial region is defined at the particle level with the same selection criteria as in the SRs. The E_T^{miss} computation at particle level is given by the vector sum of the transverse momenta of

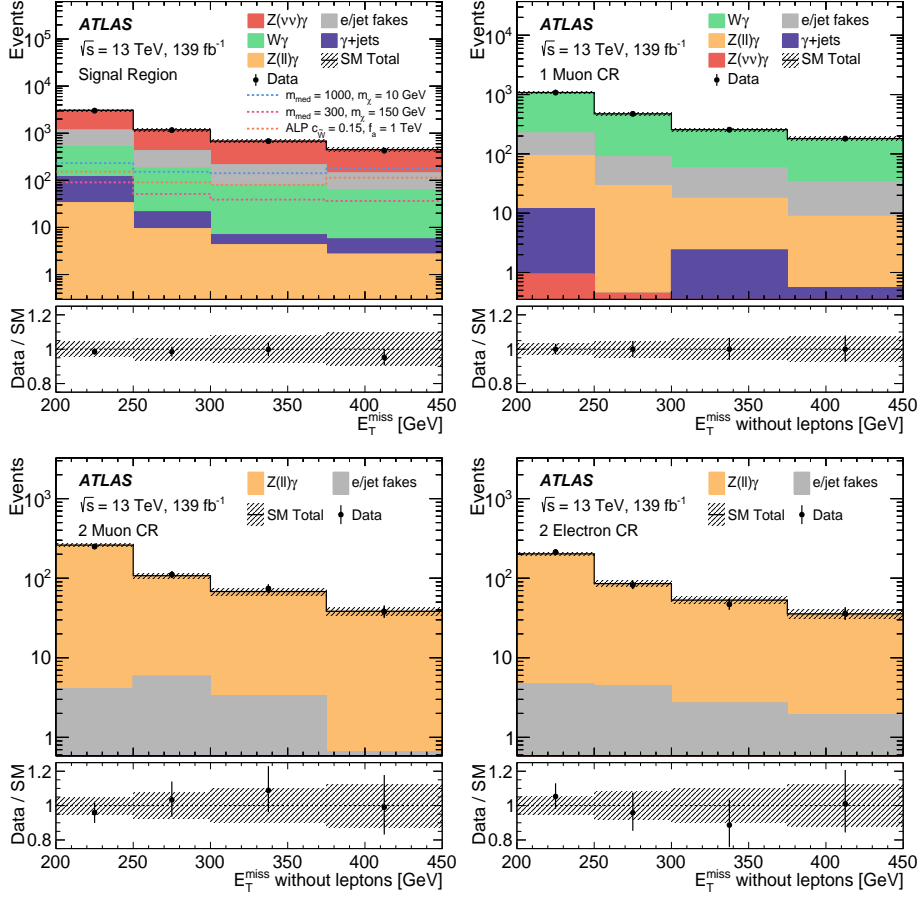


Figure 4: Distribution of E_T^{miss} in data and for the expected SM background in the SRs and CRs after performing the ‘simplified shape fit’: SRs (top left), Single-Muon CR (top right), Two-Muon CR (bottom left) and Two-Electron CR (bottom right). Overflows are included in the fourth bin of each distribution. The E_T^{miss} calculation in these CRs does not include the muon or electron contribution. The error bars are statistical, and the dashed band includes statistical and systematic uncertainties determined by the fit. The expectations for the simplified model for two different values of m_χ and m_{med} , and with $g_q = 0.25$ and $g_\chi = 1.0$ and for the ALP model are also shown. The lower panel shows the ratio of data to expected background event yields.

Table 7: The observed and expected upper limits at 95% confidence level on the visible cross section $\sigma \times A \times \epsilon$ from all signal regions. The observed limits on the number of events are also reported as well as the fiducial efficiencies, ϵ .

Signal region	$(\sigma \times A \times \epsilon)_{\text{obs}}^{95}$ [fb]	$(\sigma \times A \times \epsilon)_{\text{exp}}^{95}$ [fb]	N_{obs}^{95}	ϵ [%]
SRI1	2.45	$2.82^{+1.08}_{-0.78}$	340	76
SRI2	1.42	$1.68^{+0.63}_{-0.46}$	198	74
SRI3	0.93	$1.07^{+0.40}_{-0.29}$	129	72
SRI4	0.53	$0.63^{+0.23}_{-0.17}$	74	67
SRE1	1.80	$2.03^{+0.77}_{-0.56}$	250	75
SRE2	1.04	$1.15^{+0.43}_{-0.31}$	145	75
SRE3	0.79	$0.82^{+0.31}_{-0.22}$	109	71

all non-interacting particles. The $E_{\text{T}}^{\text{miss}}$ significance requirement is not applied, because the object-based definition is not reproducible at particle level, but the impact of this selection on signal events is treated as negligible.

Given the fiducial acceptance (A) for a particular model and the fiducial efficiency (ϵ), calculated as the ratio of the number of events passing the signal region selection at reconstruction level to the number of events passing the fiducial selection at the particle level, it is straightforward to convert the visible cross-section limit into fiducial cross-section ($\sigma \times A$) limits. Using the DM simplified model, described in Section 3, the fiducial efficiency for each SR is calculated and the lowest values, shown in Table 7, can be used to set the fiducial cross-section limit in a conservative way.

Exclusion limits for the BSM models studied are obtained from the ‘simplified shape fit’ described in Section 5. A fit of the background plus the signal model is performed, where the signal component is allowed to populate both the SR and CRs, with the signal strength being the freely floating signal normalisation factor. A specific signal is excluded if the upper limit on the signal strength is less than unity.

Systematic uncertainties in the signal predictions from the simplified DM and ALP models, described in Section 3, are included in the fit. The sources of experimental uncertainties are related to the physics objects as described for the main SM backgrounds. Theoretical uncertainties include uncertainties in the NLO cross section due to QCD factorisation and renormalisation scales [58] and the choice of parton distribution functions. These uncertainties are below 5% for acceptance and cross section, for different DM signals. Uncertainties in initial- and final-state radiation due to the choice of parton shower parameters used with PYTHIA 8.2 are estimated by generating MC samples with the alternative tunes described in Ref. [30], and are less than 10%. The same sources of uncertainty are considered for ALP signals and the largest uncertainty is approximately 20%, which comes mainly from QCD factorisation and renormalisation scales.

The results are presented for simplified DM models, described in Section 3, with the exchange of an axial-vector or a vector mediator in the s -channel for different couplings to quarks and leptons: $g_q = 0.25$, $g_\ell = 0$ and $g_q = 0.1$, $g_\ell = 0.1$ (0.01) [22].

As it was verified that the choice of mediator and couplings only affects the cross section and not the acceptance of the signal, the cross-section predictions for an axial-vector mediator are rescaled in order to obtain the results for a vector mediator and for different couplings. Observed and expected 95% CL exclusion contours in the m_χ - m_{med} plane are shown in Figure 5. The region of the plane under the limit curves is excluded. The band around the expected contour shows the $\pm 1\sigma$ variations including all uncertainties described in Section 6 except theoretical uncertainties affecting the signal cross section. Those uncertainties are instead indicated as dotted lines around the observed limit. The line corresponding to the DM thermal relic abundance measured by the Planck Collaboration [64] is also indicated [22]. The region not allowed due to perturbative unitarity violation is to the left of the line defined by $m_\chi = \sqrt{\pi/2}m_{\text{med}}$ [65]. The results of the search are summarised in Table 8, where the values for m_{med} and m_χ correspond to the maximum excluded values of the mediator masses and DM masses. These limits are more stringent than the limits obtained from the previous search using 36.1 fb^{-1} [9], which excluded dark-matter candidates with masses up to 340(480) GeV for axial-vector (vector) mediators, while the maximum excluded mass of the mediator was 1200 GeV for the same DM models.

Table 8: Observed limits at 95% CL on m_{med} and m_χ for the mediators and couplings to quarks, DM particles, and leptons considered for each model. The values reported for m_{med} and m_χ correspond to the maximum excluded values of mediator masses and DM masses in the search.

Mediator	g_q	g_χ	g_ℓ	m_{med} [GeV]	m_χ [GeV]
Axial-vector	0.25	1	0	1460	415
Axial-vector	0.1	1	0.1	920	280
Vector	0.25	1	0	1470	580
Vector	0.1	1	0.01	950	400

To show the complementarity with DM direct detection searches, the contours in the m_χ - m_{med} plane obtained for a specific choice of mediator and couplings can be directly translated into bounds on the χ -nucleon scattering cross section following the procedure described in Ref. [66]. Figure 6 (top left) shows the 90% CL exclusion limits on the χ -proton spin-dependent (SD) scattering cross section versus m_χ in the axial-vector model with couplings $g_q = 0.25$, $g_\chi = 1$ and $g_\ell = 0$. In Figure 6 (top right), 90% CL exclusion limits on the χ -neutron SD scattering cross section versus m_χ are shown for the same model. A comparison with the results from direct DM searches [67–72] is also shown. The search probes complementary regions with respect to direct DM searches in the full parameter space, providing greater sensitivity for m_χ values below 440 GeV for these models and parameter values. Figure 6 (bottom) shows the 90% CL exclusion limits on the χ -nucleon spin-independent (SI) scattering cross section versus m_χ for the vector model with couplings $g_q = 0.25$, $g_\chi = 1$ and $g_\ell = 0$. With the exception of small m_χ masses, lower than about 3 GeV, direct detection searches [73–76] provide stronger limits for these models and parameter values.

The results are also interpreted in terms of limits on the parameters of the ALP model described in Section 3, obtained for the first time using the full Run-2 dataset from events with a $\gamma + E_{\text{T}}^{\text{miss}}$ final state. Figure 7 shows the expected and observed limits at 95% CL on the coefficient $c_{\tilde{W}}$ as a function of the effective scale f_a for an ALP mass of 1 MeV. The limits are obtained by using the cross section to rescale the result obtained for the point generated with $c_{\tilde{W}} = 1$, $f_a = 1 \text{ TeV}$ and $m_a = 1 \text{ MeV}$. The limits on $c_{\tilde{W}}$ increase linearly with f_a . For $f_a = 1000 \text{ GeV}$ the couplings $c_{\tilde{W}} > 0.12$ (0.13) are excluded according to the observed (expected) limit. The ALP model is an EFT and it becomes invalid for $\hat{s} > f_a^2$ (\hat{s} corresponds to the invariant mass-squared of the partonic collision). The validity of the limit is verified by applying a suppression factor f_a^4/\hat{s}^2 to the events outside of the region of validity; this truncation has an almost

negligible impact for $f_a > 1000$ GeV. The largest change in the limit is 1% for $f_a = 1$ TeV, where the truncation impact is largest.

Since the signal cross section and width depend on the ratio of the operator coefficient to the effective scale, the limit is also computed for $c_{\tilde{W}}/f_a$ as a function of ALP mass in the range from 1 MeV to 1 GeV, where the acceptance is constant. The result obtained for the observed (expected) upper limit is $c_{\tilde{W}}/f_a = 1.2 \times 10^{-4}$ (1.3×10^{-4}) GeV^{-1} , constant with the ALP mass in the considered range. This limit constrains the coupling of the ALP to the electroweak gauge bosons, $|g_{aZ\gamma}| < 0.51 \text{ TeV}^{-1}$ assuming $g_{a\gamma\gamma} = 0$. In addition, using the relationship [8]:

$$\Gamma(Z \rightarrow a\gamma) = \frac{m_Z^3}{384\pi} g_{aZ\gamma}^2 \left(1 - \frac{m_a^2}{m_Z^2}\right)^3,$$

and assuming $m_a = 1$ MeV, a contribution to the Z boson width of $\Gamma(Z \rightarrow a\gamma) < 0.17$ MeV at 95% CL is estimated. The most stringent limit is set from LEP, $\Gamma(Z \rightarrow X\gamma) < 2.5$ keV for photons with energy above 30 GeV in e^+e^- annihilation events at the Z resonance can be inferred from Ref. [77], where X refers to a stable, weakly interacting particle.

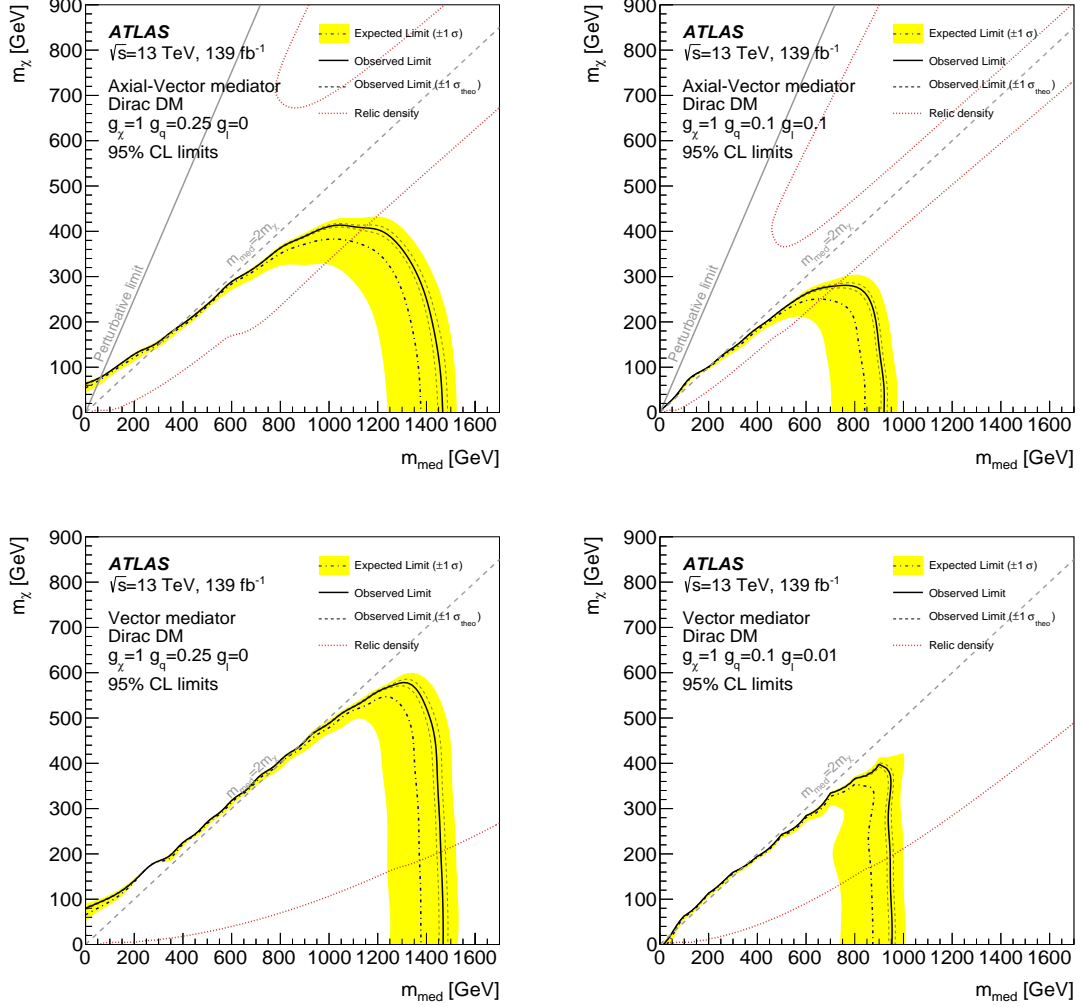


Figure 5: The observed (solid line) and expected (dot-dashed line) 95% CL exclusion contours in the m_χ – m_{med} plane for a simplified DM model involving an axial-vector mediator with couplings $g_\chi = 1$, $g_q = 0.25$ and $g_\ell = 0$ (top left) and $g_\chi = 1$, $g_q = 0.1$ and $g_\ell = 0.1$ (top right). The same is shown for a vector mediator with couplings $g_\chi = 1$, $g_q = 0.25$ and $g_\ell = 0$ (bottom left) and $g_\chi = 1$, $g_q = 0.1$ and $g_\ell = 0.01$ (bottom right). The area under the limit curve is excluded. The region to the left of the line defined by $m_\chi = \sqrt{\pi/2} m_{\text{med}}$ is excluded by the perturbative limit which is relevant for axial-vector mediators. The relic density curve [64] is also shown. The area below the relic density curve in the on-shell region (or above in the off-shell region in the axial-vector mediator case) corresponds to a predicted DM overabundance.

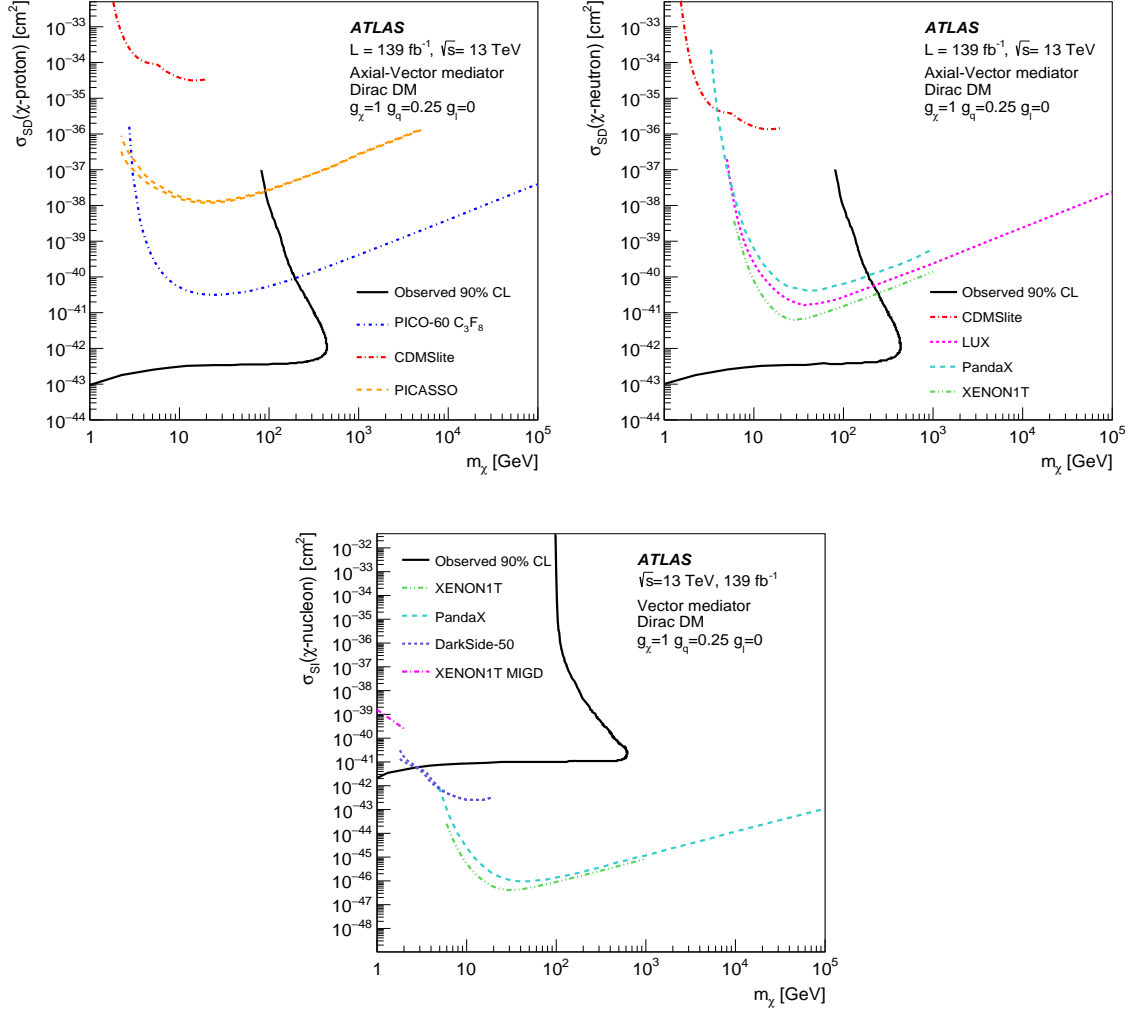


Figure 6: The 90% CL exclusion limit on the χ -proton spin-dependent scattering cross section (top left) and on the χ -neutron spin-dependent scattering cross section (top right) in an axial-vector model with couplings $g_\chi = 1$, $g_q = 0.25$ and $g_\ell = 0$ as a function of the dark-matter mass m_χ . The 90% CL exclusion limit is displayed only in the regime where the theory is perturbative. Results at 90% CL from direct DM searches [67–72] are also shown. The 90% CL exclusion limit on the χ -nucleon spin-independent scattering cross section (bottom) in a vector model with couplings $g_\chi = 1$, $g_q = 0.25$ and $g_\ell = 0$ as a function of the dark-matter mass m_χ . Results at 90% CL from direct DM searches [73–76] are also shown.

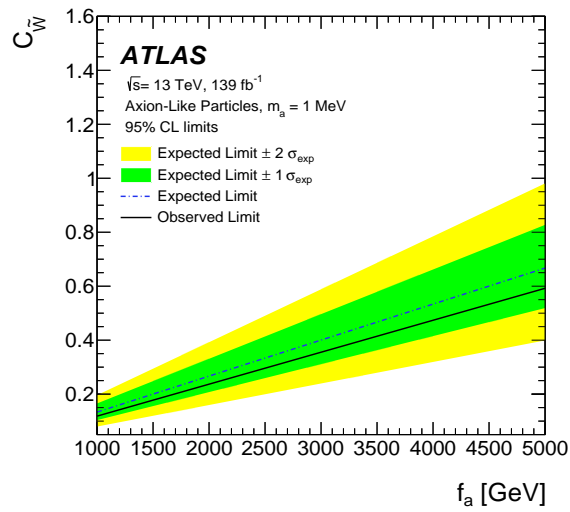


Figure 7: Observed (solid line) and expected (dot-dashed line) exclusions at 95% CL on the coupling $c_{\tilde{W}}$ as a function of the effective scale f_a for an ALP mass of 1 MeV. The region above the limit lines is excluded.

8 Conclusion

A search for an excess of events in a $\gamma + E_{\text{T}}^{\text{miss}}$ final state over the SM prediction is performed using 139 fb^{-1} of proton–proton data collected by the ATLAS experiment at the LHC at a centre-of-mass energy of $\sqrt{s} = 13 \text{ TeV}$. Events with an isolated photon with transverse energy above 150 GeV in association with $E_{\text{T}}^{\text{miss}} > 200 \text{ GeV}$ are selected. Several signal regions (inclusive and exclusive) are defined for different $E_{\text{T}}^{\text{miss}}$ ranges to improve the sensitivity, and control regions are adopted to estimate the main backgrounds, decreasing the impact of the experimental and theoretical uncertainties with a data-driven approach. The observed data are consistent with the SM expectation. Model-independent 95% CL upper limits are set on the visible cross section for events beyond the Standard Model ranging from 2.45 to 0.5 fb in signal regions corresponding to different $E_{\text{T}}^{\text{miss}}$ ranges. Model-dependent 95% CL limits are placed on parameters of simplified dark-matter models. Dark-matter candidates are excluded for masses up to 415 (580) GeV for axial-vector (vector) mediators, while the maximum excluded mass of an axial-vector (vector) mediator is 1460 (1470) GeV. The results are also translated into limits on the parameters of the axion-like particle (ALP) model. The 95% CL limits on the coupling $c_{\tilde{W}}$ are computed as a function of the effective scale f_a for an ALP mass of 1 MeV. For $f_a = 1 \text{ TeV}$, values of the couplings $c_{\tilde{W}} > 0.12$ (0.13) are excluded according to the observed (expected) limit. The observed limit constrains the coupling of the ALP to the electroweak gauge bosons to be $|g_{aZ\gamma}| < 0.51 \text{ TeV}^{-1}$, assuming $g_{a\gamma\gamma} = 0$.

The ATLAS Collaboration

G. Aad¹⁰², B. Abbott¹²⁸, D.C. Abbott¹⁰³, A. Abed Abud³⁶, K. Abeling⁵³, D.K. Abhayasinghe⁹⁴, S.H. Abidi¹⁶⁷, O.S. AbouZeid⁴⁰, N.L. Abraham¹⁵⁶, H. Abramowicz¹⁶¹, H. Abreu¹⁶⁰, Y. Abulaiti⁶, B.S. Acharya^{67a,67b,n}, B. Achkar⁵³, L. Adam¹⁰⁰, C. Adam Bourdarios⁵, L. Adamczyk^{84a}, L. Adamek¹⁶⁷, J. Adelman¹²¹, M. Adersberger¹¹⁴, A. Adiguzel^{12c,ae}, S. Adorni⁵⁴, T. Adye¹⁴³, A.A. Affolder¹⁴⁵, Y. Afik¹⁶⁰, C. Agapopoulou⁶⁵, M.N. Agaras³⁸, A. Aggarwal¹¹⁹, C. Agheorghiesei^{27c}, J.A. Aguilar-Saavedra^{139f,139a,ad}, A. Ahmad³⁶, F. Ahmadov⁸⁰, W.S. Ahmed¹⁰⁴, X. Ai¹⁸, G. Aielli^{74a,74b}, S. Akatsuka⁸⁶, M. Akbiyik¹⁰⁰, T.P.A. Åkesson⁹⁷, E. Akilli⁵⁴, A.V. Akimov¹¹¹, K. Al Houry⁶⁵, G.L. Alberghi^{23b,23a}, J. Albert¹⁷⁶, M.J. Alconada Verzini¹⁶¹, S. Alderweireldt³⁶, M. Aleksa³⁶, I.N. Aleksandrov⁸⁰, C. Alexa^{27b}, T. Alexopoulos¹⁰, A. Alfonsi¹²⁰, F. Alfonsi^{23b,23a}, M. Alhroob¹²⁸, B. Ali¹⁴¹, S. Ali¹⁵⁸, M. Aliev¹⁶⁶, G. Alimonti^{69a}, C. Allaire³⁶, B.M.M. Allbrooke¹⁵⁶, B.W. Allen¹³¹, P.P. Allport²¹, A. Aloisio^{70a,70b}, F. Alonso⁸⁹, C. Alpigiani¹⁴⁸, E. Alunno Camelia^{74a,74b}, M. Alvarez Estevez⁹⁹, M.G. Alviggi^{70a,70b}, Y. Amaral Coutinho^{81b}, A. Ambler¹⁰⁴, L. Ambroz¹³⁴, C. Amelung²⁶, D. Amidei¹⁰⁶, S.P. Amor Dos Santos^{139a}, S. Amoroso⁴⁶, C.S. Amrouche⁵⁴, F. An⁷⁹, C. Anastopoulos¹⁴⁹, N. Andari¹⁴⁴, T. Andeen¹¹, J.K. Anders²⁰, S.Y. Andrean^{45a,45b}, A. Andreazza^{69a,69b}, V. Andrei^{61a}, C.R. Anelli¹⁷⁶, S. Angelidakis⁹, A. Angerami³⁹, A.V. Anisenkov^{122b,122a}, A. Annovi^{72a}, C. Antel⁵⁴, M.T. Anthony¹⁴⁹, E. Antipov¹²⁹, M. Antonelli⁵¹, D.J.A. Antrim¹⁷¹, F. Anulli^{73a}, M. Aoki⁸², J.A. Aparisi Pozo¹⁷⁴, M.A. Aparo¹⁵⁶, L. Aperio Bella⁴⁶, N. Aranzabal³⁶, V. Araujo Ferraz^{81a}, R. Araujo Pereira^{81b}, C. Arcangeletti⁵¹, A.T.H. Arce⁴⁹, F.A. Arduh⁸⁹, J-F. Arguin¹¹⁰, S. Argyropoulos⁵², J.-H. Arling⁴⁶, A.J. Armbruster³⁶, A. Armstrong¹⁷¹, O. Arnaez¹⁶⁷, H. Arnold¹²⁰, Z.P. Arrubarrena Tame¹¹⁴, G. Artoni¹³⁴, H. Asada¹¹⁷, K. Asai¹²⁶, S. Asai¹⁶³, T. Asawatavonvanich¹⁶⁵, N. Asbah⁵⁹, E.M. Asimakopoulou¹⁷², L. Asquith¹⁵⁶, J. Assahsah^{35e}, K. Assamagan²⁹, R. Astalos^{28a}, R.J. Atkin^{33a}, M. Atkinson¹⁷³, N.B. Atlay¹⁹, H. Atmani⁶⁵, K. Augsten¹⁴¹, V.A. Austrup¹⁸², G. Avolio³⁶, M.K. Ayoub^{15a}, G. Azeulos^{110,am}, H. Bachacou¹⁴⁴, K. Bachas¹⁶², F. Backman^{45a,45b}, P. Bagnaia^{73a,73b}, M. Bahmani⁸⁵, H. Bahrasemani¹⁵², A.J. Bailey¹⁷⁴, V.R. Bailey¹⁷³, J.T. Baines¹⁴³, C. Bakalis¹⁰, O.K. Baker¹⁸³, P.J. Bakker¹²⁰, E. Bakos¹⁶, D. Bakshi Gupta⁸, S. Balaji¹⁵⁷, R. Balasubramanian¹²⁰, E.M. Baldin^{122b,122a}, P. Balek¹⁸⁰, F. Balli¹⁴⁴, W.K. Balunas¹³⁴, J. Balz¹⁰⁰, E. Banas⁸⁵, M. Bandieramonte¹³⁸, A. Bandyopadhyay²⁴, Sw. Banerjee^{181,i}, L. Barak¹⁶¹, W.M. Barbe³⁸, E.L. Barberio¹⁰⁵, D. Barberis^{55b,55a}, M. Barbero¹⁰², G. Barbour⁹⁵, T. Barillari¹¹⁵, M-S. Barisits³⁶, J. Barkeloo¹³¹, T. Barklow¹⁵³, R. Barnea¹⁶⁰, B.M. Barnett¹⁴³, R.M. Barnett¹⁸, Z. Barnovska-Blenessy^{60a}, A. Baroncelli^{60a}, G. Barone²⁹, A.J. Barr¹³⁴, L. Barranco Navarro^{45a,45b}, F. Barreiro⁹⁹, J. Barreiro Guimarães da Costa^{15a}, U. Barron¹⁶¹, S. Barsov¹³⁷, F. Bartels^{61a}, R. Bartoldus¹⁵³, G. Bartolini¹⁰², A.E. Barton⁹⁰, P. Bartos^{28a}, A. Basalae⁴⁶, A. Basan¹⁰⁰, A. Bassalat^{65,aj}, M.J. Basso¹⁶⁷, R.L. Bates⁵⁷, S. Batlamous^{35f}, J.R. Batley³², B. Batool¹⁵¹, M. Battaglia¹⁴⁵, M. Baue^{73a,73b}, F. Bauer¹⁴⁴, P. Bauer²⁴, H.S. Bawa³¹, A. Bayirli^{12c}, J.B. Beacham⁴⁹, T. Beau¹³⁵, P.H. Beauchemin¹⁷⁰, F. Becherer⁵², P. Bechtel²⁴, H.C. Beck⁵³, H.P. Beck^{20,p}, K. Becker¹⁷⁸, C. Becot⁴⁶, A. Beddall^{12d}, A.J. Beddall^{12a}, V.A. Bednyakov⁸⁰, M. Bedognetti¹²⁰, C.P. Bee¹⁵⁵, T.A. Beermann¹⁸², M. Begalli^{81b}, M. Begel²⁹, A. Behera¹⁵⁵, J.K. Behr⁴⁶, F. Beisiegel²⁴, M. Belfkir⁵, A.S. Bell⁹⁵, G. Bella¹⁶¹, L. Bellagamba^{23b}, A. Bellerive³⁴, P. Bellos⁹, K. Beloborodov^{122b,122a}, K. Belotskiy¹¹², N.L. Belyaev¹¹², D. Benchekroun^{35a}, N. Benekos¹⁰, Y. Benhammou¹⁶¹, D.P. Benjamin⁶, M. Benoit²⁹, J.R. Bensinger²⁶, S. Bentvelsen¹²⁰, L. Beresford¹³⁴, M. Beretta⁵¹, D. Berge¹⁹, E. Bergeaas Kuutmann¹⁷², N. Berger⁵, B. Bergmann¹⁴¹, L.J. Bergsten²⁶, J. Beringer¹⁸, S. Berlendis⁷, G. Bernardi¹³⁵, C. Bernius¹⁵³, F.U. Bernlochner²⁴, T. Berry⁹⁴, P. Berta¹⁰⁰, A. Berthold⁴⁸, I.A. Bertram⁹⁰, O. Bessidskaia Bylund¹⁸², N. Besson¹⁴⁴, A. Bethani¹⁰¹, S. Bethke¹¹⁵, A. Betti⁴², A.J. Bevan⁹³, J. Beyer¹¹⁵, D.S. Bhattacharya¹⁷⁷, P. Bhattarai²⁶, V.S. Bhopatkar⁶, R. Bi¹³⁸, R.M. Bianchi¹³⁸, O. Biebel¹¹⁴, D. Biedermann¹⁹, R. Bielski³⁶, K. Bierwagen¹⁰⁰, N.V. Biesuz^{72a,72b}, M. Biglietti^{75a}, T.R.V. Billoud¹⁴¹, M. Bindi⁵³, A. Bingul^{12d},

C. Bini^{73a,73b}, S. Biondi^{23b,23a}, C.J. Birch-sykes¹⁰¹, M. Birman¹⁸⁰, T. Bisanz³⁶, J.P. Biswal³,
 D. Biswas^{181,i}, A. Bitadze¹⁰¹, C. Bittrich⁴⁸, K. Bjørke¹³³, T. Blazek^{28a}, I. Bloch⁴⁶, C. Blocker²⁶, A. Blue⁵⁷,
 U. Blumenschein⁹³, G.J. Bobbink¹²⁰, V.S. Bobrovnikov^{122b,122a}, S.S. Bocchetta⁹⁷, D. Bogavac¹⁴,
 A.G. Bogdanchikov^{122b,122a}, C. Bohm^{45a}, V. Boisvert⁹⁴, P. Bokan^{172,53}, T. Bold^{84a}, A.E. Bolz^{61b},
 M. Bomben¹³⁵, M. Bona⁹³, J.S. Bonilla¹³¹, M. Boonekamp¹⁴⁴, C.D. Booth⁹⁴, A.G. Borbély⁵⁷,
 H.M. Borecka-Bielska⁹¹, L.S. Borgna⁹⁵, A. Borisov¹²³, G. Borissov⁹⁰, D. Bortoletto¹³⁴, D. Boscherini^{23b},
 M. Bosman¹⁴, J.D. Bossio Sola¹⁰⁴, K. Bouaouda^{35a}, J. Boudreau¹³⁸, E.V. Bouhova-Thacker⁹⁰,
 D. Boumediene³⁸, A. Boveia¹²⁷, J. Boyd³⁶, D. Boye^{33c}, I.R. Boyko⁸⁰, A.J. Bozson⁹⁴, J. Bracnik²¹,
 N. Brahim^{60d,60c}, G. Brandt¹⁸², O. Brandt³², F. Braren⁴⁶, B. Brau¹⁰³, J.E. Brau¹³¹,
 W.D. Breaden Madden⁵⁷, K. Brendlinger⁴⁶, R. Brenner¹⁶⁰, L. Brenner³⁶, R. Brenner¹⁷², S. Bressler¹⁸⁰,
 B. Brickwedde¹⁰⁰, D.L. Briglin²¹, D. Britton⁵⁷, D. Britzger¹¹⁵, I. Brock²⁴, R. Brock¹⁰⁷, G. Brooijmans³⁹,
 W.K. Brooks^{146d}, E. Brost²⁹, P.A. Bruckman de Renstrom⁸⁵, B. Brüers⁴⁶, D. Bruncko^{28b}, A. Bruni^{23b},
 G. Bruni^{23b}, M. Bruschi^{23b}, N. Brusino^{73a,73b}, L. Bryngemark¹⁵³, T. Buanes¹⁷, Q. Buat¹⁵⁵,
 P. Buchholz¹⁵¹, A.G. Buckley⁵⁷, I.A. Budagov⁸⁰, M.K. Bugge¹³³, F. Bühner⁵², O. Bulekov¹¹²,
 B.A. Bullard⁵⁹, T.J. Burch¹²¹, S. Burdin⁹¹, C.D. Burgard¹²⁰, A.M. Burger¹²⁹, B. Burghgrave⁸,
 J.T.P. Burr⁴⁶, C.D. Burton¹¹, J.C. Burzynski¹⁰³, V. Büscher¹⁰⁰, E. Buschmann⁵³, P.J. Bussey⁵⁷,
 J.M. Butler²⁵, C.M. Buttar⁵⁷, J.M. Butterworth⁹⁵, P. Butti³⁶, W. Buttinger¹⁴³, C.J. Buxo Vazquez¹⁰⁷,
 A. Buzatu¹⁵⁸, A.R. Buzykaev^{122b,122a}, G. Cabras^{23b,23a}, S. Cabrera Urbán¹⁷⁴, D. Caforio⁵⁶, H. Cai¹³⁸,
 V.M.M. Cairo¹⁵³, O. Cakir^{4a}, N. Calace³⁶, P. Calafiura¹⁸, G. Calderini¹³⁵, P. Calfayan⁶⁶, G. Callea⁵⁷,
 L.P. Caloba^{81b}, A. Caltabiano^{74a,74b}, S. Calvente Lopez⁹⁹, D. Calvet³⁸, S. Calvet³⁸, T.P. Calvet¹⁰²,
 M. Calvetti^{72a,72b}, R. Camacho Toro¹³⁵, S. Camarda³⁶, D. Camarero Munoz⁹⁹, P. Camarri^{74a,74b},
 M.T. Camerlingo^{75a,75b}, D. Cameron¹³³, C. Camincher³⁶, S. Campana³⁶, M. Campanelli⁹⁵, A. Camplani⁴⁰,
 V. Canale^{70a,70b}, A. Canesse¹⁰⁴, M. Cano Bret⁷⁸, J. Cantero¹²⁹, T. Cao¹⁶¹, Y. Cao¹⁷³,
 M.D.M. Capeans Garrido³⁶, M. Capua^{41b,41a}, R. Cardarelli^{74a}, F. Cardillo¹⁷⁴, G. Carducci^{41b,41a},
 I. Carli¹⁴², T. Carli³⁶, G. Carlino^{70a}, B.T. Carlson¹³⁸, E.M. Carlson^{176,168a}, L. Carminati^{69a,69b},
 R.M.D. Carney¹⁵³, S. Caron¹¹⁹, E. Carquin^{146d}, S. Carrá⁴⁶, G. Carratta^{23b,23a}, J.W.S. Carter¹⁶⁷,
 T.M. Carter⁵⁰, M.P. Casado^{14,f}, A.F. Casha¹⁶⁷, E.G. Castiglia¹⁸³, F.L. Castillo¹⁷⁴, L. Castillo Garcia¹⁴,
 V. Castillo Gimenez¹⁷⁴, N.F. Castro^{139a,139e}, A. Catinaccio³⁶, J.R. Catmore¹³³, A. Cattai³⁶, V. Cavaliere²⁹,
 D. Cavalli^{69b}, V. Cavasinni^{72a,72b}, E. Celebi^{12b}, F. Celli¹³⁴, K. Cerny¹³⁰, A.S. Cerqueira^{81a}, A. Cerri¹⁵⁶,
 L. Cerrito^{74a,74b}, F. Cerutti¹⁸, A. Cervelli^{23b,23a}, S.A. Cetin^{12b}, Z. Chadi^{35a}, D. Chakraborty¹²¹, J. Chan¹⁸¹,
 W.S. Chan¹²⁰, W.Y. Chan⁹¹, J.D. Chapman³², B. Chargeishvili^{159b}, D.G. Charlton²¹, T.P. Charman⁹³,
 M. Chatterjee²⁰, C.C. Chau³⁴, S. Che¹²⁷, S. Chekanov⁶, S.V. Chekulaev^{168a}, G.A. Chelkov^{80,ah}, B. Chen⁷⁹,
 C. Chen^{60a}, C.H. Chen⁷⁹, H. Chen^{15c}, H. Chen²⁹, J. Chen^{60a}, J. Chen³⁹, J. Chen²⁶, S. Chen¹³⁶,
 S.J. Chen^{15c}, X. Chen^{15b}, Y. Chen^{60a}, Y-H. Chen⁴⁶, H.C. Cheng^{63a}, H.J. Cheng^{15a}, A. Cheplakov⁸⁰,
 E. Cheremushkina¹²³, R. Cherkaoui El Moursli^{35f}, E. Cheu⁷, K. Cheung⁶⁴, T.J.A. Chevaléras¹⁴⁴,
 L. Chevalier¹⁴⁴, V. Chiarella⁵¹, G. Chiarelli^{72a}, G. Chiodini^{68a}, A.S. Chisholm²¹, A. Chitan^{27b}, I. Chiu¹⁶³,
 Y.H. Chiu¹⁷⁶, M.V. Chizhov⁸⁰, K. Choi¹¹, A.R. Chomont^{73a,73b}, Y.S. Chow¹²⁰, L.D. Christopher^{33e},
 M.C. Chu^{63a}, X. Chu^{15a,15d}, J. Chudoba¹⁴⁰, J.J. Chwastowski⁸⁵, L. Chytka¹³⁰, D. Cieri¹¹⁵, K.M. Ciesla⁸⁵,
 V. Cindro⁹², I.A. Cioară^{27b}, A. Ciocio¹⁸, F. Ciotto^{70a,70b}, Z.H. Citron^{180j}, M. Citterio^{69a},
 D.A. Ciubotaru^{27b}, B.M. Ciungu¹⁶⁷, A. Clark⁵⁴, M.R. Clark³⁹, P.J. Clark⁵⁰, S.E. Clawson¹⁰¹,
 C. Clement^{45a,45b}, Y. Coadou¹⁰², M. Cobal^{167a,67c}, A. Coccaro^{55b}, J. Cochran⁷⁹, R. Coelho Lopes De Sa¹⁰³,
 H. Cohen¹⁶¹, A.E.C. Coimbra³⁶, B. Cole³⁹, A.P. Colijn¹²⁰, J. Collot⁵⁸, P. Conde Muiño^{139a,139h},
 S.H. Connell^{33c}, I.A. Connelly⁵⁷, S. Constantinescu^{27b}, F. Conventi^{70a,an}, A.M. Cooper-Sarkar¹³⁴,
 F. Cormier¹⁷⁵, K.J.R. Cormier¹⁶⁷, L.D. Corpe⁹⁵, M. Corradi^{73a,73b}, E.E. Corrigan⁹⁷, F. Corriveau^{104,ab},
 M.J. Costa¹⁷⁴, F. Costanza⁵, D. Costanzo¹⁴⁹, G. Cowan⁹⁴, J.W. Cowley³², J. Crane¹⁰¹, K. Cranmer¹²⁵,
 R.A. Creager¹³⁶, S. Crépe-Renaudin⁵⁸, F. Crescioli¹³⁵, M. Cristinziani²⁴, V. Croft¹⁷⁰, G. Crosetti^{41b,41a},
 A. Cueto⁵, T. Cuhadar Donszelmann¹⁷¹, H. Cui^{15a,15d}, A.R. Cukierman¹⁵³, W.R. Cunningham⁵⁷,

S. Czekierda⁸⁵, P. Czodrowski³⁶, M.M. Czurylo^{61b}, M.J. Da Cunha Sargedas De Sousa^{60b},
 J.V. Da Fonseca Pinto^{81b}, C. Da Via¹⁰¹, W. Dabrowski^{84a}, F. Dachs³⁶, T. Dado⁴⁷, S. Dahbi^{33e}, T. Dai¹⁰⁶,
 C. Dallapiccola¹⁰³, M. Dam⁴⁰, G. D'amen²⁹, V. D'Amico^{75a,75b}, J. Damp¹⁰⁰, J.R. Dandoy¹³⁶,
 M.F. Daneri³⁰, M. Danninger¹⁵², V. Dao³⁶, G. Darbo^{55b}, O. Dartsis⁵, A. Dattagupta¹³¹, T. Daubney⁴⁶,
 S. D'Auria^{69a,69b}, C. David^{168b}, T. Davidek¹⁴², D.R. Davis⁴⁹, I. Dawson¹⁴⁹, K. De⁸, R. De Asmundis^{70a},
 M. De Beurs¹²⁰, S. De Castro^{23b,23a}, N. De Groot¹¹⁹, P. de Jong¹²⁰, H. De la Torre¹⁰⁷, A. De Maria^{15c},
 D. De Pedis^{73a}, A. De Salvo^{73a}, U. De Sanctis^{74a,74b}, M. De Santis^{74a,74b}, A. De Santo¹⁵⁶,
 J.B. De Vivie De Regie⁶⁵, D.V. Dedovich⁸⁰, A.M. Deiana⁴², J. Del Peso⁹⁹, Y. Delabat Diaz⁴⁶,
 D. Delgove⁶⁵, F. Deliot¹⁴⁴, C.M. Delitzsch⁷, M. Della Pietra^{70a,70b}, D. Della Volpe⁵⁴, A. Dell'Acqua³⁶,
 L. Dell'Asta^{74a,74b}, M. Delmastro⁵, C. Delporte⁶⁵, P.A. Delsart⁵⁸, D.A. DeMarco¹⁶⁷, S. Demers¹⁸³,
 M. Demichev⁸⁰, G. Demontigny¹¹⁰, S.P. Denisov¹²³, L. D'Eramo¹²¹, D. Derendarz⁸⁵, J.E. Derkaoui^{35e},
 F. Derue¹³⁵, P. Dervan⁹¹, K. Desch²⁴, K. Dette¹⁶⁷, C. Deutsch²⁴, M.R. Devesa³⁰, P.O. Deviveiros³⁶,
 F.A. Di Bello^{73a,73b}, A. Di Ciaccio^{74a,74b}, L. Di Ciaccio⁵, W.K. Di Clemente¹³⁶, C. Di Donato^{70a,70b},
 A. Di Girolamo³⁶, G. Di Gregorio^{72a,72b}, B. Di Micco^{75a,75b}, R. Di Nardo^{75a,75b}, K.F. Di Petrillo⁵⁹,
 R. Di Sipio¹⁶⁷, C. Diaconu¹⁰², F.A. Dias¹²⁰, T. Dias Do Vale^{139a}, M.A. Diaz^{146a}, F.G. Diaz Capriles²⁴,
 J. Dickinson¹⁸, M. Didenko¹⁶⁶, E.B. Diehl¹⁰⁶, J. Dietrich¹⁹, S. Díez Cornell⁴⁶, C. Diez Pardos¹⁵¹,
 A. Dimitrievska¹⁸, W. Ding^{15b}, J. Dingfelder²⁴, S.J. Dittmeier^{61b}, F. Dittus³⁶, F. Djama¹⁰², T. Djobava^{159b},
 J.I. Djuvsland¹⁷, M.A.B. Do Vale¹⁴⁷, M. Dobre^{27b}, D. Dodsworth²⁶, C. Doglioni⁹⁷, J. Dolejsi¹⁴²,
 Z. Dolezal¹⁴², M. Donadelli^{81c}, B. Dong^{60c}, J. Donini³⁸, A. D'onofrio^{15c}, M. D'Onofrio⁹¹, J. Dopke¹⁴³,
 A. Doria^{70a}, M.T. Dova⁸⁹, A.T. Doyle⁵⁷, E. Drechsler¹⁵², E. Dreyer¹⁵², T. Dreyer⁵³, A.S. Drobac¹⁷⁰,
 D. Du^{60b}, T.A. du Pree¹²⁰, Y. Duan^{60d}, F. Dubinin¹¹¹, M. Dubovsky^{28a}, A. Dubreuil⁵⁴, E. Duchovni¹⁸⁰,
 G. Duckeck¹¹⁴, O.A. Ducu^{36,27b}, D. Duda¹¹⁵, A. Dudarev³⁶, A.C. Dudder¹⁰⁰, E.M. Duffield¹⁸,
 M. D'uffizi¹⁰¹, L. Duflot⁶⁵, M. Dührssen³⁶, C. Dülsen¹⁸², M. Dumancic¹⁸⁰, A.E. Dumitriu^{27b},
 M. Dunford^{61a}, S. Dungs⁴⁷, A. Duperrin¹⁰², H. Duran Yildiz^{4a}, M. Düren⁵⁶, A. Durglishvili^{159b},
 D. Duschinger⁴⁸, B. Dutta⁴⁶, D. Duvnjak¹, G.I. Dyckes¹³⁶, M. Dyndal³⁶, S. Dysch¹⁰¹, B.S. Dziedzic⁸⁵,
 M.G. Eggleston⁴⁹, T. Eifert⁸, G. Eigen¹⁷, K. Einsweiler¹⁸, T. Ekelof¹⁷², H. El Jarrari^{35f}, V. Ellajosyula¹⁷²,
 M. Ellert¹⁷², F. Ellinghaus¹⁸², A.A. Elliot⁹³, N. Ellis³⁶, J. Elmsheuser²⁹, M. Elsing³⁶, D. Emeliyanov¹⁴³,
 A. Emerman³⁹, Y. Enari¹⁶³, M.B. Epland⁴⁹, J. Erdmann⁴⁷, A. Ereditato²⁰, P.A. Erland⁸⁵, M. Errenst¹⁸²,
 M. Escalier⁶⁵, C. Escobar¹⁷⁴, O. Estrada Pastor¹⁷⁴, E. Etzion¹⁶¹, G. Evans^{139a,139b}, H. Evans⁶⁶,
 M.O. Evans¹⁵⁶, A. Ezhilov¹³⁷, F. Fabbri⁵⁷, L. Fabbri^{23b,23a}, V. Fabiani¹¹⁹, G. Facini¹⁷⁸,
 R.M. Fakhruddinov¹²³, S. Falciano^{73a}, P.J. Falke²⁴, S. Falke³⁶, J. Faltova¹⁴², Y. Fang^{15a}, Y. Fang^{15a},
 G. Fanourakis⁴⁴, M. Fanti^{69a,69b}, M. Faraj^{67a,67c}, A. Farbin⁸, A. Farilla^{75a}, E.M. Farina^{71a,71b},
 T. Farooque¹⁰⁷, S.M. Farrington⁵⁰, P. Farthouat³⁶, F. Fassi^{35f}, P. Fassnacht³⁶, D. Fassouliotis⁹,
 M. Fauci Giannelli⁵⁰, W.J. Fawcett³², L. Fayard⁶⁵, O.L. Fedin^{137,o}, W. Fedorko¹⁷⁵, A. Fehr²⁰,
 M. Feickert¹⁷³, L. Feligioni¹⁰², A. Fell¹⁴⁹, C. Feng^{60b}, M. Feng⁴⁹, M.J. Fenton¹⁷¹, A.B. Fenyuk¹²³,
 S.W. Ferguson⁴³, J. Ferrando⁴⁶, A. Ferrante¹⁷³, A. Ferrari¹⁷², P. Ferrari¹²⁰, R. Ferrari^{71a},
 D.E. Ferreira de Lima^{61b}, A. Ferrer¹⁷⁴, D. Ferrere⁵⁴, C. Ferretti¹⁰⁶, F. Fiedler¹⁰⁰, A. Filipčić⁹²,
 F. Filthaut¹¹⁹, K.D. Finelli²⁵, M.C.N. Fiolhais^{139a,139c,a}, L. Fiorini¹⁷⁴, F. Fischer¹¹⁴, J. Fischer¹⁰⁰,
 W.C. Fisher¹⁰⁷, T. Fitschen²¹, I. Fleck¹⁵¹, P. Fleischmann¹⁰⁶, T. Flick¹⁸², B.M. Flierl¹¹⁴, L. Flores¹³⁶,
 L.R. Flores Castillo^{63a}, F.M. Follega^{76a,76b}, N. Fomin¹⁷, J.H. Foo¹⁶⁷, G.T. Forcolin^{76a,76b}, B.C. Forland⁶⁶,
 A. Formica¹⁴⁴, F.A. Förster¹⁴, A.C. Forti¹⁰¹, E. Fortin¹⁰², M.G. Foti¹³⁴, D. Fournier⁶⁵, H. Fox⁹⁰,
 P. Francavilla^{72a,72b}, S. Francescato^{73a,73b}, M. Franchini^{23b,23a}, S. Franchino^{61a}, D. Francis³⁶, L. Franco⁵,
 L. Franconi²⁰, M. Franklin⁵⁹, G. Frattari^{73a,73b}, A.N. Fray⁹³, P.M. Freeman²¹, B. Freund¹¹⁰,
 W.S. Freund^{81b}, E.M. Freundlich⁴⁷, D.C. Frizzell¹²⁸, D. Froidevaux³⁶, J.A. Frost¹³⁴, G. Fugante^{69b},
 M. Fujimoto¹²⁶, C. Fukunaga¹⁶⁴, E. Fullana Torregrosa¹⁷⁴, T. Fusayasu¹¹⁶, J. Fuster¹⁷⁴, A. Gabrielli^{23b,23a},
 A. Gabrielli³⁶, S. Gadatsch⁵⁴, P. Gadow¹¹⁵, G. Gagliardi^{55b,55a}, L.G. Gagnon¹¹⁰, G.E. Gallardo¹³⁴,
 E.J. Gallas¹³⁴, B.J. Gallop¹⁴³, R. Gamboa Goni⁹³, K.K. Gan¹²⁷, S. Ganguly¹⁸⁰, J. Gao^{60a}, Y. Gao⁵⁰,

Y.S. Gao^{31,l}, F.M. Garay Walls^{146a}, C. García¹⁷⁴, J.E. García Navarro¹⁷⁴, J.A. García Pascual^{15a},
 C. Garcia-Argos⁵², M. Garcia-Sciveres¹⁸, R.W. Gardner³⁷, N. Garelli¹⁵³, S. Gargiulo⁵², C.A. Garner¹⁶⁷,
 V. Garonne¹³³, S.J. Gasiorowski¹⁴⁸, P. Gaspar^{81b}, A. Gaudiello^{55b,55a}, G. Gaudio^{71a}, P. Gauzzi^{73a,73b},
 I.L. Gavrilenko¹¹¹, A. Gavriilyuk¹²⁴, C. Gay¹⁷⁵, G. Gaycken⁴⁶, E.N. Gazis¹⁰, A.A. Geanta^{27b}, C.M. Gee¹⁴⁵,
 C.N.P. Gee¹⁴³, J. Geisen⁹⁷, M. Geisen¹⁰⁰, C. Gemme^{55b}, M.H. Genest⁵⁸, C. Geng¹⁰⁶, S. Gentile^{73a,73b},
 S. George⁹⁴, T. Geralis⁴⁴, L.O. Gerlach⁵³, P. Gessinger-Befurt¹⁰⁰, G. Gessner⁴⁷, S. Ghasemi¹⁵¹,
 M. Ghasemi Bostanabad¹⁷⁶, M. Ghneimat¹⁵¹, A. Ghosh⁶⁵, A. Ghosh⁷⁸, B. Giacobbe^{23b}, S. Giagu^{73a,73b},
 N. Giangiacomi^{23b,23a}, P. Giannetti^{72a}, A. Giannini^{70a,70b}, G. Giannini¹⁴, S.M. Gibson⁹⁴, M. Gignac¹⁴⁵,
 D.T. Gil^{84b}, B.J. Gilbert³⁹, D. Gillberg³⁴, G. Gilles¹⁸², N.E.K. Gillwald⁴⁶, D.M. Gingrich^{3,am},
 M.P. Giordani^{67a,67c}, P.F. Giraud¹⁴⁴, G. Giugliarelli^{67a,67c}, D. Giugni^{69a}, F. Giuli^{74a,74b}, S. Gkaitatzis¹⁶²,
 I. Gkialas^{9,g}, E.L. Gkoukousis¹⁴, P. Gkoutoumis¹⁰, L.K. Gladilin¹¹³, C. Glasman⁹⁹, J. Glatzer¹⁴,
 P.C.F. Glaysher⁴⁶, A. Glazov⁴⁶, G.R. Gledhill¹³¹, I. Gnesi^{41b,b}, M. Goblirsch-Kolb²⁶, D. Godin¹¹⁰,
 S. Goldfarb¹⁰⁵, T. Golling⁵⁴, D. Golubkov¹²³, A. Gomes^{139a,139b}, R. Goncalves Gama⁵³,
 R. Gonçalves^{139a,139c}, G. Gonella¹³¹, L. Gonella²¹, A. Gongadze⁸⁰, F. Gonnella²¹, J.L. Gonski³⁹,
 S. González de la Hoz¹⁷⁴, S. Gonzalez Fernandez¹⁴, R. Gonzalez Lopez⁹¹, C. Gonzalez Renteria¹⁸,
 R. Gonzalez Suarez¹⁷², S. Gonzalez-Sevilla⁵⁴, G.R. Gonzalvo Rodriguez¹⁷⁴, L. Goossens³⁶,
 N.A. Gorasia²¹, P.A. Gorbounov¹²⁴, H.A. Gordon²⁹, B. Gorini³⁶, E. Gorini^{68a,68b}, A. Gorišek⁹²,
 A.T. Goshaw⁴⁹, M.I. Gostkin⁸⁰, C.A. Gottardo¹¹⁹, M. Gouighri^{35b}, A.G. Goussiou¹⁴⁸, N. Govender^{33c},
 C. Goy⁵, I. Grabowska-Bold^{84a}, E.C. Graham⁹¹, J. Gramling¹⁷¹, E. Gramstad¹³³, S. Grancagnolo¹⁹,
 M. Grandi¹⁵⁶, V. Gratchev¹³⁷, P.M. Gravila^{27f}, F.G. Gravili^{68a,68b}, C. Gray⁵⁷, H.M. Gray¹⁸, C. Grefe²⁴,
 K. Gregersen⁹⁷, I.M. Gregor⁴⁶, P. Grenier¹⁵³, K. Grevtsov⁴⁶, C. Grieco¹⁴, N.A. Grieser¹²⁸, A.A. Grillo¹⁴⁵,
 K. Grimm^{31,k}, S. Grinstein^{14,w}, J.-F. Grivaz⁶⁵, S. Groh¹⁰⁰, E. Gross¹⁸⁰, J. Grosse-Knetter⁵³, Z.J. Grout⁹⁵,
 C. Grud¹⁰⁶, A. Grummer¹¹⁸, J.C. Grundy¹³⁴, L. Guan¹⁰⁶, W. Guan¹⁸¹, C. Gubbels¹⁷⁵, J. Guenther⁷⁷,
 A. Guerguichon⁶⁵, J.G.R. Guerrero Rojas¹⁷⁴, F. Guescini¹¹⁵, D. Guest¹⁷¹, R. Gugel¹⁰⁰, A. Guida⁴⁶,
 T. Guillemin⁵, S. Guindon³⁶, J. Guo^{60c}, W. Guo¹⁰⁶, Y. Guo^{60a}, Z. Guo¹⁰², R. Gupta⁴⁶, S. Gurbuz^{12c},
 G. Gustavino¹²⁸, M. Guth⁵², P. Gutierrez¹²⁸, C. Gutschow⁹⁵, C. Guyot¹⁴⁴, C. Gwenlan¹³⁴,
 C.B. Gwilliam⁹¹, E.S. Haaland¹³³, A. Haas¹²⁵, C. Haber¹⁸, H.K. Hadavand⁸, A. Hadeif^{60a}, M. Haleem¹⁷⁷,
 J. Haley¹²⁹, J.J. Hall¹⁴⁹, G. Halladjian¹⁰⁷, G.D. Hallewell¹⁰², K. Hamano¹⁷⁶, H. Hamdaoui^{35f}, M. Hamer²⁴,
 G.N. Hamity⁵⁰, K. Han^{60a,v}, L. Han^{15c}, L. Han^{60a}, S. Han¹⁸, Y.F. Han¹⁶⁷, K. Hanagaki^{82,t}, M. Hance¹⁴⁵,
 D.M. Handl¹¹⁴, M.D. Hank³⁷, R. Hankache¹³⁵, E. Hansen⁹⁷, J.B. Hansen⁴⁰, J.D. Hansen⁴⁰, M.C. Hansen²⁴,
 P.H. Hansen⁴⁰, E.C. Hanson¹⁰¹, K. Hara¹⁶⁹, T. Harenberg¹⁸², S. Harkusha¹⁰⁸, P.F. Harrison¹⁷⁸,
 N.M. Hartman¹⁵³, N.M. Hartmann¹¹⁴, Y. Hasegawa¹⁵⁰, A. Hasib⁵⁰, S. Hassani¹⁴⁴, S. Haug²⁰,
 R. Hauser¹⁰⁷, L.B. Havener³⁹, M. Havranek¹⁴¹, C.M. Hawkes²¹, R.J. Hawkings³⁶, S. Hayashida¹¹⁷,
 D. Hayden¹⁰⁷, C. Hayes¹⁰⁶, R.L. Hayes¹⁷⁵, C.P. Hays¹³⁴, J.M. Hays⁹³, H.S. Hayward⁹¹, S.J. Haywood¹⁴³,
 F. He^{60a}, Y. He¹⁶⁵, M.P. Heath⁵⁰, V. Hedberg⁹⁷, A.L. Heggelund¹³³, C. Heidegger⁵², K.K. Heidegger⁵²,
 W.D. Heidorn⁷⁹, J. Heilman³⁴, S. Heim⁴⁶, T. Heim¹⁸, B. Heinemann^{46,ak}, J.G. Heinlein¹³⁶, J.J. Heinrich¹³¹,
 L. Heinrich³⁶, J. Hejbal¹⁴⁰, L. Helary⁴⁶, A. Held¹²⁵, S. Hellesund¹³³, C.M. Helling¹⁴⁵, S. Hellman^{45a,45b},
 C. Helsens³⁶, R.C.W. Henderson⁹⁰, Y. Heng¹⁸¹, L. Henkelmann³², A.M. Henriques Correia³⁶, H. Herde²⁶,
 Y. Hernández Jiménez^{33e}, H. Herr¹⁰⁰, M.G. Herrmann¹¹⁴, T. Herrmann⁴⁸, G. Herten⁵², R. Hertenberger¹¹⁴,
 L. Hervas³⁶, T.C. Herwig¹³⁶, G.G. Hesketh⁹⁵, N.P. Hessey^{168a}, H. Hibi⁸³, S. Higashino⁸²,
 E. Higón-Rodríguez¹⁷⁴, K. Hildebrand³⁷, J.C. Hill³², K.K. Hill²⁹, K.H. Hiller⁴⁶, S.J. Hillier²¹, M. Hils⁴⁸,
 I. Hinchliffe¹⁸, F. Hinterkeuser²⁴, M. Hirose¹³², S. Hirose¹⁶⁹, D. Hirschbuehl¹⁸², B. Hiti⁹², O. Hladik¹⁴⁰,
 J. Hobbs¹⁵⁵, N. Hod¹⁸⁰, M.C. Hodgkinson¹⁴⁹, A. Hoecker³⁶, D. Hohn⁵², D. Hohov⁶⁵, T. Holm²⁴,
 T.R. Holmes³⁷, M. Holzbock¹¹⁵, L.B.A.H. Hommels³², T.M. Hong¹³⁸, J.C. Honig⁵², A. Hönle¹¹⁵,
 B.H. Hooberman¹⁷³, W.H. Hopkins⁶, Y. Horii¹¹⁷, P. Horn⁴⁸, L.A. Horyn³⁷, S. Hou¹⁵⁸, A. Houmada^{35a},
 J. Howarth⁵⁷, J. Hoya⁸⁹, M. Hrabovsky¹³⁰, J. Hrivnac⁶⁵, A. Hrynevich¹⁰⁹, T. Hryn'ova⁵, P.J. Hsu⁶⁴,
 S.-C. Hsu¹⁴⁸, Q. Hu²⁹, S. Hu^{60c}, Y.F. Hu^{15a,15d,ao}, D.P. Huang⁹⁵, X. Huang^{15c}, Y. Huang^{60a}, Y. Huang^{15a},

Z. Hubacek¹⁴¹, F. Hubaut¹⁰², M. Huebner²⁴, F. Huegging²⁴, T.B. Huffman¹³⁴, M. Huhtinen³⁶, R. Hulsken⁵⁸, R.F.H. Hunter³⁴, N. Huseynov^{80,ac}, J. Huston¹⁰⁷, J. Huth⁵⁹, R. Hyneman¹⁵³, S. Hyrych^{28a}, G. Iacobucci⁵⁴, G. Iakovidis²⁹, I. Ibragimov¹⁵¹, L. Iconomidou-Fayard⁶⁵, P. Iengo³⁶, R. Ignazzi⁴⁰, O. Igonkina^{120,y,*}, R. Iguchi¹⁶³, T. Iizawa⁵⁴, Y. Ikegami⁸², M. Ikeno⁸², N. Ilic^{119,167,ab}, F. Iltzsche⁴⁸, H. Imam^{35a}, G. Introzzi^{71a,71b}, M. Iodice^{75a}, K. Iordanidou^{168a}, V. Ippolito^{73a,73b}, M.F. Isacson¹⁷², M. Ishino¹⁶³, W. Islam¹²⁹, C. Issever^{19,46}, S. Istin¹⁶⁰, J.M. Iturbe Ponce^{63a}, R. Iuppa^{76a,76b}, A. Ivina¹⁸⁰, J.M. Izen⁴³, V. Izzo^{70a}, P. Jacka¹⁴⁰, P. Jackson¹, R.M. Jacobs⁴⁶, B.P. Jaeger¹⁵², V. Jain², G. Jäkel¹⁸², K.B. Jakobi¹⁰⁰, K. Jakobs⁵², T. Jakoubek¹⁸⁰, J. Jamieson⁵⁷, K.W. Janas^{84a}, R. Jansky⁵⁴, M. Janus⁵³, P.A. Janus^{84a}, G. Jarlskog⁹⁷, A.E. Jaspan⁹¹, N. Javadov^{80,ac}, T. Javûrek³⁶, M. Javurkova¹⁰³, F. Jeanneau¹⁴⁴, L. Jeanty¹³¹, J. Jejelava^{159a}, P. Jenni^{52,c}, N. Jeong⁴⁶, S. Jézéquel⁵, H. Ji¹⁸¹, J. Jia¹⁵⁵, Z. Jia^{15c}, H. Jiang⁷⁹, Y. Jiang^{60a}, Z. Jiang¹⁵³, S. Jiggins⁵², F.A. Jimenez Morales³⁸, J. Jimenez Pena¹¹⁵, S. Jin^{15c}, A. Jinaru^{27b}, O. Jinnouchi¹⁶⁵, H. Jivan^{33e}, P. Johansson¹⁴⁹, K.A. Johns⁷, C.A. Johnson⁶⁶, E. Jones¹⁷⁸, R.W.L. Jones⁹⁰, S.D. Jones¹⁵⁶, T.J. Jones⁹¹, J. Jongmanns^{61a}, J. Jovicevic³⁶, X. Ju¹⁸, J.J. Junggeburth¹¹⁵, A. Juste Rozas^{14,w}, A. Kaczmarzka⁸⁵, M. Kado^{73a,73b}, H. Kagan¹²⁷, M. Kagan¹⁵³, A. Kahn³⁹, C. Kahra¹⁰⁰, T. Kaji¹⁷⁹, E. Kajomovitz¹⁶⁰, C.W. Kalderon²⁹, A. Kaluza¹⁰⁰, A. Kamenshchikov¹²³, M. Kaneda¹⁶³, N.J. Kang¹⁴⁵, S. Kang⁷⁹, Y. Kano¹¹⁷, J. Kanzaki⁸², L.S. Kaplan¹⁸¹, D. Kar^{33e}, K. Karava¹³⁴, M.J. Kareem^{168b}, I. Karkanias¹⁶², S.N. Karpov⁸⁰, Z.M. Karpova⁸⁰, V. Kartvelishvili⁹⁰, A.N. Karyukhin¹²³, E. Kasimi¹⁶², A. Kastanas^{45a,45b}, C. Kato^{60d}, J. Katzy⁴⁶, K. Kawade¹⁵⁰, K. Kawagoe⁸⁸, T. Kawaguchi¹¹⁷, T. Kawamoto¹⁴⁴, G. Kawamura⁵³, E.F. Kay¹⁷⁶, S. Kazakos¹⁴, V.F. Kazanin^{122b,122a}, J.M. Keaveney^{33a}, R. Keeler¹⁷⁶, J.S. Keller³⁴, E. Kellermann⁹⁷, D. Kelsey¹⁵⁶, J.J. Kempster²¹, J. Kendrick²¹, K.E. Kennedy³⁹, O. Kepka¹⁴⁰, S. Kersten¹⁸², B.P. Kerševan⁹², S. Ketabchi Haghighat¹⁶⁷, M. Khader¹⁷³, F. Khalil-Zada¹³, M. Khandoga¹⁴⁴, A. Khanov¹²⁹, A.G. Kharlamov^{122b,122a}, T. Kharlamova^{122b,122a}, E.E. Khoda¹⁷⁵, A. Khodinov¹⁶⁶, T.J. Khoo⁷⁷, G. Khorauli¹⁷⁷, E. Khramov⁸⁰, J. Khubua^{159b}, S. Kido⁸³, M. Kiehn³⁶, E. Kim¹⁶⁵, Y.K. Kim³⁷, N. Kimura⁹⁵, A. Kirchhoff⁵³, D. Kirchmeier⁴⁸, J. Kirk¹⁴³, A.E. Kiryunin¹¹⁵, T. Kishimoto¹⁶³, D.P. Kisliuk¹⁶⁷, V. Kitali⁴⁶, C. Kitsaki¹⁰, O. Kivernyk²⁴, T. Klapdor-Kleingrothaus⁵², M. Klassen^{61a}, C. Klein³⁴, M.H. Klein¹⁰⁶, M. Klein⁹¹, U. Klein⁹¹, K. Kleinknecht¹⁰⁰, P. Klimek³⁶, A. Klimentov²⁹, T. Klingl²⁴, T. Klioutchnikova³⁶, F.F. Klitzner¹¹⁴, P. Kluit¹²⁰, S. Kluth¹¹⁵, E. Kneringer⁷⁷, E.B.F.G. Knoop¹⁰², A. Knue⁵², D. Kobayashi⁸⁸, M. Kobel⁴⁸, M. Kocian¹⁵³, T. Kodama¹⁶³, P. Kodys¹⁴², D.M. Koeck¹⁵⁶, P.T. Koenig²⁴, T. Koffas³⁴, N.M. Köhler³⁶, M. Kolb¹⁴⁴, I. Koletsou⁵, T. Komarek¹³⁰, T. Kondo⁸², K. Köneke⁵², A.X.Y. Kong¹, A.C. König¹¹⁹, T. Kono¹²⁶, V. Konstantinides⁹⁵, N. Konstantinidis⁹⁵, B. Konya⁹⁷, R. Kopeliansky⁶⁶, S. Koperny^{84a}, K. Korcyl⁸⁵, K. Kordas¹⁶², G. Koren¹⁶¹, A. Korn⁹⁵, I. Korolkov¹⁴, E.V. Korolkova¹⁴⁹, N. Korotkova¹¹³, O. Kortner¹¹⁵, S. Kortner¹¹⁵, V.V. Kostyukhin^{149,166}, A. Kotsokchagia⁶⁵, A. Kotwal⁴⁹, A. Koulouris¹⁰, A. Kourkoumeli-Charalampidi^{71a,71b}, C. Kourkoumelis⁹, E. Kourlitis⁶, V. Kouskoura²⁹, R. Kowalewski¹⁷⁶, W. Kozanecki¹⁰¹, A.S. Kozhin¹²³, V.A. Kramarenko¹¹³, G. Kramberger⁹², D. Krasnopevtsev^{60a}, M.W. Krasny¹³⁵, A. Krasznahorkay³⁶, D. Krauss¹¹⁵, J.A. Kremer¹⁰⁰, J. Kretzschmar⁹¹, P. Krieger¹⁶⁷, F. Krieter¹¹⁴, A. Krishnan^{61b}, M. Krivos¹⁴², K. Krizka¹⁸, K. Kroeninger⁴⁷, H. Kroha¹¹⁵, J. Kroll¹⁴⁰, J. Kroll¹³⁶, K.S. Krowpman¹⁰⁷, U. Kruchonak⁸⁰, H. Krüger²⁴, N. Krumnack⁷⁹, M.C. Kruse⁴⁹, J.A. Krzysiak⁸⁵, A. Kubota¹⁶⁵, O. Kuchinskaia¹⁶⁶, S. Kудay^{4b}, D. Kuechler⁴⁶, J.T. Kuechler⁴⁶, S. Kuehn³⁶, T. Kuhl⁴⁶, V. Kukhtin⁸⁰, Y. Kulchitsky^{108,af}, S. Kuleshov^{146b}, Y.P. Kulinich¹⁷³, M. Kuna⁵⁸, A. Kupco¹⁴⁰, T. Kupfer⁴⁷, O. Kuprash⁵², H. Kurashige⁸³, L.L. Kurchaninov^{168a}, Y.A. Kurochkin¹⁰⁸, A. Kurova¹¹², M.G. Kurth^{15a,15d}, E.S. Kuwertz³⁶, M. Kuze¹⁶⁵, A.K. Kvam¹⁴⁸, J. Kvita¹³⁰, T. Kwan¹⁰⁴, F. La Ruffa^{41b,41a}, C. Lacasta¹⁷⁴, F. Lacava^{73a,73b}, D.P.J. Lack¹⁰¹, H. Lacker¹⁹, D. Lacour¹³⁵, E. Ladygin⁸⁰, R. Lafaye⁵, B. Laforge¹³⁵, T. Lagouri^{146c}, S. Lai⁵³, I.K. Lakomic^{84a}, J.E. Lambert¹²⁸, S. Lammers⁶⁶, W. Lampl⁷, C. Lampoudis¹⁶², E. Lançon²⁹, U. Landgraf⁵², M.P.J. Landon⁹³, V.S. Lang⁵², J.C. Lange⁵³, R.J. Langenberg¹⁰³, A.J. Lankford¹⁷¹, F. Lanni²⁹, K. Lantzscht²⁴, A. Lanza^{71a}, A. Lapertosa^{55b,55a}, J.F. Laporte¹⁴⁴, T. Lari^{69a}, F. Lasagni Manghi^{23b,23a}, M. Lassnig³⁶, V. Latonova¹⁴⁰, T.S. Lau^{63a},

A. Laudrain¹⁰⁰, A. Laurier³⁴, M. Lavorgna^{70a,70b}, S.D. Lawlor⁹⁴, M. Lazzaroni^{69a,69b}, B. Le¹⁰¹,
 E. Le Guirriec¹⁰², A. Lebedev⁷⁹, M. LeBlanc⁷, T. LeCompte⁶, F. Ledroit-Guillon⁵⁸, A.C.A. Lee⁹⁵,
 C.A. Lee²⁹, G.R. Lee¹⁷, L. Lee⁵⁹, S.C. Lee¹⁵⁸, S. Lee⁷⁹, B. Lefebvre^{168a}, H.P. Lefebvre⁹⁴, M. Lefebvre¹⁷⁶,
 C. Leggett¹⁸, K. Lehmann¹⁵², N. Lehmann²⁰, G. Lehmann Miotto³⁶, W.A. Leight⁴⁶, A. Leisos^{162,u},
 M.A.L. Leite^{81c}, C.E. Leitgeb¹¹⁴, R. Leitner¹⁴², K.J.C. Leney⁴², T. Lenz²⁴, S. Leone^{72a},
 C. Leonidopoulos⁵⁰, A. Leopold¹³⁵, C. Leroy¹¹⁰, R. Les¹⁰⁷, C.G. Lester³², M. Levchenko¹³⁷, J. Levêque⁵,
 D. Levin¹⁰⁶, L.J. Levinson¹⁸⁰, D.J. Lewis²¹, B. Li^{15b}, B. Li¹⁰⁶, C-Q. Li^{60c,60d}, F. Li^{60c}, H. Li^{60a}, H. Li^{60b},
 J. Li^{60c}, K. Li¹⁴⁸, L. Li^{60c}, M. Li^{15a,15d}, Q. Li^{15a,15d}, Q.Y. Li^{60a}, S. Li^{60d,60c}, X. Li⁴⁶, Y. Li⁴⁶, Z. Li^{60b},
 Z. Li¹³⁴, Z. Li¹⁰⁴, Z. Liang^{15a}, M. Liberatore⁴⁶, B. Liberti^{74a}, K. Lie^{63c}, S. Lim²⁹, C.Y. Lin³², K. Lin¹⁰⁷,
 R.A. Linck⁶⁶, R.E. Lindley⁷, J.H. Lindon²¹, A. Linss⁴⁶, A.L. Lioni⁵⁴, E. Lipeles¹³⁶, A. Lipniacka¹⁷,
 T.M. Liss^{173,al}, A. Lister¹⁷⁵, J.D. Little⁸, B. Liu⁷⁹, B.X. Liu¹⁵², H.B. Liu²⁹, J.B. Liu^{60a}, J.K.K. Liu³⁷,
 K. Liu^{60d,60c}, M. Liu^{60a}, M.Y. Liu^{60a}, P. Liu^{15a}, X. Liu^{60a}, Y. Liu⁴⁶, Y. Liu^{15a,15d}, Y.L. Liu¹⁰⁶, Y.W. Liu^{60a},
 M. Livan^{71a,71b}, A. Lleres⁵⁸, J. Llorente Merino¹⁵², S.L. Lloyd⁹³, C.Y. Lo^{63b}, E.M. Lobodzinska⁴⁶,
 P. Loch⁷, S. Loffredo^{74a,74b}, T. Lohse¹⁹, K. Lohwasser¹⁴⁹, M. Lokajicek¹⁴⁰, J.D. Long¹⁷³, R.E. Long⁹⁰,
 I. Longarini^{73a,73b}, L. Longo³⁶, K.A. Looper¹²⁷, I. Lopez Paz¹⁰¹, A. Lopez Solis¹⁴⁹, J. Lorenz¹¹⁴,
 N. Lorenzo Martinez⁵, A.M. Lory¹¹⁴, P.J. Lösel¹¹⁴, A. Lösle⁵², X. Lou^{45a,45b}, X. Lou^{15a}, A. Lounis⁶⁵,
 J. Love⁶, P.A. Love⁹⁰, J.J. Lozano Bahilo¹⁷⁴, M. Lu^{60a}, Y.J. Lu⁶⁴, H.J. Lubatti¹⁴⁸, C. Luci^{73a,73b},
 F.L. Lucio Alves^{15c}, A. Lucotte⁵⁸, F. Luehring⁶⁶, I. Luise¹⁵⁵, L. Luminari^{73a}, B. Lund-Jensen¹⁵⁴,
 N.A. Luongo¹³¹, M.S. Lutz¹⁶¹, D. Lynn²⁹, H. Lyons⁹¹, R. Lysak¹⁴⁰, E. Lytken⁹⁷, F. Lyu^{15a},
 V. Lyubushkin⁸⁰, T. Lyubushkina⁸⁰, H. Ma²⁹, L.L. Ma^{60b}, Y. Ma⁹⁵, D.M. Mac Donell¹⁷⁶, G. Maccarrone⁵¹,
 A. Macchiolo¹¹⁵, C.M. Macdonald¹⁴⁹, J.C. MacDonald¹⁴⁹, J. Machado Miguens¹³⁶, D. Madaffari¹⁷⁴,
 R. Madar³⁸, W.F. Mader⁴⁸, M. Madugoda Ralalage Don¹²⁹, N. Madysa⁴⁸, J. Maeda⁸³, T. Maeno²⁹,
 M. Maerker⁴⁸, V. Magerl⁵², N. Magini⁷⁹, J. Magro^{67a,67c,q}, D.J. Mahon³⁹, C. Maidantchik^{81b}, T. Maier¹¹⁴,
 A. Maio^{139a,139b,139d}, K. Maj^{84a}, O. Majersky^{28a}, S. Majewski¹³¹, Y. Makida⁸², N. Makovec⁶⁵,
 B. Malaescu¹³⁵, Pa. Malecki⁸⁵, V.P. Maleev¹³⁷, F. Malek⁵⁸, D. Malito^{41b,41a}, U. Mallik⁷⁸, C. Malone³²,
 S. Maltezos¹⁰, S. Malyukov⁸⁰, J. Mamuzic¹⁷⁴, G. Mancini⁵¹, C. Mancuso^{69b}, I. Mandić⁹²,
 L. Manhaes de Andrade Filho^{81a}, I.M. Maniatis¹⁶², J. Manjarres Ramos⁴⁸, K.H. Mankinen⁹⁷, A. Mann¹¹⁴,
 A. Manousos⁷⁷, B. Mansoulie¹⁴⁴, I. Mantos¹⁶², S. Manzoni¹²⁰, A. Marantis¹⁶², G. Marceca³⁰,
 L. Marchese¹³⁴, G. Marchiori¹³⁵, M. Marcisovsky¹⁴⁰, L. Marcoccia^{74a,74b}, C. Marcon⁹⁷, M. Marjanovic¹²⁸,
 Z. Marshall¹⁸, M.U.F. Martensson¹⁷², S. Marti-Garcia¹⁷⁴, C.B. Martin¹²⁷, T.A. Martin¹⁷⁸, V.J. Martin⁵⁰,
 B. Martin dit Latour¹⁷, L. Martinelli^{75a,75b}, M. Martinez^{14,w}, P. Martinez Agullo¹⁷⁴,
 V.I. Martinez Outschoorn¹⁰³, S. Martin-Haugh¹⁴³, V.S. Martoiu^{27b}, A.C. Martyniuk⁹⁵, A. Marzin³⁶,
 S.R. Maschek¹¹⁵, L. Masetti¹⁰⁰, T. Mashimo¹⁶³, R. Mashinistov¹¹¹, J. Masik¹⁰¹, A.L. Maslennikov^{122b,122a},
 L. Massa^{23b,23a}, P. Massarotti^{70a,70b}, P. Mastrandrea^{72a,72b}, A. Mastroberardino^{41b,41a}, T. Masubuchi¹⁶³,
 D. Matakias²⁹, A. Matic¹¹⁴, N. Matsuzawa¹⁶³, P. Mättig²⁴, J. Maurer^{27b}, B. Maček⁹²,
 D.A. Maximov^{122b,122a}, R. Mazini¹⁵⁸, I. Maznas¹⁶², S.M. Mazza¹⁴⁵, E. Mazzeo^{69b}, J.P. Mc Gowan¹⁰⁴,
 S.P. Mc Kee¹⁰⁶, T.G. McCarthy¹¹⁵, W.P. McCormack¹⁸, E.F. McDonald¹⁰⁵, A.E. McDougall¹²⁰,
 J.A. Mcfayden¹⁸, G. Mchedlidze^{159b}, M.A. McKay⁴², K.D. McLean¹⁷⁶, S.J. McMahon¹⁴³,
 P.C. McNamara¹⁰⁵, C.J. McNicol¹⁷⁸, R.A. McPherson^{176,ab}, J.E. Mdhluli^{33e}, Z.A. Meadows¹⁰³,
 S. Meehan³⁶, T. Megy³⁸, S. Mehlhase¹¹⁴, A. Mehta⁹¹, B. Meirose⁴³, D. Melini¹⁶⁰, B.R. Mellado Garcia^{33e},
 J.D. Mellenthin⁵³, M. Melo^{28a}, F. Meloni⁴⁶, A. Melzer²⁴, E.D. Mendes Gouveia^{139a,139e},
 A.M. Mendes Jacques Da Costa²¹, L. Meng³⁶, X.T. Meng¹⁰⁶, S. Menke¹¹⁵, E. Meoni^{41b,41a},
 S. Mergelmeyer¹⁹, S.A.M. Merkt¹³⁸, C. Merlassino¹³⁴, P. Mermod⁵⁴, L. Merola^{70a,70b}, C. Meroni^{69a},
 G. Merz¹⁰⁶, O. Meshkov^{113,111}, J.K.R. Meshreki¹⁵¹, J. Metcalfe⁶, A.S. Mete⁶, C. Meyer⁶⁶, J-P. Meyer¹⁴⁴,
 M. Michetti¹⁹, R.P. Middleton¹⁴³, L. Mijović⁵⁰, G. Mikenberg¹⁸⁰, M. Mikestikova¹⁴⁰, M. Mikuž⁹²,
 H. Mildner¹⁴⁹, A. Milic¹⁶⁷, C.D. Milke⁴², D.W. Miller³⁷, L.S. Miller³⁴, A. Milov¹⁸⁰, D.A. Milstead^{45a,45b},
 R.A. Mina¹⁵³, A.A. Minaenko¹²³, I.A. Minashvili^{159b}, L. Mince⁵⁷, A.I. Mincer¹²⁵, B. Mindur^{84a},

M. Mineev⁸⁰, Y. Minegishi¹⁶³, Y. Mino⁸⁶, L.M. Mir¹⁴, M. Mironova¹³⁴, K.P. Mistry¹³⁶, T. Mitani¹⁷⁹,
J. Mitrevski¹¹⁴, V.A. Mitsou¹⁷⁴, M. Mittal^{60c}, O. Miu¹⁶⁷, A. Miucci²⁰, P.S. Miyagawa⁹³, A. Mizukami⁸²,
J.U. Mjörnmark⁹⁷, T. Mkrtchyan^{61a}, M. Mlynarikova¹²¹, T. Moa^{45a,45b}, S. Mobius⁵³, K. Mochizuki¹¹⁰,
P. Moder⁴⁶, P. Mogg¹¹⁴, S. Mohapatra³⁹, R. Moles-Valls²⁴, K. Mönig⁴⁶, E. Monnier¹⁰², A. Montalbano¹⁵²,
J. Montejo Berlingen³⁶, M. Montella⁹⁵, F. Monticelli⁸⁹, S. Monzani^{69a}, N. Morange⁶⁵,
A.L. Moreira De Carvalho^{139a}, D. Moreno^{22a}, M. Moreno Llácer¹⁷⁴, C. Moreno Martinez¹⁴,
P. Morettini^{55b}, M. Morgenstern¹⁶⁰, S. Morgenstern⁴⁸, D. Mori¹⁵², M. Morii⁵⁹, M. Morinaga¹⁷⁹,
V. Morisbak¹³³, A.K. Morley³⁶, G. Mornacchi³⁶, A.P. Morris⁹⁵, L. Morvaj¹⁵⁵, P. Moschovakos³⁶,
B. Moser¹²⁰, M. Mosidze^{159b}, T. Moskalets¹⁴⁴, P. Moskvitina¹¹⁹, J. Moss^{31,m}, E.J.W. Moyse¹⁰³,
S. Muanza¹⁰², J. Mueller¹³⁸, R.S.P. Mueller¹¹⁴, D. Muenstermann⁹⁰, G.A. Mullier⁹⁷, D.P. Mungo^{69a,69b},
J.L. Munoz Martinez¹⁴, F.J. Munoz Sanchez¹⁰¹, P. Murin^{28b}, W.J. Murray^{178,143}, A. Murrone^{69a,69b},
J.M. Muse¹²⁸, M. Muškinja¹⁸, C. Mwewa^{33a}, A.G. Myagkov^{123,ah}, A.A. Myers¹³⁸, G. Myers⁶⁶,
J. Myers¹³¹, M. Myska¹⁴¹, B.P. Nachman¹⁸, O. Nackenhorst⁴⁷, A.Nag Nag⁴⁸, K. Nagai¹³⁴, K. Nagano⁸²,
Y. Nagasaka⁶², J.L. Nagle²⁹, E. Nagy¹⁰², A.M. Nairz³⁶, Y. Nakahama¹¹⁷, K. Nakamura⁸², T. Nakamura¹⁶³,
H. Nanjo¹³², F. Napolitano^{61a}, R.F. Naranjo Garcia⁴⁶, R. Narayan⁴², I. Naryshkin¹³⁷, L. Nasella^{69b},
M. Naseri³⁴, T. Naumann⁴⁶, G. Navarro^{22a}, P.Y. Nechaeva¹¹¹, F. Nechansky⁴⁶, T.J. Neep²¹, A. Negri^{71a,71b},
M. Negrini^{23b}, C. Nellist¹¹⁹, C. Nelson¹⁰⁴, M.E. Nelson^{45a,45b}, S. Nemecek¹⁴⁰, M. Nessi^{36,e},
M.S. Neubauer¹⁷³, F. Neuhaus¹⁰⁰, M. Neumann¹⁸², R. Newhouse¹⁷⁵, P.R. Newman²¹, C.W. Ng¹³⁸,
Y.S. Ng¹⁹, Y.W.Y. Ng¹⁷¹, B. Ngair^{35f}, H.D.N. Nguyen¹⁰², T. Nguyen Manh¹¹⁰, E. Nibigira³⁸,
R.B. Nickerson¹³⁴, R. Nicolaidou¹⁴⁴, D.S. Nielsen⁴⁰, J. Nielsen¹⁴⁵, M. Niemeyer⁵³, N. Nikiforou¹¹,
V. Nikolaenko^{123,ah}, I. Nikolic-Audit¹³⁵, K. Nikolopoulos²¹, P. Nilsson²⁹, H.R. Nindhito⁵⁴, A. Nisati^{73a},
N. Nishu^{60c}, R. Nisius¹¹⁵, I. Nitsche⁴⁷, T. Nitta¹⁷⁹, T. Nobe¹⁶³, D.L. Noel³², Y. Noguchi⁸⁶, I. Nomidis¹³⁵,
M.A. Nomura²⁹, M. Nordberg³⁶, J. Novak⁹², T. Novak⁹², O. Novgorodova⁴⁸, R. Novotny¹⁴¹, L. Nozka¹³⁰,
K. Ntekas¹⁷¹, E. Nurse⁹⁵, F.G. Oakham^{34,am}, H. Oberlack¹¹⁵, J. Ocariz¹³⁵, A. Ochi⁸³, I. Ochoa³⁹,
J.P. Ochoa-Ricoux^{146a}, K. O'Connor²⁶, S. Oda⁸⁸, S. Odaka⁸², S. Oerdek⁵³, A. Ogrodnik^{84a}, A. Oh¹⁰¹,
C.C. Ohm¹⁵⁴, H. Oide¹⁶⁵, M.L. Ojeda¹⁶⁷, H. Okawa¹⁶⁹, Y. Okazaki⁸⁶, M.W. O'Keefe⁹¹, Y. Okumura¹⁶³,
A. Olariu^{27b}, L.F. Oleiro Seabra^{139a}, S.A. Olivares Pino^{146a}, D. Oliveira Damazio²⁹, J.L. Oliver¹,
M.J.R. Olsson¹⁷¹, A. Olszewski⁸⁵, J. Olszowska⁸⁵, Ö.O. Öncel²⁴, D.C. O'Neil¹⁵², A.P. O'Neill¹³⁴,
A. Onofre^{139a,139e}, P.U.E. Onyisi¹¹, H. Oppen¹³³, R.G. Oreamuno Madriz¹²¹, M.J. Oreglia³⁷,
G.E. Orellana⁸⁹, D. Orestano^{75a,75b}, N. Orlando¹⁴, R.S. Orr¹⁶⁷, V. O'Shea⁵⁷, R. Ospanov^{60a},
G. Otero y Garzon³⁰, H. Otono⁸⁸, P.S. Ott^{61a}, G.J. Ottino¹⁸, M. Ouchrif^{35e}, J. Ouellette²⁹,
F. Ould-Saada¹³³, A. Ouraou^{144,*}, Q. Ouyang^{15a}, M. Owen⁵⁷, R.E. Owen¹⁴³, V.E. Ozcan^{12c}, N. Ozturk⁸,
J. Pacalt¹³⁰, H.A. Pacey³², K. Pachal⁴⁹, A. Pacheco Pages¹⁴, C. Padilla Aranda¹⁴, S. Pagan Griso¹⁸,
G. Palacino⁶⁶, S. Palazzo⁵⁰, S. Palestini³⁶, M. Palka^{84b}, P. Palmi^{84a}, C.E. Pandini⁵⁴,
J.G. Panduro Vazquez⁹⁴, P. Pani⁴⁶, G. Panizzo^{67a,67c}, L. Paolozzi⁵⁴, C. Papadatos¹¹⁰, K. Papageorgiou^{9,g},
S. Parajuli⁴², A. Paramonov⁶, C. Paraskevopoulos¹⁰, D. Paredes Hernandez^{63b}, S.R. Paredes Saenz¹³⁴,
B. Parida¹⁸⁰, T.H. Park¹⁶⁷, A.J. Parker³¹, M.A. Parker³², F. Parodi^{55b,55a}, E.W. Parrish¹²¹, J.A. Parsons³⁹,
U. Parzefall⁵², L. Pascual Dominguez¹³⁵, V.R. Pascuzzi¹⁸, J.M.P. Pasner¹⁴⁵, F. Pasquali¹²⁰,
E. Pasqualucci^{73a}, S. Passaggio^{55b}, F. Pastore⁹⁴, P. Pasuwan^{45a,45b}, S. Patariaia¹⁰⁰, J.R. Pater¹⁰¹,
A. Pathak^{181,i}, J. Patton⁹¹, T. Pauly³⁶, J. Parkes¹⁵³, B. Pearson¹¹⁵, M. Pedersen¹³³, L. Pedraza Diaz¹¹⁹,
R. Pedro^{139a}, T. Peiffer⁵³, S.V. Peleganchuk^{122b,122a}, O. Penc¹⁴⁰, C. Peng^{63b}, H. Peng^{60a}, B.S. Peralva^{81a},
M.M. Perego⁶⁵, A.P. Pereira Peixoto^{139a}, L. Pereira Sanchez^{45a,45b}, D.V. Perepelitsa²⁹, E. Perez Codina^{168a},
F. Peri¹⁹, L. Perini^{69a,69b}, H. Pernegger³⁶, S. Perrella³⁶, A. Perrevoort¹²⁰, K. Peters⁴⁶, R.F.Y. Peters¹⁰¹,
B.A. Petersen³⁶, T.C. Petersen⁴⁰, E. Petit¹⁰², V. Petousis¹⁴¹, C. Petridou¹⁶², F. Petrucci^{75a,75b}, M. Pettee¹⁸³,
N.E. Pettersson¹⁰³, K. Petukhova¹⁴², A. Peyaud¹⁴⁴, R. Pezoa^{146d}, L. Pezzotti^{71a,71b}, T. Pham¹⁰⁵,
P.W. Phillips¹⁴³, M.W. Phipps¹⁷³, G. Piacquadio¹⁵⁵, E. Pianori¹⁸, F. Piazza^{69b}, A. Picazio¹⁰³,
R.H. Pickles¹⁰¹, R. Piegai³⁰, D. Pietreanu^{27b}, J.E. Pilcher³⁷, A.D. Pilkington¹⁰¹, M. Pinamonti^{67a,67c},

J.L. Pinfeld³, C. Pitman Donaldson⁹⁵, M. Pitt¹⁶¹, L. Pizzimento^{74a,74b}, A. Pizzini¹²⁰, M.-A. Pleier²⁹, V. Plesanovs⁵², V. Pleskot¹⁴², E. Plotnikova⁸⁰, P. Podberezko^{122b,122a}, R. Poettgen⁹⁷, R. Poggi⁵⁴, L. Poggioli¹³⁵, I. Pogrebnyak¹⁰⁷, D. Pohl²⁴, I. Pokharel⁵³, G. Polesello^{71a}, A. Poley^{152,168a}, A. Policicchio^{73a,73b}, R. Polifka¹⁴², A. Polini^{23b}, C.S. Pollard⁴⁶, V. Polychronakos²⁹, D. Ponomarenko¹¹², L. Pontecorvo³⁶, S. Popa^{27a}, G.A. Popeneciu^{27d}, L. Portales⁵, D.M. Portillo Quintero⁵⁸, S. Pospisil¹⁴¹, K. Potamianos⁴⁶, I.N. Potrap⁸⁰, C.J. Potter³², H. Potti¹¹, T. Poulsen⁹⁷, J. Poveda¹⁷⁴, T.D. Powell¹⁴⁹, G. Pownall⁴⁶, M.E. Pozo Astigarraga³⁶, A. Prades Ibanez¹⁷⁴, P. Pralavorio¹⁰², M.M. Prapa⁴⁴, S. Prell⁷⁹, D. Price¹⁰¹, M. Primavera^{68a}, M.L. Proffitt¹⁴⁸, N. Proklova¹¹², K. Prokofiev^{63c}, F. Prokoshin⁸⁰, S. Protopopescu²⁹, J. Proudfoot⁶, M. Przybycien^{84a}, D. Pudzha¹³⁷, A. Puri¹⁷³, P. Puzo⁶⁵, D. Pyatiizbyantseva¹¹², J. Qian¹⁰⁶, Y. Qin¹⁰¹, A. Quadt⁵³, M. Queitsch-Maitland³⁶, M. Racko^{28a}, F. Ragusa^{69a,69b}, G. Rahal⁹⁸, J.A. Raine⁵⁴, S. Rajagopalan²⁹, A. Ramirez Morales⁹³, K. Ran^{15a,15d}, D.M. Rauch⁴⁶, F. Rauscher¹¹⁴, S. Rave¹⁰⁰, B. Ravina⁵⁷, I. Ravinovich¹⁸⁰, J.H. Rawling¹⁰¹, M. Raymond³⁶, A.L. Read¹³³, N.P. Readioff¹⁴⁹, M. Reale^{68a,68b}, D.M. Rebutzi^{71a,71b}, G. Redlinger²⁹, K. Reeves⁴³, D. Reikher¹⁶¹, A. Reiss¹⁰⁰, A. Rej¹⁵¹, C. Rembser³⁶, A. Renardi⁴⁶, M. Renda^{27b}, M.B. Rendel¹¹⁵, A.G. Rennie⁵⁷, S. Resconi^{69a}, E.D. Resseguie¹⁸, S. Rettie⁹⁵, B. Reynolds¹²⁷, E. Reynolds²¹, O.L. Rezanova^{122b,122a}, P. Reznicek¹⁴², E. Ricci^{76a,76b}, R. Richter¹¹⁵, S. Richter⁴⁶, E. Richter-Was^{84b}, M. Ridel¹³⁵, P. Rieck¹¹⁵, O. Rifki⁴⁶, M. Rijssenbeek¹⁵⁵, A. Rimoldi^{71a,71b}, M. Rimoldi⁴⁶, L. Rinaldi^{23b}, T.T. Rinn¹⁷³, G. Ripellino¹⁵⁴, I. Riu¹⁴, P. Rivadeneira⁴⁶, J.C. Rivera Vergara¹⁷⁶, F. Rizatdinova¹²⁹, E. Rizvi⁹³, C. Rizzi³⁶, S.H. Robertson^{104,ab}, M. Robin⁴⁶, D. Robinson³², C.M. Robles Gajardo^{146d}, M. Robles Manzano¹⁰⁰, A. Robson⁵⁷, A. Rocchi^{74a,74b}, E. Rocco¹⁰⁰, C. Roda^{72a,72b}, S. Rodriguez Bosca¹⁷⁴, A. Rodriguez Rodriguez⁵², A.M. Rodríguez Vera^{168b}, S. Roe³⁶, J. Roggel¹⁸², O. Røhne¹³³, R. Röhrig¹¹⁵, R.A. Rojas^{146d}, B. Roland⁵², C.P.A. Roland⁶⁶, J. Roloff²⁹, A. Romaniouk¹¹², M. Romano^{23b,23a}, N. Rompotis⁹¹, M. Ronzani¹²⁵, L. Roos¹³⁵, S. Rosati^{73a}, G. Rosin¹⁰³, B.J. Rosser¹³⁶, E. Rossi⁴⁶, E. Rossi^{75a,75b}, E. Rossi^{70a,70b}, L.P. Rossi^{55b}, L. Rossini⁴⁶, R. Rosten¹⁴, M. Rotaru^{27b}, B. Rottler⁵², D. Rousseau⁶⁵, G. Rovelli^{71a,71b}, A. Roy¹¹, D. Roy^{33e}, A. Rozanov¹⁰², Y. Rozen¹⁶⁰, X. Ruan^{33e}, T.A. Ruggeri¹, F. Rühr⁵², A. Ruiz-Martinez¹⁷⁴, A. Rummeler³⁶, Z. Rurikova⁵², N.A. Rusakovich⁸⁰, H.L. Russell¹⁰⁴, L. Rustige^{38,47}, J.P. Rutherford⁷, E.M. Rüttinger¹⁴⁹, M. Rybar¹⁴², G. Rybkin⁶⁵, E.B. Rye¹³³, A. Ryzhov¹²³, J.A. Sabater Iglesias⁴⁶, P. Sabatini¹⁷⁴, L. Sabetta^{73a,73b}, S. Sacerdoti⁶⁵, H.F.W. Sadrozinski¹⁴⁵, R. Sadykov⁸⁰, F. Safai Tehrani^{73a}, B. Safarzadeh Samani¹⁵⁶, M. Safdari¹⁵³, P. Saha¹²¹, S. Saha¹⁰⁴, M. Sahinsoy¹¹⁵, A. Sahu¹⁸², M. Saimpert³⁶, M. Saito¹⁶³, T. Saito¹⁶³, H. Sakamoto¹⁶³, D. Salamani⁵⁴, G. Salamanna^{75a,75b}, A. Salnikov¹⁵³, J. Salt¹⁷⁴, A. Salvador Salas¹⁴, D. Salvatore^{41b,41a}, F. Salvatore¹⁵⁶, A. Salvucci^{63a}, A. Salzburger³⁶, J. Samarati³⁶, D. Sammel⁵², D. Sampsonidis¹⁶², D. Sampsonidou¹⁶², J. Sánchez¹⁷⁴, A. Sanchez Pineda^{67a,36,67c}, H. Sandaker¹³³, C.O. Sander⁴⁶, I.G. Sanderswood⁹⁰, M. Sandhoff¹⁸², C. Sandoval^{22b}, D.P.C. Sankey¹⁴³, M. Sannino^{55b,55a}, Y. Sano¹¹⁷, A. Sansoni⁵¹, C. Santoni³⁸, H. Santos^{139a,139b}, S.N. Santpur¹⁸, A. Santra¹⁷⁴, K.A. Saoucha¹⁴⁹, A. Saprnov⁸⁰, J.G. Saraiva^{139a,139d}, O. Sasaki⁸², K. Sato¹⁶⁹, F. Sauerburger⁵², E. Sauvan⁵, P. Savard^{167,am}, R. Sawada¹⁶³, C. Sawyer¹⁴³, L. Sawyer^{96,ag}, I. Sayago Galvan¹⁷⁴, C. Sbarra^{23b}, A. Sbrizzi^{67a,67c}, T. Scanlon⁹⁵, J. Schaarschmidt¹⁴⁸, P. Schacht¹¹⁵, D. Schaefer³⁷, L. Schaefer¹³⁶, U. Schäfer¹⁰⁰, A.C. Schaffer⁶⁵, D. Schaile¹¹⁴, R.D. Schamberger¹⁵⁵, E. Schanet¹¹⁴, C. Scharf¹⁹, N. Scharmberg¹⁰¹, V.A. Schegelsky¹³⁷, D. Scheirich¹⁴², F. Schenck¹⁹, M. Schernau¹⁷¹, C. Schiavi^{55b,55a}, L.K. Schildgen²⁴, Z.M. Schillaci²⁶, E.J. Schioppa^{68a,68b}, M. Schioppa^{41b,41a}, K.E. Schleicher⁵², S. Schlenker³⁶, K.R. Schmidt-Sommerfeld¹¹⁵, K. Schmieden¹⁰⁰, C. Schmitt¹⁰⁰, S. Schmitt⁴⁶, L. Schoeffel¹⁴⁴, A. Schoening^{61b}, P.G. Scholer⁵², E. Schopf¹³⁴, M. Schott¹⁰⁰, J.F.P. Schouwenberg¹¹⁹, J. Schovancova³⁶, S. Schramm⁵⁴, F. Schroeder¹⁸², A. Schulte¹⁰⁰, H-C. Schultz-Coulon^{61a}, M. Schumacher⁵², B.A. Schumm¹⁴⁵, Ph. Schune¹⁴⁴, A. Schwartzman¹⁵³, T.A. Schwarz¹⁰⁶, Ph. Schwemling¹⁴⁴, R. Schwienhorst¹⁰⁷, A. Sciandra¹⁴⁵, G. Sciolla²⁶, M. Scornajenghi^{41b,41a}, F. Scuri^{72a}, F. Scutti¹⁰⁵, L.M. Scyboz¹¹⁵, C.D. Sebastiani⁹¹, K. Sedlaczek⁴⁷, P. Seema¹⁹, S.C. Seidel¹¹⁸, A. Seiden¹⁴⁵,

B.D. Seidlitz²⁹, T. Seiss³⁷, C. Seitz⁴⁶, J.M. Seixas^{81b}, G. Sekhniadze^{70a}, S.J. Sekula⁴²,
 N. Semprini-Cesari^{23b,23a}, S. Sen⁴⁹, C. Serfon²⁹, L. Serin⁶⁵, L. Serkin^{67a,67b}, M. Sessa^{60a}, H. Severini¹²⁸,
 S. Sevova¹⁵³, F. Sforza^{55b,55a}, A. Sfyrla⁵⁴, E. Shabalina⁵³, J.D. Shahinian¹³⁶, N.W. Shaikh^{45a,45b},
 D. Shaked Renous¹⁸⁰, L.Y. Shan^{15a}, M. Shapiro¹⁸, A. Sharma³⁶, A.S. Sharma¹, P.B. Shatalov¹²⁴,
 K. Shaw¹⁵⁶, S.M. Shaw¹⁰¹, M. Shehade¹⁸⁰, Y. Shen¹²⁸, A.D. Sherman²⁵, P. Sherwood⁹⁵, L. Shi⁹⁵,
 C.O. Shimmin¹⁸³, Y. Shimogama¹⁷⁹, M. Shimojima¹¹⁶, J.D. Shinner⁹⁴, I.P.J. Shipsey¹³⁴, S. Shirabe¹⁶⁵,
 M. Shiyakova^{80,z}, J. Shlomi¹⁸⁰, A. Shmeleva¹¹¹, M.J. Shochet³⁷, J. Shojaii¹⁰⁵, D.R. Shope¹⁵⁴,
 S. Shrestha¹²⁷, E.M. Shrif^{33e}, M.J. Shroff¹⁷⁶, E. Shulga¹⁸⁰, P. Sicho¹⁴⁰, A.M. Sickles¹⁷³,
 E. Sideras Haddad^{33e}, O. Sidiropoulou³⁶, A. Sidoti^{23b,23a}, F. Siegert⁴⁸, Dj. Sijacki¹⁶, M.Jr. Silva¹⁸¹,
 M.V. Silva Oliveira³⁶, S.B. Silverstein^{45a}, S. Simion⁶⁵, R. Simoniello¹⁰⁰, C.J. Simpson-allso²¹,
 S. Simsek^{12b}, P. Sinervo¹⁶⁷, V. Sinetckii¹¹³, S. Singh¹⁵², M. Sioli^{23b,23a}, I. Siral¹³¹, S.Yu. Sivoklov¹¹³,
 J. Sjölin^{45a,45b}, A. Skaf⁵³, E. Skorda⁹⁷, P. Skubic¹²⁸, M. Slawinska⁸⁵, K. Sliwa¹⁷⁰, R. Slovak¹⁴²,
 V. Smakhtin¹⁸⁰, B.H. Smart¹⁴³, J. Smiesko^{28b}, N. Smirnov¹¹², S.Yu. Smirnov¹¹², Y. Smirnov¹¹²,
 L.N. Smirnova^{113,r}, O. Smirnova⁹⁷, E.A. Smith³⁷, H.A. Smith¹³⁴, M. Smizanska⁹⁰, K. Smolek¹⁴¹,
 A. Smykiewicz⁸⁵, A.A. Snasarev¹¹¹, H.L. Snoek¹²⁰, I.M. Snyder¹³¹, S. Snyder²⁹, R. Sobie^{176,ab},
 A. Soffer¹⁶¹, A. Sögaard⁵⁰, F. Sohns⁵³, C.A. Solans Sanchez³⁶, E.Yu. Soldatov¹¹², U. Soldevila¹⁷⁴,
 A.A. Solodkov¹²³, A. Soloshenko⁸⁰, O.V. Solovyanov¹²³, V. Solovyev¹³⁷, P. Sommer¹⁴⁹, H. Son¹⁷⁰,
 A. Sonay¹⁴, W. Song¹⁴³, W.Y. Song^{168b}, A. Sopczak¹⁴¹, A.L. Soppio⁹⁵, F. Sopkova^{28b},
 S. Sottocornola^{71a,71b}, R. Soualah^{67a,67c}, A.M. Soukharev^{122b,122a}, D. South⁴⁶, S. Spagnolo^{68a,68b},
 M. Spalla¹¹⁵, M. Spangenberg¹⁷⁸, F. Spanò⁹⁴, D. Sperlich⁵², T.M. Spieker^{61a}, G. Spigo³⁶, M. Spina¹⁵⁶,
 D.P. Spiteri⁵⁷, M. Spousta¹⁴², A. Stabile^{69a,69b}, B.L. Stamas¹²¹, R. Stamen^{61a}, M. Stamenkovic¹²⁰,
 A. Stampeki²¹, E. Stanecka⁸⁵, B. Stanislaus¹³⁴, M.M. Stanitzki⁴⁶, M. Stankaityte¹³⁴, B. Stapf¹²⁰,
 E.A. Starchenko¹²³, G.H. Stark¹⁴⁵, J. Stark⁵⁸, P. Staroba¹⁴⁰, P. Starovoitov^{61a}, S. Stärz¹⁰⁴, R. Staszewski⁸⁵,
 G. Stavropoulos⁴⁴, M. Stegler⁴⁶, P. Steinberg²⁹, A.L. Steinhebel¹³¹, B. Stelzer^{152,168a}, H.J. Stelzer¹³⁸,
 O. Stelzer-Chilton^{168a}, H. Stenzel⁵⁶, T.J. Stevenson¹⁵⁶, G.A. Stewart³⁶, M.C. Stockton³⁶, G. Stoicea^{27b},
 M. Stolarski^{139a}, S. Stonjek¹¹⁵, A. Straessner⁴⁸, J. Strandberg¹⁵⁴, S. Strandberg^{45a,45b}, M. Strauss¹²⁸,
 T. Strebler¹⁰², P. Strizenec^{28b}, R. Ströhmer¹⁷⁷, D.M. Strom¹³¹, R. Stroynowski⁴², A. Strubig^{45a,45b},
 S.A. Stucci²⁹, B. Stugu¹⁷, J. Stupak¹²⁸, N.A. Styles⁴⁶, D. Su¹⁵³, W. Su^{60c,148}, X. Su^{60a}, V.V. Sulin¹¹¹,
 M.J. Sullivan⁹¹, D.M.S. Sultan⁵⁴, S. Sultansoy^{4c}, T. Sumida⁸⁶, S. Sun¹⁰⁶, X. Sun¹⁰¹, C.J.E. Suster¹⁵⁷,
 M.R. Sutton¹⁵⁶, S. Suzuki⁸², M. Svatos¹⁴⁰, M. Swiatlowski^{168a}, S.P. Swift², T. Swirski¹⁷⁷,
 A. Sydorenko¹⁰⁰, I. Sykora^{28a}, M. Sykora¹⁴², T. Sykora¹⁴², D. Ta¹⁰⁰, K. Tackmann^{46,x}, J. Taenzer¹⁶¹,
 A. Taffard¹⁷¹, R. Tafirout^{168a}, E. Tagiev¹²³, R. Takashima⁸⁷, K. Takeda⁸³, T. Takeshita¹⁵⁰, E.P. Takeva⁵⁰,
 Y. Takubo⁸², M. Talby¹⁰², A.A. Talyshev^{122b,122a}, K.C. Tam^{63b}, N.M. Tamir¹⁶¹, J. Tanaka¹⁶³, R. Tanaka⁶⁵,
 S. Tapia Araya¹⁷³, S. Tapprogge¹⁰⁰, A. Tarek Abouelfadl Mohamed¹⁰⁷, S. Tarem¹⁶⁰, K. Tariq^{60b},
 G. Tarna^{27b,d}, G.F. Tartarelli^{69a}, P. Tas¹⁴², M. Tasevsky¹⁴⁰, E. Tassi^{41b,41a}, A. Tavares Delgado^{139a},
 Y. Tayalati^{35f}, A.J. Taylor⁵⁰, G.N. Taylor¹⁰⁵, W. Taylor^{168b}, H. Teagle⁹¹, A.S. Tee⁹⁰,
 R. Teixeira De Lima¹⁵³, P. Teixeira-Dias⁹⁴, H. Ten Kate³⁶, J.J. Teoh¹²⁰, K. Terashi¹⁶³, J. Terron⁹⁹,
 S. Terzo¹⁴, M. Testa⁵¹, R.J. Teuscher^{167,ab}, S.J. Thais¹⁸³, N. Themistokleous⁵⁰, T. Thevenaux-Pelzer⁴⁶,
 F. Thiele⁴⁰, D.W. Thomas⁹⁴, J.O. Thomas⁴², J.P. Thomas²¹, E.A. Thompson⁴⁶, P.D. Thompson²¹,
 E. Thomson¹³⁶, E.J. Thorpe⁹³, R.E. Ticse Torres⁵³, V.O. Tikhomirov^{111,ai}, Yu.A. Tikhonov^{122b,122a},
 S. Timoshenko¹¹², P. Tipton¹⁸³, S. Tisserant¹⁰², K. Todome^{23b,23a}, S. Todorova-Nova¹⁴², S. Todt⁴⁸,
 J. Tojo⁸⁸, S. Tokár^{28a}, K. Tokushuku⁸², E. Tolley¹²⁷, R. Tombs³², K.G. Tomiwa^{33e}, M. Tomoto^{82,117},
 L. Tompkins¹⁵³, P. Tornambe¹⁰³, E. Torrence¹³¹, H. Torres⁴⁸, E. Torró Pastor¹⁷⁴, M. Toscani³⁰,
 C. Toscirri¹³⁴, J. Toth^{102,aa}, D.R. Tovey¹⁴⁹, A. Traet¹⁷, C.J. Treado¹²⁵, T. Trefzger¹⁷⁷, F. Tresoldi¹⁵⁶,
 A. Tricoli²⁹, I.M. Trigger^{168a}, S. Trincaz-Duvoid¹³⁵, D.A. Trischuk¹⁷⁵, W. Trischuk¹⁶⁷, B. Trocme⁵⁸,
 A. Trofymov⁶⁵, C. Troncon^{69a}, F. Trovato¹⁵⁶, L. Truong^{33c}, M. Trzebinski⁸⁵, A. Trzupek⁸⁵, F. Tsai⁴⁶,
 J.C-L. Tseng¹³⁴, P.V. Tsiarshka^{108,af}, A. Tsirigotis^{162,u}, V. Tsiskaridze¹⁵⁵, E.G. Tskhadadze^{159a},

M. Tsopoulou¹⁶², I.I. Tsukerman¹²⁴, V. Tsulaia¹⁸, S. Tsuno⁸², D. Tsybychev¹⁵⁵, Y. Tu^{63b}, A. Tudorache^{27b},
V. Tudorache^{27b}, T.T. Tulbure^{27a}, A.N. Tuna⁵⁹, S. Turchikhin⁸⁰, D. Turgeman¹⁸⁰, I. Turk Cakir^{4b,s},
R.J. Turner²¹, R. Turra^{69a}, P.M. Tuts³⁹, S. Tzamarias¹⁶², E. Tzovara¹⁰⁰, K. Uchida¹⁶³, F. Ukegawa¹⁶⁹,
G. Unal³⁶, M. Unal¹¹, A. Undrus²⁹, G. Unel¹⁷¹, F.C. Ungaro¹⁰⁵, Y. Unno⁸², K. Uno¹⁶³, J. Urban^{28b},
P. Urquijo¹⁰⁵, G. Usai⁸, Z. Uysal^{12d}, V. Vacek¹⁴¹, B. Vachon¹⁰⁴, K.O.H. Vadla¹³³, T. Vafeiadis³⁶,
A. Vaidya⁹⁵, C. Valderanis¹¹⁴, E. Valdes Santurio^{45a,45b}, M. Valente^{168a}, S. Valentini^{23b,23a},
A. Valero¹⁷⁴, L. Valéry⁴⁶, R.A. Vallance²¹, A. Vallier³⁶, J.A. Valls Ferrer¹⁷⁴, T.R. Van Daalen¹⁴,
P. Van Gemmeren⁶, S. Van Stroud⁹⁵, I. Van Vulpen¹²⁰, M. Vanadia^{74a,74b}, W. Vandelli³⁶,
M. Vandenbroucke¹⁴⁴, E.R. Vandewall¹²⁹, A. Vaniachine¹⁶⁶, D. Vannicola^{73a,73b}, R. Vari^{73a}, E.W. Varnes⁷,
C. Varni^{55b,55a}, T. Varol¹⁵⁸, D. Varouchas⁶⁵, K.E. Varvell¹⁵⁷, M.E. Vasile^{27b}, G.A. Vasquez¹⁷⁶,
F. Vazeille³⁸, D. Vazquez Furelos¹⁴, T. Vazquez Schroeder³⁶, J. Veatch⁵³, V. Vecchio¹⁰¹, M.J. Veen¹²⁰,
L.M. Veloce¹⁶⁷, F. Veloso^{139a,139c}, S. Veneziano^{73a}, A. Ventura^{68a,68b}, A. Verbytskyi¹¹⁵, V. Vercesi^{71a},
M. Verducci^{72a,72b}, C.M. Vergel Infante⁷⁹, C. Vergis²⁴, W. Verkerke¹²⁰, A.T. Vermeulen¹²⁰,
J.C. Vermeulen¹²⁰, C. Vernieri¹⁵³, P.J. Verschuuren⁹⁴, M.C. Vetterli^{152,am}, N. Viaux Maira^{146d},
T. Vickey¹⁴⁹, O.E. Vickey Boeriu¹⁴⁹, G.H.A. Viehhauser¹³⁴, L. Vignani^{61b}, M. Villa^{23b,23a},
M. Villaplana Perez³, E.M. Villhauer⁵⁰, E. Vilucchi⁵¹, M.G. Vincker³⁴, G.S. Virdee²¹, A. Vishwakarma⁵⁰,
C. Vittori^{23b,23a}, I. Vivarelli¹⁵⁶, M. Vogel¹⁸², P. Vokac¹⁴¹, S.E. von Buddenbrock^{33e}, E. Von Toerne²⁴,
V. Vorobel¹⁴², K. Vorobev¹¹², M. Vos¹⁷⁴, J.H. Vosseveld⁹¹, M. Vozak¹⁰¹, N. Vranjes¹⁶,
M. Vranjes Milosavljevic¹⁶, V. Vrba¹⁴¹, M. Vreeswijk¹²⁰, N.K. Vu¹⁰², R. Vuillermet³⁶, I. Vukotic³⁷,
S. Wada¹⁶⁹, P. Wagner²⁴, W. Wagner¹⁸², J. Wagner-Kuhr¹¹⁴, S. Wahdan¹⁸², H. Wahlberg⁸⁹, R. Wakasa¹⁶⁹,
V.M. Walbrecht¹¹⁵, J. Walder¹⁴³, R. Walker¹¹⁴, S.D. Walker⁹⁴, W. Walkowiak¹⁵¹, V. Wallangen^{45a,45b},
A.M. Wang⁵⁹, A.Z. Wang¹⁸¹, C. Wang^{60a}, C. Wang^{60c}, F. Wang¹⁸¹, H. Wang¹⁸, H. Wang³, J. Wang^{63a},
P. Wang⁴², Q. Wang¹²⁸, R.-J. Wang¹⁰⁰, R. Wang^{60a}, R. Wang⁶, S.M. Wang¹⁵⁸, W.T. Wang^{60a}, W. Wang^{15c},
W.X. Wang^{60a}, Y. Wang^{60a}, Z. Wang¹⁰⁶, C. Wanotayaroj⁴⁶, A. Warburton¹⁰⁴, C.P. Ward³², R.J. Ward²¹,
N. Warrack⁵⁷, A.T. Watson²¹, M.F. Watson²¹, G. Watts¹⁴⁸, B.M. Waugh⁹⁵, A.F. Webb¹¹, C. Weber²⁹,
M.S. Weber²⁰, S.A. Weber³⁴, S.M. Weber^{61a}, A.R. Weidberg¹³⁴, J. Weingarten⁴⁷, M. Weirich¹⁰⁰,
C. Weiser⁵², P.S. Wells³⁶, T. Wenaus²⁹, B. Wendland⁴⁷, T. Wengler³⁶, S. Wenig³⁶, N. Wermes²⁴,
M. Wessels^{61a}, T.D. Weston²⁰, K. Whalen¹³¹, A.M. Wharton⁹⁰, A.S. White¹⁰⁶, A. White⁸, M.J. White¹,
D. Whiteson¹⁷¹, B.W. Whitmore⁹⁰, W. Wiedenmann¹⁸¹, C. Wiel⁴⁸, M. Wielers¹⁴³, N. Wieseotte¹⁰⁰,
C. Wiglesworth⁴⁰, L.A.M. Wiik-Fuchs⁵², H.G. Wilkens³⁶, L.J. Wilkins⁹⁴, H.H. Williams¹³⁶,
S. Williams³², S. Willocq¹⁰³, P.J. Windischhofer¹³⁴, I. Wingerter-Seez⁵, E. Winkels¹⁵⁶, F. Winklmeier¹³¹,
B.T. Winter⁵², M. Wittgen¹⁵³, M. Wobisch⁹⁶, A. Wolf¹⁰⁰, R. Wölker¹³⁴, J. Wollrath⁵², M.W. Wolter⁸⁵,
H. Wolters^{139a,139c}, V.W.S. Wong¹⁷⁵, N.L. Woods¹⁴⁵, S.D. Worm⁴⁶, B.K. Wosiek⁸⁵, K.W. Woźniak⁸⁵,
K. Wraight⁵⁷, S.L. Wu¹⁸¹, X. Wu⁵⁴, Y. Wu^{60a}, J. Wuerzinger¹³⁴, T.R. Wyatt¹⁰¹, B.M. Wynne⁵⁰, S. Xella⁴⁰,
L. Xia¹⁷⁸, J. Xiang^{63c}, X. Xiao¹⁰⁶, X. Xie^{60a}, I. Xiotidis¹⁵⁶, D. Xu^{15a}, H. Xu^{60a}, H. Xu^{60a}, L. Xu²⁹,
T. Xu¹⁴⁴, W. Xu¹⁰⁶, Y. Xu^{15b}, Z. Xu^{60b}, Z. Xu¹⁵³, B. Yabsley¹⁵⁷, S. Yacoub^{33a}, D.P. Yallup⁹⁵,
N. Yamaguchi⁸⁸, Y. Yamaguchi¹⁶⁵, A. Yamamoto⁸², M. Yamatani¹⁶³, T. Yamazaki¹⁶³, Y. Yamazaki⁸³,
J. Yan^{60c}, Z. Yan²⁵, H.J. Yang^{60c,60d}, H.T. Yang¹⁸, S. Yang^{60a}, T. Yang^{63c}, X. Yang^{60b,58}, Y. Yang¹⁶³,
Z. Yang^{60a}, W.-M. Yao¹⁸, Y.C. Yap⁴⁶, E. Yatsenko^{60c}, H. Ye^{15c}, J. Ye⁴², S. Ye²⁹, I. Yeletsikh⁸⁰,
M.R. Yexley⁹⁰, E. Yigitbasi²⁵, P. Yin³⁹, K. Yorita¹⁷⁹, K. Yoshihara⁷⁹, C.J.S. Young³⁶, C. Young¹⁵³,
J. Yu⁷⁹, R. Yuan^{60b,h}, X. Yue^{61a}, M. Zaazoua^{35f}, B. Zabinski⁸⁵, G. Zacharis¹⁰, E. Zaffaroni⁵⁴,
J. Zahreddine¹³⁵, A.M. Zaitsev^{123,ah}, T. Zakareishvili^{159b}, N. Zakharchuk³⁴, S. Zambito³⁶, D. Zanzi³⁶,
S.V. Zeißner⁴⁷, C. Zeitnitz¹⁸², G. Zemaityte¹³⁴, J.C. Zeng¹⁷³, O. Zenin¹²³, T. Ženiš^{28a}, D. Zerwas⁶⁵,
M. Zgubic¹³⁴, B. Zhang^{15c}, D.F. Zhang^{15b}, G. Zhang^{15b}, J. Zhang⁶, K. Zhang^{15a}, L. Zhang^{15c}, L. Zhang^{60a},
M. Zhang¹⁷³, R. Zhang¹⁸¹, S. Zhang¹⁰⁶, X. Zhang^{60c}, X. Zhang^{60b}, Y. Zhang^{15a,15d}, Z. Zhang^{63a},
Z. Zhang⁶⁵, P. Zhao⁴⁹, Y. Zhao¹⁴⁵, Z. Zhao^{60a}, A. Zhemchugov⁸⁰, Z. Zheng¹⁰⁶, D. Zhong¹⁷³, B. Zhou¹⁰⁶,
C. Zhou¹⁸¹, H. Zhou⁷, M.S. Zhou^{15a,15d}, M. Zhou¹⁵⁵, N. Zhou^{60c}, Y. Zhou⁷, C.G. Zhu^{60b}, C. Zhu^{15a,15d},

H.L. Zhu^{60a}, H. Zhu^{15a}, J. Zhu¹⁰⁶, Y. Zhu^{60a}, X. Zhuang^{15a}, K. Zhukov¹¹¹, V. Zhulanov^{122b,122a}, D. Zieminska⁶⁶, N.I. Zimine⁸⁰, S. Zimmermann^{52,*}, Z. Zinonos¹¹⁵, M. Ziolkowski¹⁵¹, L. Živković¹⁶, G. Zobernig¹⁸¹, A. Zoccoli^{23b,23a}, K. Zoch⁵³, T.G. Zorbas¹⁴⁹, R. Zou³⁷, L. Zwalinski³⁶.

¹Department of Physics, University of Adelaide, Adelaide; Australia.

²Physics Department, SUNY Albany, Albany NY; United States of America.

³Department of Physics, University of Alberta, Edmonton AB; Canada.

⁴(^a)Department of Physics, Ankara University, Ankara; (^b)Istanbul Aydin University, Application and Research Center for Advanced Studies, Istanbul; (^c)Division of Physics, TOBB University of Economics and Technology, Ankara; Turkey.

⁵LAPP, Université Grenoble Alpes, Université Savoie Mont Blanc, CNRS/IN2P3, Annecy; France.

⁶High Energy Physics Division, Argonne National Laboratory, Argonne IL; United States of America.

⁷Department of Physics, University of Arizona, Tucson AZ; United States of America.

⁸Department of Physics, University of Texas at Arlington, Arlington TX; United States of America.

⁹Physics Department, National and Kapodistrian University of Athens, Athens; Greece.

¹⁰Physics Department, National Technical University of Athens, Zografou; Greece.

¹¹Department of Physics, University of Texas at Austin, Austin TX; United States of America.

¹²(^a)Bahcesehir University, Faculty of Engineering and Natural Sciences, Istanbul; (^b)Istanbul Bilgi University, Faculty of Engineering and Natural Sciences, Istanbul; (^c)Department of Physics, Bogazici University, Istanbul; (^d)Department of Physics Engineering, Gaziantep University, Gaziantep; Turkey.

¹³Institute of Physics, Azerbaijan Academy of Sciences, Baku; Azerbaijan.

¹⁴Institut de Física d'Altes Energies (IFAE), Barcelona Institute of Science and Technology, Barcelona; Spain.

¹⁵(^a)Institute of High Energy Physics, Chinese Academy of Sciences, Beijing; (^b)Physics Department, Tsinghua University, Beijing; (^c)Department of Physics, Nanjing University, Nanjing; (^d)University of Chinese Academy of Science (UCAS), Beijing; China.

¹⁶Institute of Physics, University of Belgrade, Belgrade; Serbia.

¹⁷Department for Physics and Technology, University of Bergen, Bergen; Norway.

¹⁸Physics Division, Lawrence Berkeley National Laboratory and University of California, Berkeley CA; United States of America.

¹⁹Institut für Physik, Humboldt Universität zu Berlin, Berlin; Germany.

²⁰Albert Einstein Center for Fundamental Physics and Laboratory for High Energy Physics, University of Bern, Bern; Switzerland.

²¹School of Physics and Astronomy, University of Birmingham, Birmingham; United Kingdom.

²²(^a)Facultad de Ciencias y Centro de Investigaciones, Universidad Antonio Nariño, Bogotá; (^b)Departamento de Física, Universidad Nacional de Colombia, Bogotá, Colombia; Colombia.

²³(^a)INFN Bologna and Università di Bologna, Dipartimento di Fisica; (^b)INFN Sezione di Bologna; Italy.

²⁴Physikalisches Institut, Universität Bonn, Bonn; Germany.

²⁵Department of Physics, Boston University, Boston MA; United States of America.

²⁶Department of Physics, Brandeis University, Waltham MA; United States of America.

²⁷(^a)Transilvania University of Brasov, Brasov; (^b)Horia Hulubei National Institute of Physics and Nuclear Engineering, Bucharest; (^c)Department of Physics, Alexandru Ioan Cuza University of Iasi, Iasi; (^d)National Institute for Research and Development of Isotopic and Molecular Technologies, Physics Department, Cluj-Napoca; (^e)University Politehnica Bucharest, Bucharest; (^f)West University in Timisoara, Timisoara; Romania.

²⁸(^a)Faculty of Mathematics, Physics and Informatics, Comenius University, Bratislava; (^b)Department of Subnuclear Physics, Institute of Experimental Physics of the Slovak Academy of Sciences, Kosice; Slovak

Republic.

²⁹Physics Department, Brookhaven National Laboratory, Upton NY; United States of America.

³⁰Departamento de Física, Universidad de Buenos Aires, Buenos Aires; Argentina.

³¹California State University, CA; United States of America.

³²Cavendish Laboratory, University of Cambridge, Cambridge; United Kingdom.

³³(^a)Department of Physics, University of Cape Town, Cape Town; (^b)iThemba Labs, Western Cape; (^c)Department of Mechanical Engineering Science, University of Johannesburg, Johannesburg; (^d)University of South Africa, Department of Physics, Pretoria; (^e)School of Physics, University of the Witwatersrand, Johannesburg; South Africa.

³⁴Department of Physics, Carleton University, Ottawa ON; Canada.

³⁵(^a)Faculté des Sciences Ain Chock, Réseau Universitaire de Physique des Hautes Energies - Université Hassan II, Casablanca; (^b)Faculté des Sciences, Université Ibn-Tofail, Kénitra; (^c)Faculté des Sciences Semlalia, Université Cadi Ayyad, LPHEA-Marrakech; (^d)Moroccan Foundation for Advanced Science Innovation and Research (MAScIR), Rabat; (^e)Faculté des Sciences, Université Mohamed Premier and LPTPM, Oujda; (^f)Faculté des sciences, Université Mohammed V, Rabat; Morocco.

³⁶CERN, Geneva; Switzerland.

³⁷Enrico Fermi Institute, University of Chicago, Chicago IL; United States of America.

³⁸LPC, Université Clermont Auvergne, CNRS/IN2P3, Clermont-Ferrand; France.

³⁹Nevis Laboratory, Columbia University, Irvington NY; United States of America.

⁴⁰Niels Bohr Institute, University of Copenhagen, Copenhagen; Denmark.

⁴¹(^a)Dipartimento di Fisica, Università della Calabria, Rende; (^b)INFN Gruppo Collegato di Cosenza, Laboratori Nazionali di Frascati; Italy.

⁴²Physics Department, Southern Methodist University, Dallas TX; United States of America.

⁴³Physics Department, University of Texas at Dallas, Richardson TX; United States of America.

⁴⁴National Centre for Scientific Research "Demokritos", Agia Paraskevi; Greece.

⁴⁵(^a)Department of Physics, Stockholm University; (^b)Oskar Klein Centre, Stockholm; Sweden.

⁴⁶Deutsches Elektronen-Synchrotron DESY, Hamburg and Zeuthen; Germany.

⁴⁷Lehrstuhl für Experimentelle Physik IV, Technische Universität Dortmund, Dortmund; Germany.

⁴⁸Institut für Kern- und Teilchenphysik, Technische Universität Dresden, Dresden; Germany.

⁴⁹Department of Physics, Duke University, Durham NC; United States of America.

⁵⁰SUPA - School of Physics and Astronomy, University of Edinburgh, Edinburgh; United Kingdom.

⁵¹INFN e Laboratori Nazionali di Frascati, Frascati; Italy.

⁵²Physikalisches Institut, Albert-Ludwigs-Universität Freiburg, Freiburg; Germany.

⁵³II. Physikalisches Institut, Georg-August-Universität Göttingen, Göttingen; Germany.

⁵⁴Département de Physique Nucléaire et Corpusculaire, Université de Genève, Genève; Switzerland.

⁵⁵(^a)Dipartimento di Fisica, Università di Genova, Genova; (^b)INFN Sezione di Genova; Italy.

⁵⁶II. Physikalisches Institut, Justus-Liebig-Universität Giessen, Giessen; Germany.

⁵⁷SUPA - School of Physics and Astronomy, University of Glasgow, Glasgow; United Kingdom.

⁵⁸LPSC, Université Grenoble Alpes, CNRS/IN2P3, Grenoble INP, Grenoble; France.

⁵⁹Laboratory for Particle Physics and Cosmology, Harvard University, Cambridge MA; United States of America.

⁶⁰(^a)Department of Modern Physics and State Key Laboratory of Particle Detection and Electronics, University of Science and Technology of China, Hefei; (^b)Institute of Frontier and Interdisciplinary Science and Key Laboratory of Particle Physics and Particle Irradiation (MOE), Shandong University, Qingdao; (^c)School of Physics and Astronomy, Shanghai Jiao Tong University, KLPPAC-MoE, SKLPPC, Shanghai; (^d)Tsung-Dao Lee Institute, Shanghai; China.

⁶¹(^a)Kirchhoff-Institut für Physik, Ruprecht-Karls-Universität Heidelberg, Heidelberg; (^b)Physikalisches

Institut, Ruprecht-Karls-Universität Heidelberg, Heidelberg; Germany.

⁶²Faculty of Applied Information Science, Hiroshima Institute of Technology, Hiroshima; Japan.

⁶³(^a)Department of Physics, Chinese University of Hong Kong, Shatin, N.T., Hong Kong; (^b)Department of Physics, University of Hong Kong, Hong Kong; (^c)Department of Physics and Institute for Advanced Study, Hong Kong University of Science and Technology, Clear Water Bay, Kowloon, Hong Kong; China.

⁶⁴Department of Physics, National Tsing Hua University, Hsinchu; Taiwan.

⁶⁵IJCLab, Université Paris-Saclay, CNRS/IN2P3, 91405, Orsay; France.

⁶⁶Department of Physics, Indiana University, Bloomington IN; United States of America.

⁶⁷(^a)INFN Gruppo Collegato di Udine, Sezione di Trieste, Udine; (^b)ICTP, Trieste; (^c)Dipartimento Politecnico di Ingegneria e Architettura, Università di Udine, Udine; Italy.

⁶⁸(^a)INFN Sezione di Lecce; (^b)Dipartimento di Matematica e Fisica, Università del Salento, Lecce; Italy.

⁶⁹(^a)INFN Sezione di Milano; (^b)Dipartimento di Fisica, Università di Milano, Milano; Italy.

⁷⁰(^a)INFN Sezione di Napoli; (^b)Dipartimento di Fisica, Università di Napoli, Napoli; Italy.

⁷¹(^a)INFN Sezione di Pavia; (^b)Dipartimento di Fisica, Università di Pavia, Pavia; Italy.

⁷²(^a)INFN Sezione di Pisa; (^b)Dipartimento di Fisica E. Fermi, Università di Pisa, Pisa; Italy.

⁷³(^a)INFN Sezione di Roma; (^b)Dipartimento di Fisica, Sapienza Università di Roma, Roma; Italy.

⁷⁴(^a)INFN Sezione di Roma Tor Vergata; (^b)Dipartimento di Fisica, Università di Roma Tor Vergata, Roma; Italy.

⁷⁵(^a)INFN Sezione di Roma Tre; (^b)Dipartimento di Matematica e Fisica, Università Roma Tre, Roma; Italy.

⁷⁶(^a)INFN-TIFPA; (^b)Università degli Studi di Trento, Trento; Italy.

⁷⁷Institut für Astro- und Teilchenphysik, Leopold-Franzens-Universität, Innsbruck; Austria.

⁷⁸University of Iowa, Iowa City IA; United States of America.

⁷⁹Department of Physics and Astronomy, Iowa State University, Ames IA; United States of America.

⁸⁰Joint Institute for Nuclear Research, Dubna; Russia.

⁸¹(^a)Departamento de Engenharia Elétrica, Universidade Federal de Juiz de Fora (UFJF), Juiz de Fora; (^b)Universidade Federal do Rio De Janeiro COPPE/EE/IF, Rio de Janeiro; (^c)Instituto de Física, Universidade de São Paulo, São Paulo; Brazil.

⁸²KEK, High Energy Accelerator Research Organization, Tsukuba; Japan.

⁸³Graduate School of Science, Kobe University, Kobe; Japan.

⁸⁴(^a)AGH University of Science and Technology, Faculty of Physics and Applied Computer Science, Krakow; (^b)Marian Smoluchowski Institute of Physics, Jagiellonian University, Krakow; Poland.

⁸⁵Institute of Nuclear Physics Polish Academy of Sciences, Krakow; Poland.

⁸⁶Faculty of Science, Kyoto University, Kyoto; Japan.

⁸⁷Kyoto University of Education, Kyoto; Japan.

⁸⁸Research Center for Advanced Particle Physics and Department of Physics, Kyushu University, Fukuoka ; Japan.

⁸⁹Instituto de Física La Plata, Universidad Nacional de La Plata and CONICET, La Plata; Argentina.

⁹⁰Physics Department, Lancaster University, Lancaster; United Kingdom.

⁹¹Oliver Lodge Laboratory, University of Liverpool, Liverpool; United Kingdom.

⁹²Department of Experimental Particle Physics, Jožef Stefan Institute and Department of Physics, University of Ljubljana, Ljubljana; Slovenia.

⁹³School of Physics and Astronomy, Queen Mary University of London, London; United Kingdom.

⁹⁴Department of Physics, Royal Holloway University of London, Egham; United Kingdom.

⁹⁵Department of Physics and Astronomy, University College London, London; United Kingdom.

⁹⁶Louisiana Tech University, Ruston LA; United States of America.

⁹⁷Fysiska institutionen, Lunds universitet, Lund; Sweden.

- ⁹⁸Centre de Calcul de l'Institut National de Physique Nucléaire et de Physique des Particules (IN2P3), Villeurbanne; France.
- ⁹⁹Departamento de Física Teórica C-15 and CIAFF, Universidad Autónoma de Madrid, Madrid; Spain.
- ¹⁰⁰Institut für Physik, Universität Mainz, Mainz; Germany.
- ¹⁰¹School of Physics and Astronomy, University of Manchester, Manchester; United Kingdom.
- ¹⁰²CPPM, Aix-Marseille Université, CNRS/IN2P3, Marseille; France.
- ¹⁰³Department of Physics, University of Massachusetts, Amherst MA; United States of America.
- ¹⁰⁴Department of Physics, McGill University, Montreal QC; Canada.
- ¹⁰⁵School of Physics, University of Melbourne, Victoria; Australia.
- ¹⁰⁶Department of Physics, University of Michigan, Ann Arbor MI; United States of America.
- ¹⁰⁷Department of Physics and Astronomy, Michigan State University, East Lansing MI; United States of America.
- ¹⁰⁸B.I. Stepanov Institute of Physics, National Academy of Sciences of Belarus, Minsk; Belarus.
- ¹⁰⁹Research Institute for Nuclear Problems of Byelorussian State University, Minsk; Belarus.
- ¹¹⁰Group of Particle Physics, University of Montreal, Montreal QC; Canada.
- ¹¹¹P.N. Lebedev Physical Institute of the Russian Academy of Sciences, Moscow; Russia.
- ¹¹²National Research Nuclear University MEPhI, Moscow; Russia.
- ¹¹³D.V. Skobeltsyn Institute of Nuclear Physics, M.V. Lomonosov Moscow State University, Moscow; Russia.
- ¹¹⁴Fakultät für Physik, Ludwig-Maximilians-Universität München, München; Germany.
- ¹¹⁵Max-Planck-Institut für Physik (Werner-Heisenberg-Institut), München; Germany.
- ¹¹⁶Nagasaki Institute of Applied Science, Nagasaki; Japan.
- ¹¹⁷Graduate School of Science and Kobayashi-Maskawa Institute, Nagoya University, Nagoya; Japan.
- ¹¹⁸Department of Physics and Astronomy, University of New Mexico, Albuquerque NM; United States of America.
- ¹¹⁹Institute for Mathematics, Astrophysics and Particle Physics, Radboud University/Nikhef, Nijmegen; Netherlands.
- ¹²⁰Nikhef National Institute for Subatomic Physics and University of Amsterdam, Amsterdam; Netherlands.
- ¹²¹Department of Physics, Northern Illinois University, DeKalb IL; United States of America.
- ¹²²^(a) Budker Institute of Nuclear Physics and NSU, SB RAS, Novosibirsk; ^(b) Novosibirsk State University Novosibirsk; Russia.
- ¹²³Institute for High Energy Physics of the National Research Centre Kurchatov Institute, Protvino; Russia.
- ¹²⁴Institute for Theoretical and Experimental Physics named by A.I. Alikhanov of National Research Centre "Kurchatov Institute", Moscow; Russia.
- ¹²⁵Department of Physics, New York University, New York NY; United States of America.
- ¹²⁶Ochanomizu University, Otsuka, Bunkyo-ku, Tokyo; Japan.
- ¹²⁷Ohio State University, Columbus OH; United States of America.
- ¹²⁸Homer L. Dodge Department of Physics and Astronomy, University of Oklahoma, Norman OK; United States of America.
- ¹²⁹Department of Physics, Oklahoma State University, Stillwater OK; United States of America.
- ¹³⁰Palacký University, RCPTM, Joint Laboratory of Optics, Olomouc; Czech Republic.
- ¹³¹Institute for Fundamental Science, University of Oregon, Eugene, OR; United States of America.
- ¹³²Graduate School of Science, Osaka University, Osaka; Japan.
- ¹³³Department of Physics, University of Oslo, Oslo; Norway.
- ¹³⁴Department of Physics, Oxford University, Oxford; United Kingdom.
- ¹³⁵LPNHE, Sorbonne Université, Université de Paris, CNRS/IN2P3, Paris; France.

- ¹³⁶Department of Physics, University of Pennsylvania, Philadelphia PA; United States of America.
- ¹³⁷Konstantinov Nuclear Physics Institute of National Research Centre "Kurchatov Institute", PNPI, St. Petersburg; Russia.
- ¹³⁸Department of Physics and Astronomy, University of Pittsburgh, Pittsburgh PA; United States of America.
- ¹³⁹(^a)Laboratório de Instrumentação e Física Experimental de Partículas - LIP, Lisboa; (^b)Departamento de Física, Faculdade de Ciências, Universidade de Lisboa, Lisboa; (^c)Departamento de Física, Universidade de Coimbra, Coimbra; (^d)Centro de Física Nuclear da Universidade de Lisboa, Lisboa; (^e)Departamento de Física, Universidade do Minho, Braga; (^f)Departamento de Física Teórica y del Cosmos, Universidad de Granada, Granada (Spain); (^g)Dep Física and CEFITEC of Faculdade de Ciências e Tecnologia, Universidade Nova de Lisboa, Caparica; (^h)Instituto Superior Técnico, Universidade de Lisboa, Lisboa; Portugal.
- ¹⁴⁰Institute of Physics of the Czech Academy of Sciences, Prague; Czech Republic.
- ¹⁴¹Czech Technical University in Prague, Prague; Czech Republic.
- ¹⁴²Charles University, Faculty of Mathematics and Physics, Prague; Czech Republic.
- ¹⁴³Particle Physics Department, Rutherford Appleton Laboratory, Didcot; United Kingdom.
- ¹⁴⁴IRFU, CEA, Université Paris-Saclay, Gif-sur-Yvette; France.
- ¹⁴⁵Santa Cruz Institute for Particle Physics, University of California Santa Cruz, Santa Cruz CA; United States of America.
- ¹⁴⁶(^a)Departamento de Física, Pontificia Universidad Católica de Chile, Santiago; (^b)Universidad Andres Bello, Department of Physics, Santiago; (^c)Instituto de Alta Investigación, Universidad de Tarapacá; (^d)Departamento de Física, Universidad Técnica Federico Santa María, Valparaíso; Chile.
- ¹⁴⁷Universidade Federal de São João del Rei (UFSJ), São João del Rei; Brazil.
- ¹⁴⁸Department of Physics, University of Washington, Seattle WA; United States of America.
- ¹⁴⁹Department of Physics and Astronomy, University of Sheffield, Sheffield; United Kingdom.
- ¹⁵⁰Department of Physics, Shinshu University, Nagano; Japan.
- ¹⁵¹Department Physik, Universität Siegen, Siegen; Germany.
- ¹⁵²Department of Physics, Simon Fraser University, Burnaby BC; Canada.
- ¹⁵³SLAC National Accelerator Laboratory, Stanford CA; United States of America.
- ¹⁵⁴Physics Department, Royal Institute of Technology, Stockholm; Sweden.
- ¹⁵⁵Departments of Physics and Astronomy, Stony Brook University, Stony Brook NY; United States of America.
- ¹⁵⁶Department of Physics and Astronomy, University of Sussex, Brighton; United Kingdom.
- ¹⁵⁷School of Physics, University of Sydney, Sydney; Australia.
- ¹⁵⁸Institute of Physics, Academia Sinica, Taipei; Taiwan.
- ¹⁵⁹(^a)E. Andronikashvili Institute of Physics, Iv. Javakhishvili Tbilisi State University, Tbilisi; (^b)High Energy Physics Institute, Tbilisi State University, Tbilisi; Georgia.
- ¹⁶⁰Department of Physics, Technion, Israel Institute of Technology, Haifa; Israel.
- ¹⁶¹Raymond and Beverly Sackler School of Physics and Astronomy, Tel Aviv University, Tel Aviv; Israel.
- ¹⁶²Department of Physics, Aristotle University of Thessaloniki, Thessaloniki; Greece.
- ¹⁶³International Center for Elementary Particle Physics and Department of Physics, University of Tokyo, Tokyo; Japan.
- ¹⁶⁴Graduate School of Science and Technology, Tokyo Metropolitan University, Tokyo; Japan.
- ¹⁶⁵Department of Physics, Tokyo Institute of Technology, Tokyo; Japan.
- ¹⁶⁶Tomsk State University, Tomsk; Russia.
- ¹⁶⁷Department of Physics, University of Toronto, Toronto ON; Canada.
- ¹⁶⁸(^a)TRIUMF, Vancouver BC; (^b)Department of Physics and Astronomy, York University, Toronto ON;

Canada.

¹⁶⁹Division of Physics and Tomonaga Center for the History of the Universe, Faculty of Pure and Applied Sciences, University of Tsukuba, Tsukuba; Japan.

¹⁷⁰Department of Physics and Astronomy, Tufts University, Medford MA; United States of America.

¹⁷¹Department of Physics and Astronomy, University of California Irvine, Irvine CA; United States of America.

¹⁷²Department of Physics and Astronomy, University of Uppsala, Uppsala; Sweden.

¹⁷³Department of Physics, University of Illinois, Urbana IL; United States of America.

¹⁷⁴Instituto de Física Corpuscular (IFIC), Centro Mixto Universidad de Valencia - CSIC, Valencia; Spain.

¹⁷⁵Department of Physics, University of British Columbia, Vancouver BC; Canada.

¹⁷⁶Department of Physics and Astronomy, University of Victoria, Victoria BC; Canada.

¹⁷⁷Fakultät für Physik und Astronomie, Julius-Maximilians-Universität Würzburg, Würzburg; Germany.

¹⁷⁸Department of Physics, University of Warwick, Coventry; United Kingdom.

¹⁷⁹Waseda University, Tokyo; Japan.

¹⁸⁰Department of Particle Physics and Astrophysics, Weizmann Institute of Science, Rehovot; Israel.

¹⁸¹Department of Physics, University of Wisconsin, Madison WI; United States of America.

¹⁸²Fakultät für Mathematik und Naturwissenschaften, Fachgruppe Physik, Bergische Universität Wuppertal, Wuppertal; Germany.

¹⁸³Department of Physics, Yale University, New Haven CT; United States of America.

^a Also at Borough of Manhattan Community College, City University of New York, New York NY; United States of America.

^b Also at Centro Studi e Ricerche Enrico Fermi; Italy.

^c Also at CERN, Geneva; Switzerland.

^d Also at CPPM, Aix-Marseille Université, CNRS/IN2P3, Marseille; France.

^e Also at Département de Physique Nucléaire et Corpusculaire, Université de Genève, Genève; Switzerland.

^f Also at Departament de Física de la Universitat Autònoma de Barcelona, Barcelona; Spain.

^g Also at Department of Financial and Management Engineering, University of the Aegean, Chios; Greece.

^h Also at Department of Physics and Astronomy, Michigan State University, East Lansing MI; United States of America.

ⁱ Also at Department of Physics and Astronomy, University of Louisville, Louisville, KY; United States of America.

^j Also at Department of Physics, Ben Gurion University of the Negev, Beer Sheva; Israel.

^k Also at Department of Physics, California State University, East Bay; United States of America.

^l Also at Department of Physics, California State University, Fresno; United States of America.

^m Also at Department of Physics, California State University, Sacramento; United States of America.

ⁿ Also at Department of Physics, King's College London, London; United Kingdom.

^o Also at Department of Physics, St. Petersburg State Polytechnical University, St. Petersburg; Russia.

^p Also at Department of Physics, University of Fribourg, Fribourg; Switzerland.

^q Also at Dipartimento di Matematica, Informatica e Fisica, Università di Udine, Udine; Italy.

^r Also at Faculty of Physics, M.V. Lomonosov Moscow State University, Moscow; Russia.

^s Also at Giresun University, Faculty of Engineering, Giresun; Turkey.

^t Also at Graduate School of Science, Osaka University, Osaka; Japan.

^u Also at Hellenic Open University, Patras; Greece.

^v Also at IJCLab, Université Paris-Saclay, CNRS/IN2P3, 91405, Orsay; France.

^w Also at Institutio Catalana de Recerca i Estudis Avancats, ICREA, Barcelona; Spain.

^x Also at Institut für Experimentalphysik, Universität Hamburg, Hamburg; Germany.

- ^y Also at Institute for Mathematics, Astrophysics and Particle Physics, Radboud University/Nikhef, Nijmegen; Netherlands.
- ^z Also at Institute for Nuclear Research and Nuclear Energy (INRNE) of the Bulgarian Academy of Sciences, Sofia; Bulgaria.
- ^{aa} Also at Institute for Particle and Nuclear Physics, Wigner Research Centre for Physics, Budapest; Hungary.
- ^{ab} Also at Institute of Particle Physics (IPP); Canada.
- ^{ac} Also at Institute of Physics, Azerbaijan Academy of Sciences, Baku; Azerbaijan.
- ^{ad} Also at Instituto de Fisica Teorica, IFT-UAM/CSIC, Madrid; Spain.
- ^{ae} Also at Istanbul University, Dept. of Physics, Istanbul; Turkey.
- ^{af} Also at Joint Institute for Nuclear Research, Dubna; Russia.
- ^{ag} Also at Louisiana Tech University, Ruston LA; United States of America.
- ^{ah} Also at Moscow Institute of Physics and Technology State University, Dolgoprudny; Russia.
- ^{ai} Also at National Research Nuclear University MEPhI, Moscow; Russia.
- ^{aj} Also at Physics Department, An-Najah National University, Nablus; Palestine.
- ^{ak} Also at Physikalisches Institut, Albert-Ludwigs-Universität Freiburg, Freiburg; Germany.
- ^{al} Also at The City College of New York, New York NY; United States of America.
- ^{am} Also at TRIUMF, Vancouver BC; Canada.
- ^{an} Also at Università di Napoli Parthenope, Napoli; Italy.
- ^{ao} Also at University of Chinese Academy of Sciences (UCAS), Beijing; China.
- * Deceased

Acknowledgements

We thank CERN for the very successful operation of the LHC, as well as the support staff from our institutions without whom ATLAS could not be operated efficiently.

We acknowledge the support of ANPCyT, Argentina; YerPhI, Armenia; ARC, Australia; BMWFW and FWF, Austria; ANAS, Azerbaijan; SSTC, Belarus; CNPq and FAPESP, Brazil; NSERC, NRC and CFI, Canada; CERN; ANID, Chile; CAS, MOST and NSFC, China; COLCIENCIAS, Colombia; MSMT CR, MPO CR and VSC CR, Czech Republic; DNRF and DNSRC, Denmark; IN2P3-CNRS and CEA-DRF/IRFU, France; SRNSFG, Georgia; BMBF, HGF and MPG, Germany; GSRT, Greece; RGC and Hong Kong SAR, China; ISF and Benozio Center, Israel; INFN, Italy; MEXT and JSPS, Japan; CNRST, Morocco; NWO, Netherlands; RCN, Norway; MNiSW and NCN, Poland; FCT, Portugal; MNE/IFA, Romania; JINR; MES of Russia and NRC KI, Russian Federation; MESTD, Serbia; MSSR, Slovakia; ARRS and MIZŠ, Slovenia; DST/NRF, South Africa; MICINN, Spain; SRC and Wallenberg Foundation, Sweden; SERI, SNSF and Cantons of Bern and Geneva, Switzerland; MOST, Taiwan; TAEK, Turkey; STFC, United Kingdom; DOE and NSF, United States of America. In addition, individual groups and members have received support from BCKDF, CANARIE, Compute Canada, CRC and IVADO, Canada; Beijing Municipal Science & Technology Commission, China; COST, ERC, ERDF, Horizon 2020 and Marie Skłodowska-Curie Actions, European Union; Investissements d’Avenir Labex, Investissements d’Avenir Idex and ANR, France; DFG and AvH Foundation, Germany; Herakleitos, Thales and Aristeia programmes co-financed by EU-ESF and the Greek NSRF, Greece; BSF-NSF and GIF, Israel; La Caixa Banking Foundation, CERCA Programme Generalitat de Catalunya and PROMETEO and GenT Programmes Generalitat Valenciana, Spain; Göran Gustafssons Stiftelse, Sweden; The Royal Society and Leverhulme Trust, United Kingdom.

The crucial computing support from all WLCG partners is acknowledged gratefully, in particular from CERN, the ATLAS Tier-1 facilities at TRIUMF (Canada), NDGF (Denmark, Norway, Sweden), CC-IN2P3 (France), KIT/GridKA (Germany), INFN-CNAF (Italy), NL-T1 (Netherlands), PIC (Spain), ASGC (Taiwan), RAL (UK) and BNL (USA), the Tier-2 facilities worldwide and large non-WLCG resource providers. Major contributors of computing resources are listed in Ref. [78].

References

- [1] D. Clowe et al., *A Direct Empirical Proof of the Existence of Dark Matter*, *The Astrophysical Journal* **648** (2006) L109, arXiv: [astro-ph/0608407](#).
- [2] J. Goodman et al., *Constraints on dark matter from colliders*, *Phys. Rev. D* **82** (2010) 116010, arXiv: [1008.1783 \[hep-ph\]](#).
- [3] R. D. Peccei and H. R. Quinn, *CP Conservation in the Presence of Pseudoparticles*, *Phys. Rev. Lett.* **38** (1977) 1440.
- [4] J. Preskill, M. B. Wise and F. Wilczek, *Cosmology of the invisible axion*, *Phys. Lett. B* **120** (1983) 127.
- [5] M. Bauer, M. Heiles, M. Neubert and A. Thamm, *Axion-like particles at future colliders*, *Eur. Phys. J. C* **79** (2019) 74, arXiv: [1808.10323 \[hep-ph\]](#).
- [6] J. Jaeckel, M. Jankowiak and M. Spannowsky, *LHC probes the hidden sector*, *Phys. Dark Univ.* **2** (2013) 111, arXiv: [1212.3620 \[hep-ex\]](#).

- [7] K. Mimasu and V. Sanz, *ALPs at colliders*, *JHEP* **06** (2015) 173, arXiv: [1409.4792 \[hep-ph\]](#).
- [8] I. Brivio et al., *ALPs effective field theory and collider signatures*, *Eur. Phys. J. C* **77** (2017) 572, arXiv: [1701.05379 \[hep-ph\]](#).
- [9] ATLAS Collaboration, *Search for dark matter at $\sqrt{s} = 13$ TeV in final states containing an energetic photon and large missing transverse momentum with the ATLAS detector*, *Eur. Phys. J. C* **77** (2017) 393, arXiv: [1704.03848 \[hep-ex\]](#).
- [10] CMS Collaboration, *Search for new physics in final states with a single photon and missing transverse momentum in proton-proton collisions at $\sqrt{s} = 13$ TeV*, *JHEP* **02** (2019) 074, arXiv: [1810.00196 \[hep-ex\]](#).
- [11] ATLAS Collaboration, *Search for dark matter and other new phenomena in events with an energetic jet and large missing transverse momentum using the ATLAS detector*, *JHEP* **01** (2018) 126, arXiv: [1711.03301 \[hep-ex\]](#).
- [12] CMS Collaboration, *Search for new physics in final states with an energetic jet or a hadronically decaying W or Z boson and transverse momentum imbalance at $\sqrt{s} = 13$ TeV*, *Phys. Rev. D* **97** (2018) 092005, arXiv: [1712.02345 \[hep-ex\]](#).
- [13] ATLAS Collaboration, *Search for dark matter produced in association with bottom or top quarks in $\sqrt{s} = 13$ TeV pp collisions with the ATLAS detector*, *Eur. Phys. J. C* **78** (2018) 18, arXiv: [1710.11412 \[hep-ex\]](#).
- [14] CMS Collaboration, *Search for dark matter in events with energetic, hadronically decaying top quarks and missing transverse momentum at $\sqrt{s} = 13$ TeV*, *JHEP* **06** (2018) 027, arXiv: [1801.08427 \[hep-ex\]](#).
- [15] CMS Collaboration, *Search for dark matter and unparticles in events with a Z boson and missing transverse momentum in proton-proton collisions at $\sqrt{s} = 13$ TeV*, *JHEP* **03** (2017) 061, arXiv: [1701.02042 \[hep-ex\]](#),
Erratum: *Search for dark matter and unparticles in events with a Z boson and missing transverse momentum in proton-proton collisions at $\sqrt{s} = 13$ TeV*, *JHEP* **09** (2017) 106.
- [16] ATLAS Collaboration, *Search for dark matter in events with a hadronically decaying vector boson and missing transverse momentum in pp collisions at $\sqrt{s} = 13$ TeV with the ATLAS detector*, *JHEP* **10** (2018) 180, arXiv: [1807.11471 \[hep-ex\]](#).
- [17] ATLAS Collaboration, *Search for dark matter in association with a Higgs boson decaying to two photons at $\sqrt{s} = 13$ TeV with the ATLAS detector*, *Phys. Rev. D* **96** (2017) 112004, arXiv: [1706.03948 \[hep-ex\]](#).
- [18] CMS Collaboration, *Search for associated production of dark matter with a Higgs boson decaying to $b\bar{b}$ or $\gamma\gamma$ at $\sqrt{s} = 13$ TeV*, *JHEP* **10** (2017) 180, arXiv: [1703.05236 \[hep-ex\]](#).
- [19] J. Abdallah et al., *Simplified models for dark matter searches at the LHC*, *Phys. Dark Univ.* **9-10** (2015) 8, arXiv: [1506.03116 \[hep-ph\]](#).
- [20] O. Buchmueller, M. J. Dolan, S. A. Malik and C. McCabe, *Characterising dark matter searches at colliders and direct detection experiments: vector mediators*, *JHEP* **01** (2015) 037, arXiv: [1407.8257 \[hep-ph\]](#).
- [21] D. Abercrombie et al., *Dark Matter benchmark models for early LHC Run-2 Searches: Report of the ATLAS/CMS Dark Matter Forum*, *Phys. Dark Univ.* **27** (2020) 100371, arXiv: [1507.00966 \[hep-ex\]](#).

- [22] A. Albert et al., *Recommendations of the LHC Dark Matter Working Group: Comparing LHC searches for dark matter mediators in visible and invisible decay channels and calculations of the thermal relic density*, *Phys. Dark Univ.* **26** (2019) 100377, arXiv: 1703.05703 [hep-ex].
- [23] ATLAS Collaboration, *The ATLAS Experiment at the CERN Large Hadron Collider*, *JINST* **3** (2008) S08003.
- [24] ATLAS Collaboration, *ATLAS Insertable B-Layer Technical Design Report*, ATLAS-TDR-19, 2010, URL: <https://cds.cern.ch/record/1291633>,
ATLAS Insertable B-Layer Technical Design Report Addendum, ATLAS-TDR-19-ADD-1, 2012, URL: <https://cds.cern.ch/record/1451888>.
- [25] B. Abbott et al., *Production and integration of the ATLAS Insertable B-Layer*, *JINST* **13** (2018) T05008, arXiv: 1803.00844 [physics.ins-det].
- [26] ATLAS Collaboration, *Performance of the ATLAS trigger system in 2015*, *Eur. Phys. J. C* **77** (2017) 317, arXiv: 1611.09661 [hep-ex].
- [27] ATLAS Collaboration, *Luminosity determination in pp collisions at $\sqrt{s} = 13$ TeV using the ATLAS detector at the LHC*, ATLAS-CONF-2019-021, 2019, URL: <https://cds.cern.ch/record/2677054>.
- [28] G. Avoni et al, *The new LUCID-2 detector for luminosity measurement and monitoring in ATLAS*, *JINST* **13** (2018) P07017.
- [29] T. Sjöstrand, S. Mrenna and P. Skands, *A brief introduction to PYTHIA 8.1*, *Comput. Phys. Comm.* **178** (2008) 852, arXiv: 0710.3820 [hep-ph].
- [30] ATLAS Collaboration, *ATLAS Pythia 8 tunes to 7 TeV data*, ATL-PHYS-PUB-2014-021, 2014, URL: <https://cds.cern.ch/record/1966419>.
- [31] G. Watt and R. S. Thorne, *Study of Monte Carlo approach to experimental uncertainty propagation with MSTW 2008 PDFs*, *JHEP* **08** (2012) 052, arXiv: 1205.4024 [hep-ph].
- [32] J. Alwall et al., *The automated computation of tree-level and next-to-leading order differential cross sections, and their matching to parton shower simulations*, *JHEP* **07** (2014) 079, arXiv: 1405.0301 [hep-ph].
- [33] NNPDF Collaboration, R. D. Ball et al., *Parton distributions for the LHC run II*, *JHEP* **04** (2015) 040, arXiv: 1410.8849 [hep-ph].
- [34] M. Backović et al., *Higher-order QCD predictions for dark matter production at the LHC in simplified models with s-channel mediators*, *Eur. Phys. J. C* **75** (2015) 482, arXiv: 1508.05327 [hep-ph].
- [35] T. Gleisberg et al., *Event generation with SHERPA 1.1*, *JHEP* **02** (2009) 007, arXiv: 0811.4622 [hep-ph].
- [36] E. Bothmann et al, *Event generation with SHERPA 2.2*, *SciPost Phys.* **7** (2019) 034, arXiv: 1905.09127 [hep-ph].
- [37] T. Gleisberg and S. Höche, *Comix, a new matrix element generator*, *JHEP* **12** (2008) 039, arXiv: 0808.3674 [hep-ph].
- [38] F. Cascioli, P. Maierhöfer and S. Pozzorini, *Scattering Amplitudes with Open Loops*, *Phys. Rev. Lett.* **108** (2012) 111601, arXiv: 1111.5206 [hep-ph].

- [39] S. Höche, F. Krauss, S. Schumann and F. Siegert, *QCD matrix elements and truncated showers*, *JHEP* **05** (2009) 053, arXiv: [0903.1219](#) [[hep-ph](#)].
- [40] S. Schumann and F. Krauss, *A parton shower algorithm based on Catani-Seymour dipole factorisation*, *JHEP* **03** (2008) 038, arXiv: [0709.1027](#) [[hep-ph](#)].
- [41] ATLAS Collaboration, *Monte Carlo Generators for the Production of a W or Z/ γ^* Boson in Association with Jets at ATLAS in Run 2*, ATL-PHYS-PUB-2016-003, 2016, URL: <https://cds.cern.ch/record/2120133>.
- [42] ATLAS Collaboration, *The ATLAS Simulation Infrastructure*, *Eur. Phys. J. C* **70** (2010) 823, arXiv: [1005.4568](#) [[physics.ins-det](#)].
- [43] S. Agostinelli et al., *GEANT4 – a simulation toolkit*, *Nucl. Instrum. Meth. A* **506** (2003) 250.
- [44] ATLAS Collaboration, *Performance of electron and photon triggers in ATLAS during LHC Run 2*, *Eur. Phys. J. C* **80** (2020) 47, arXiv: [1909.00761](#) [[hep-ex](#)].
- [45] ATLAS Collaboration, *Vertex Reconstruction Performance of the ATLAS Detector at $\sqrt{s} = 13$ TeV*, ATL-PHYS-PUB-2015-026, 2015, URL: <https://cds.cern.ch/record/2037717>.
- [46] ATLAS Collaboration, *Selection of jets produced in 13 TeV proton–proton collisions with the ATLAS detector*, ATLAS-CONF-2015-029, 2015, URL: <https://cds.cern.ch/record/2037702>.
- [47] ATLAS Collaboration, *Electron and photon performance measurements with the ATLAS detector using the 2015-2017 LHC proton-proton collision data*, *JINST* **14** (2019) P12006, arXiv: [1908.00005](#) [[hep-ex](#)].
- [48] ATLAS Collaboration, *Muon reconstruction performance of the ATLAS detector in proton–proton collision data at $\sqrt{s} = 13$ TeV*, *Eur. Phys. J. C* **76** (2016) 292, arXiv: [1603.05598](#) [[hep-ex](#)].
- [49] ATLAS Collaboration, *Topological cell clustering in the ATLAS calorimeters and its performance in LHC Run 1*, *Eur. Phys. J. C* **77** (2017) 490, arXiv: [1603.02934](#) [[hep-ex](#)].
- [50] M. Cacciari, G. P. Salam and G. Soyez, *The anti- k_t jet clustering algorithm*, *JHEP* **04** (2008) 063, arXiv: [0802.1189](#) [[hep-ph](#)].
- [51] M. Cacciari, G. P. Salam and G. Soyez, *FastJet user manual*, *Eur. Phys. J. C* **72** (2012) 1896, arXiv: [1111.6097](#) [[hep-ph](#)].
- [52] ATLAS Collaboration, *Jet energy scale measurements and their systematic uncertainties in proton-proton collisions at $\sqrt{s} = 13$ TeV with the ATLAS detector*, *Phys. Rev. D* **96** (2017) 072002, arXiv: [1703.09665](#) [[hep-ex](#)].
- [53] ATLAS Collaboration, *Tagging and suppression of pileup jets with the ATLAS detector*, ATLAS-CONF-2014-018, 2014, URL: <https://cds.cern.ch/record/1700870>.
- [54] ATLAS Collaboration, *Measurement of the tau lepton reconstruction and identification performance in the ATLAS experiment using pp collisions at $\sqrt{s} = 13$ TeV*, ATLAS-CONF-2017-029, 2017, URL: <https://cds.cern.ch/record/2261772>.
- [55] ATLAS Collaboration, *Performance of missing transverse momentum reconstruction with the ATLAS detector using proton-proton collisions at $\sqrt{s} = 13$ TeV*, *Eur. Phys. J. C* **78** (2018) 903, arXiv: [1802.08168](#) [[hep-ex](#)].

- [56] ATLAS Collaboration, *Object-based missing transverse momentum significance in the ATLAS Detector*, ATLAS-CONF-2018-038, 2018, URL: <https://cds.cern.ch/record/2630948>.
- [57] ATLAS Collaboration, *Measurement of the inclusive isolated prompt photon cross section in pp collisions at $\sqrt{s} = 7$ TeV with the ATLAS detector*, *Phys. Rev. D* **83** (2011) 052005, arXiv: [1012.4389](https://arxiv.org/abs/1012.4389) [[hep-ex](#)].
- [58] E. Bothmann, M. Schönherr and S. Schumann, *Reweighting QCD matrix-element and parton-shower calculations*, *Eur. Phys. J. C* **76** (2016) 590, arXiv: [1606.08753](https://arxiv.org/abs/1606.08753) [[hep-ph](#)].
- [59] M. Botje et al., *The PDF4LHC Working Group Interim Recommendations*, (2011), arXiv: [1101.0538](https://arxiv.org/abs/1101.0538) [[hep-ph](#)].
- [60] G. Choudalakis and D. Casadei, *Plotting the differences between data and expectation*, *Eur. Phys. J. Plus* **127** (2012) 25, arXiv: [1111.2062](https://arxiv.org/abs/1111.2062) [[physics.data-an](#)].
- [61] M. Baak et al., *HistFitter software framework for statistical data analysis*, *Eur. Phys. J. C* **75** (2015) 153, arXiv: [1410.1280](https://arxiv.org/abs/1410.1280) [[hep-ex](#)].
- [62] A. L. Read, *Presentation of search results: the CL_s technique*, *J. Phys. G* **28** (2002) 2693.
- [63] G. Cowan, K. Cranmer, E. Gross and O. Vitells, *Asymptotic formulae for likelihood-based tests of new physics*, *Eur. Phys. J. C* **71** (2011) 1554, arXiv: [1007.1727](https://arxiv.org/abs/1007.1727) [[physics.data-an](#)].
- [64] Planck Collaboration, P. A. R. Ade et al, *Planck 2015 results. XIII. Cosmological parameters*, *Astron. Astrophys.* **594** (2016) A13, arXiv: [1502.01589](https://arxiv.org/abs/1502.01589) [[astro-ph.CO](#)].
- [65] F. Kahlhoefer, K. Schmidt-Hoberg, T. Schwetz and S. Vogl, *Implications of unitarity and gauge invariance for simplified dark matter models*, *JHEP* **02** (2016) 016, arXiv: [1510.02110](https://arxiv.org/abs/1510.02110) [[hep-ph](#)].
- [66] A. Boveia et al., *Recommendations on presenting LHC searches for missing transverse energy signals using simplified s-channel models of dark matter*, *Phys. Dark Univ.* **27** (2020) 100365, arXiv: [1603.04156](https://arxiv.org/abs/1603.04156) [[hep-ex](#)].
- [67] PICASSO Collaboration, *Final results of the PICASSO dark matter search experiment*, *Astropart. Phys.* **90** (2017) 85, arXiv: [1611.01499](https://arxiv.org/abs/1611.01499) [[hep-ex](#)].
- [68] XENON Collaboration, *Constraining the Spin-Dependent WIMP-Nucleon Cross Sections with XENON1T*, *Phys. Rev. Lett.* **122** (2019) 141301, arXiv: [1902.03234](https://arxiv.org/abs/1902.03234) [[astro-ph.CO](#)].
- [69] SuperCDMS Collaboration, *Low-mass dark matter search with CDMSlite*, *Phys. Rev. D* **97** (2018) 022002, arXiv: [1707.01632](https://arxiv.org/abs/1707.01632) [[astro-ph.CO](#)].
- [70] LUX Collaboration, *Limits on Spin-Dependent WIMP-Nucleon Cross Section Obtained from the Complete LUX Exposure*, *Phys. Rev. Lett.* **118** (2017) 251302, arXiv: [1705.03380](https://arxiv.org/abs/1705.03380) [[astro-ph.CO](#)].
- [71] PICO Collaboration, *Dark matter search results from the complete exposure of the PICO-60 C₃F₈ bubble chamber*, *Phys. Rev. D* **100** (2019) 022001.

- [72] PandaX-II Collaboration, *Spin-Dependent Weakly-Interacting-Massive-Particle–Nucleon Cross Section Limits from First Data of PandaX-II Experiment*, *Phys. Rev. Lett.* **118** (2017) 071301, arXiv: [1611.06553v3](https://arxiv.org/abs/1611.06553v3) [[hep-ex](#)],
Erratum: *Spin-Dependent Weakly-Interacting-Massive-Particle–Nucleon Cross Section Limits from First Data of PandaX-II Experiment*, *Phys. Rev. Lett.* **120** (2018) 049902.
- [73] XENON Collaboration, *Dark Matter Search Results from a Ton-Year Exposure of XENON1T*, *Phys. Rev. Lett.* **121** (2018) 111302, arXiv: [1805.12562v2](https://arxiv.org/abs/1805.12562v2) [[astro-ph.CO](#)].
- [74] XENON Collaboration, *Search for Light Dark Matter Interactions Enhanced by the Migdal effect or Bremsstrahlung in XENON1T*, *Phys. Rev. Lett.* **123** (2019) 241803, arXiv: [1907.12771](https://arxiv.org/abs/1907.12771) [[hep-ex](#)].
- [75] PandaX-II Collaboration,
Dark Matter Results From 54-Ton-Day Exposure of PandaX-II Experiment,
Phys. Rev. Lett. **119** (2017) 181302, arXiv: [1708.06917v2](https://arxiv.org/abs/1708.06917v2) [[astro-ph.CO](#)].
- [76] DarkSide Collaboration, *Low-Mass Dark Matter Search with the DarkSide-50 Experiment*, *Phys. Rev. Lett.* **121** (2018) 081307, arXiv: [1802.06994v3](https://arxiv.org/abs/1802.06994v3) [[astro-ph.HE](#)].
- [77] L3 Collaboration, *Search for new physics in energetic single photon production in e^+e^- annihilation at the Z resonance*, *Phys. Lett. B* **412** (1997) 201.
- [78] ATLAS Collaboration, *ATLAS Computing Acknowledgements*, ATL-SOFT-PUB-2020-001, URL: <https://cds.cern.ch/record/2717821>.